WETLAID CELLULOSE FIBER-THERMOPLASTIC HYBRID COMPOSITES – EFFECTS OF LYOCELL AND STEAM EXPLODED WOOD FIBER BLENDS

Richard Kwesi Johnson

Thesis submitted to the Faculty of the
Virginia Polytechnic Institute and State University
In partial fulfillment of requirements for the degree of

Master of Science
In
Wood Science and Forest Products

Audrey Zink-Sharp

Wolfgang G Glasser

Charles E Frazier

June 18 2004
Blacksburg, Virginia

Keywords: hybrid composites, lyocell, mechanical properties, random wetlay process, sorption, steam exploded wood, viscoelastic properties

Wetlaid Cellulose Fiber-Thermoplastic Hybrid Composites – Effects Of Lyocell And Steam Exploded Wood Fiber Blends

Richard Kwesi Johnson

ABSTRACT

Fiber hybridization involves the blending of high and low performance fibers in a common matrix to yield a composite with a balance of properties that cannot be achieved by using either fiber alone. In this study, the random wetlay process was used as a compounding method to investigate the effects of fiber hybridization on the mechanical, viscoelastic, and sorption characteristics of steam-exploded wood (SEW) and lyocell (high performance regenerated cellulose) fiber-reinforced polypropylene (PP) composites. The two fiber types were blended in varying proportions within a fixed total fiber content of 50 wt. % and compared with non-hybrid lyocell- and SEW-PP controls.

Using PP matrix as basis, it was observed that moduli of all composites generally increased with increasing lyocell concentration, ranging from a minimum 66 % for SP 50 (SEW/PP control) to a maximum 233 % for LP 50 (lyocell/PP control). Ultimate strengths on the other hand, declined for SP 50 but increased with the inclusion of lyocell fibers.

Comparisons of hybrid (having 5 – 20 wt % lyocell) with non-hybrid (having 25 – 50 wt. % lyocell) composites revealed a surprisingly greater strength and modulus-building efficiency (by as much as 2.6 times) in the hybrid composites. This observation indicated possible synergism between lyocell and SEW. Analyses of composite property gains as a function of fiber cost also showed greater cost benefits (highest for tensile modulus) in favor of hybridization.

The advantages of fiber hybridization on composite properties were again evident under dynamic mechanical analysis where no significant differences in the storage moduli were found

between a hybrid composite with 20 wt. % lyocell and a non-hybrid composite with 50 wt. % lyocell loading. Application of the time-temperature superposition principle (TTSP) made it possible to predict storage moduli over extended frequencies for PP and its composites. Comparison of shift factor versus temperature plots revealed decreasing relaxation times of PP with increasing lyocell concentration, which indicated that PP interacted better with lyocell than with SEW fibers.

Finally, it was observed from sorption tests that hybrid composites absorbed less moisture than non-hybrid counterparts of either fiber type. The reasons for this observation were not apparent. It is however possible that moisture transport mechanisms within the composites may have been modified as a result of hybridization.

Dedication

This work is dedicated to my parents, Cdr. and Mrs. Johnson for all the love and support they have given me throughout my life. I wish to thank them both for the numerous sacrifices they have made for me and for always believing in me and being there for me. Mom and Dad, may God richly bless you. I also wish to express my appreciation to my siblings and other family members whose prayers, support and words of encouragement have sustained me and kept me on the right track. I thank them all for being part of my life.

Acknowledgement

My utmost thanks go to the Almighty God for giving me the strength, wisdom, and protection to make it through another important step of my life.

I would like to express my sincere gratitude to my co-advisors, Drs. Wolfgang Glasser and Audrey Zink-Sharp for offering me this wonderful opportunity to work on this project. I would like to thank them both for providing me with the invaluable support and guidance that has seen me through to the end. My sincere thanks also go to Dr. Charles Frazier for accepting to be on my advisory committee and for his very useful contributions to this work, particularly, DMA.

I would also wish to show my appreciation to the following people. My colleague and friend Dr. Scott Renneckar for his constant support and encouragement, Joe Price O'Brien and Dr Todd Bullions for their time and help towards wetlay and mechanical testing, Bob Wright for his efforts in steam-explosion, Steve McCartney for his help with SEM, Dr. Jim Fuller, Rick Caudill, and David Jones all of the Brooks Forest Products Center for their various contributions towards the successful execution of this research. Sudipto Das (PhD student) and Dr. Francisco Fraguela Lopez Suevos (aka Fuco), your help with DMA data analysis is greatly appreciated.

Finally, I would like to thank our Department Head, Dr. Paul Winistorfer as well as all faculty and staff members of the Wood Science and Forest Products Department of Virginia Tech. whose dedication to duty and desire for excellence has made the study of Wood Science in Virginia Tech a truly worthwhile experience for me. God bless you all.

Table of Contents

List of Figures

List of Tables

1 Introduction

For many years, lignocellulosic fillers such as powdered cellulose (from the paper industry) and wood flour (from the wood processing industry) have been used as low-cost extenders in thermosetting polymers, particularly phenolic resins [1, 2]. However, in recent years, research into the use of lignocellulosic fibers for reinforcement in thermoplastics has increased significantly. The positive impact of such sustained research is evident in today's increasing demand and expanding applications for lignocellulosic fiber-filled thermoplastics by the transportation, housing, infrastructure, industrial, and consumer products sectors [3]. Lignocellulosic fibers possess many advantages such as lightweight (low density), non-abrasiveness to processing equipment, high specific strength (strength to density ratio), renewability, biodegradability, affordability and availability. These qualities make them attractive alternatives to synthetic fibers, particularly for short fiber-reinforced thermoplastic products, which are generally designed for low to moderate mechanical performances. According to Kardos [4], mechanical property performances of short fiber-reinforced polymer composites are bounded on the lower and upper limits by particulate (sphere)-filled and continuous fiber-reinforced systems respectively. Despite the stated benefits, lignocellulosics remain underutilized as reinforcing fibers in composites industry because of certain practical problems associated with their use. Some of these are common to all lignocellulosic materials and include thermal instability of cellulose at elevated temperatures (> 200oC) [2], high moisture absorption (from high concentration of polar hydroxyl groups on cellulose), and incompatibility with common hydrophobic thermoplastics (particularly polyolefins). Furthermore, short lignocellulosic fibers, mostly wood fibers, suffer from low aspect (fiber length to diameter) ratio, surface roughness, and non-uniformity in shape and length. These limitations tend to pose challenges for the use of wood fibers as reinforcements in thermoplastic polymers. Several examples can be found in the literature where attempts to use wood fibers as reinforcements in commodity thermoplastics like polyethylene (PE), polypropylene (PP), polyvinyl chloride (PVC), and polystyrene (PS) have resulted in composites with improved moduli but reduced strengths compared with the matrix polymer [5, 6]. Strength deterioration in these situations result mainly from poor stress transfer, which in turn result from such factors as poor fiber dispersion, poor fiber-matrix adhesion, and low fiber aspect ratio among others. Also worthy of

note is the fact that preferred compounding methods for short fiber-reinforced thermoplastics such as extrusion and injection molding often lead to fiber breakages and further decrease fiber aspect ratio [4].

Remedies to the above problems include, 1) chemical modification of fiber surfaces such as acetylation of cellulose fibers [7], use of coupling and dispersion agents e.g. silanes, isocyanates, carboxylic waxes, and maleic anhydride-grafted polypropylene (MAPP) [2, 5, 8]; and 2) physical treatments such as corona discharge, calendaring, cold plasma treatment, thermotreatment, and fiber hybridization [9]. Chemical modification represents the most common approach to improving composite properties due to its effectiveness and ease of application. It however introduces additional costs and is also limited in flexibility (limited control over composite properties). Fiber hybridization is one suitable method of developing composites with properties that can be tailored to suit specific requirements [10].

Fiber hybridization involves blending two or more fibers together in a common matrix to generate a composite with a balance of properties that cannot be achieved when the individual fibers are used separately. Through hybridization, the beneficial properties of constituent fibers can be exploited while simultaneously mitigating their undesirable properties [10]. A hybrid composite typically combines a relatively expensive, high stiffness / strength fiber with a cheaper, relatively weaker one, which often contributes toughness and extensibility to the composite. Investigations into the use of lignocellulosic and glass fibers to create low-cost, lightweight hybrid composites of improved mechanical properties have been performed with wood pulp (chemithermomechanical pulp [CTMP]) [11], sawdust [12], bamboo [13], and other natural fibers in polyolefin matrices. Moduli and strengths of such hybrid composites have generally been observed to increase with increasing glass fiber content. Reasons for such observations include greater stiffness and strength as well the uniform morphological properties of glass compared to lignocellulosic fibers. Moisture sorption properties of hybrid composites such as weight gain and dimensional instability have also been found to decline with addition of glass fibers [11]. Failure strains on the other hand, have been found to increase with increasing lignocellulosic fiber content due to the greater flexibility of lignocellulosic fibers.

An important approach to characterizing polymers and polymer composites is to consider their time and temperature dependent behaviors. Polymers undergo thermal transitions such as the glass transition wherein amorphous components undergo large scale molecular motions

leading to drastic property changes over very narrow temperature ranges. Dynamic mechanical analysis (DMA) represents one comprehensive way to monitor changes in polymer mechanical and physical properties. Through DMA, viscoelastic functions like storage modulus and damping of a polymer or polymer composite can be continuously measured as a function of frequency (or time) and temperature. For lignocellulosic fiber-filled thermoplastics, the practical significance of having such knowledge can be appreciated from their increasing applications in the automotive and building industries where vibrations and temperature variations are likely to be encountered.

Research Objectives

In this study, the possibility of improving composite properties through hybridization of two cellulose–based fibers was investigated. Low concentrations of lyocell (a high cost, high performance regenerated cellulose fiber) were blended with cheaper steam-exploded red oak (*Quercus rubra)* fibers (in higher concentrations) in a PP matrix. The mechanical, dynamic mechanical, and sorption properties of the hybrid composites were evaluated and compared with non-hybrid (SEW/PP and lyocell/PP) controls. Specifically, the effects of fiber composition on hybrid composite properties were evaluated and compared with those of non-hybrid controls. The random wetlay process, an alternative compounding process that maximizes fiber dispersion and eliminates fiber attrition was used.

2 Literature Review

2.1 Lignocellulosic Fibers

Natural fibers are broadly classified according to origin. They may be obtained from plant, animal or mineral sources [14, 9]. In practice however, plant or lignocellulosic (so called because of their cellulose and lignin contents) fibers represent the most commonly used natural fibers for thermoplastic reinforcement. Plant fibers are themselves composite materials comprised of three major constituents namely cellulose, hemicelluloses, and lignin. Cellulose is a linear high molecular weight polysaccharide constituted of D-anhydroglucopyranose units joined together by β-1,4-glycosidic bonds [15]. Within the plant cell wall, cellulose molecules exist as semicrystalline chains held together strongly by hydrogen bonds. Hemicelluloses are relatively low molecular weight polysaccharides (with average degrees of polymerization of about 200) and are comprised primarily of D-glucose, D-mannose, D-xylose, D-galactose, and L-arabinose while lignin exists as a high molecular weight polymer made up of phenylpropane units [15]. Lignin and hemicelluloses serve as amorphous matrices in which the cellulose microfibrils are embedded. Cellulose contributes primarily to cell wall stiffness and strength while lignin imparts toughness and is primarily responsible for the rigidity of the plant cell wall [16].

The physical and mechanical properties of lignocellulosic fibers vary widely according to plant type and origin as exemplified by a selected few in Table 2.1 [17].

Table 2.1 Physical and mechanical properties of selected plant fibers [17]

Fiber	Density (g/cm^3)	Stiffness (GPa)	Tensile Strength (MPa)	Elongation at break, %
Flax	1.5	28.5	351.6	2.5
Hemp	1.48	29.6	820.5	3.5
Jute	1.5	26.2	579.2	1.5
Sisal	1.45	17.2	524	2.8
Cotton	1.5 – 1.6	8.2	551.6	5
Softwood Kraft pulp	1.5	40.0	1000	-

Lignocellulosic fibers have several beneficial characteristics that have made them attractive

alternatives to synthetic fibers. They are lighter than glass fibers, which offer a potential for less fuel consumption when used in automobile parts [14]. For example, it was found that replacing glass fibers with lignocellulosic fibers in car door panels led to weight savings of about 4 kg [14]. Lignocellulosic fibers are non-abrasive. The wearing of equipment parts that is common with the use of synthetic fibers such as glass is significantly reduced with the use of natural fibers [14,18]. Lignocellulosic fibers also possess high specific properties (property to density ratio) due to their relatively low densities [19]. They are also renewable and affordable [14, 18, 20].

These advantages notwithstanding, lignocellulosic fibers pose some important challenges to their potential for increased usage in thermoplastics. One important limitation of lignocellulosic fibers is low thermal resistance. Lignocellulosic fibers have a potential to chemically degrade and/or emit volatiles around 200^{o}C [21], thus limiting their use to commodity thermoplastics usually polyolefins e.g. polyethylene (PE) and polypropylene (PP) [9]. Another source of concern for lignocellulosic fibers is their hygroscopic character, which is attributed to the high concentration of hydroxyl groups in their constituent polymers. This leads to problems of dimensional instability and weight gain in composites [21]. Sorption problems have been successfully controlled by fiber modification techniques such as acetylation [7] and the use of coupling agents such as silanes and maleic anhydride grafted PP (MAPP) [22]. These remedies, however, come with increases in production costs.

2.2 Lignocellulosic Fiber-Reinforced Thermoplastics

On a total volume basis, the bulk of reinforcing fibers used in thermoplastic composites comes from synthetic sources, with glass, carbon, and aramid (Kevlar) fibers accounting for over 95% of the industrial market [24]. However, in recent years, particularly in the last 15 to 20 years, research into lignocellulosic fiber-reinforced thermoplastics has grown rapidly due to increasing demand for lignocellulosics as alternative fibers in automotive parts and building materials [14, 3]. The automotive and building materials industries of Europe and North America respectively represent the fastest growing segments in demand of lignocellulosic fiber-reinforced thermoplastic composites [14, 3]. For example, European automotive industry consumption rose from 7,000 tons in 1996 to 22,000 tons in 2000 [14], while total US consumption reached 590,000 tons in 2002 with over 80% of this quantity going to the building industry [3]. Tables

2.2and 2.3 respectively list some vehicle brands utilizing lignocellulosic fiber-filled thermoplastics and typical weights of fiber used per vehicle part [14].

Table 2.2 Vehicle Brands and their Components Utilizing Natural Fiber Composites adapted from Suddell and Evans [14]

Brand	Components
Audi	Seat backs, side and back door panels, trunk lining, hat rack, spare tire lining
BMW	Door panels, headliner panel, trunk lining, seat backs
Daimler-Chrysler	Door panels, windshield / dashboard, business table, pillar cover panel
Fiat, Ford	Door panels, B-pillar, trunk liner
Peugeot, Renault, Rover	Insulation, rear storage shelf / panel
Saab, SEAT, Opel GM	Headliner panel, door panels, pillar cover panel, instrument panel
Volkswagen, Volvo	Door panel, seat back, trunk lid finish panel, trunk liner

Table 2.3 Typical Weight of Natural Fibers Used per Vehicle – adapted from Suddell and Evans [14]

Part	Weight used
Front door liners	1.2 to 1.8 kg
Rear door liners	0.8 to 1.5 kg
Trunk liners	1.5 to 2.5 kg
Parcel shelves	< 2 kg
Seat backs	1.6 to 2 kg
Sunroof interior shields	< 0.4 kg
Headrests	~ 2.5 kg

2.2.1 Properties of Lignocellulosic Fiber-Reinforced Thermoplastics

The properties of lignocellulosic fiber-reinforced composites depend on the properties of the constituent materials (fibers and matrices) as well as the compounding and consolidation methods used. Some important properties of lignocellulosic fiber-reinforced composites are

discussed next.

2.2.1.1 Mechanical Properties

Mechanical properties are generally regarded as the most important properties of polymer composites since they represent the ultimate performance measurement criteria for a given end-use [1]. Many studies on composites characterization have involved strength, modulus, impact resistance, and fracture properties. Most lignocellulosic fiber-polymer composites fall under short fiber-reinforced systems due to length limitations of natural fibers. The mechanical properties of lignocellulosic fiber-reinforced thermoplastics are controlled by many of the factors that affect discontinuous fiber-reinforced composites. These factors include:

1) Fiber concentration
2) Fiber dispersion
3) Fiber length and fiber length distribution
4) Fiber aspect ratio
5) Fiber orientation
6) Fiber-matrix adhesion
7) Fiber strength properties
8) Matrix strength properties

2.2.1.2 Dynamic Mechanical Properties

Dynamic mechanical analysis is a technique used to measure the response of a material under a sinusoidal or other periodic stress [25]. A polymer (or polymer composite) subjected to a sinusoidal stress would generate a corresponding sinusoidal strain response as long as a linear load-deformation relationship is maintained. Due to the viscoelastic nature of polymers, the applied stress and the strain response under dynamic deformation would exhibit a phase lag (or phase angle) (Figure 2.1) between them. The magnitude of the phase lag (δ) would depend on the relative proportions of the viscous and elastic components as well as the test conditions. The dynamic modulus for such a system is represented as a complex modulus (E^*) that can be further resolved (as a vector) into a storage modulus – E' (a measure of system's ability to store energy) and a loss modulus – E'' (a measure of the system's ability to dissipate energy in the form of heat) (Figure 2.2). From Figure 2.2, the ratio E'' to E' gives $\tan \delta$ (loss factor), which measures the damping ability of the material. Dynamic mechanical analysis is a sensitive technique for measuring changes in polymer properties as a function of temperature or frequency (time). The

glass transition, for example, is a significant thermal transition, which involves drastic changes to polymer physical and mechanical properties as polymers interconvert between glassy and rubbery states. According to Menard [26], the glass transition temperature (T_g) of a polymer (or polymer composite) defines one end of its usable range also known as its operating range.

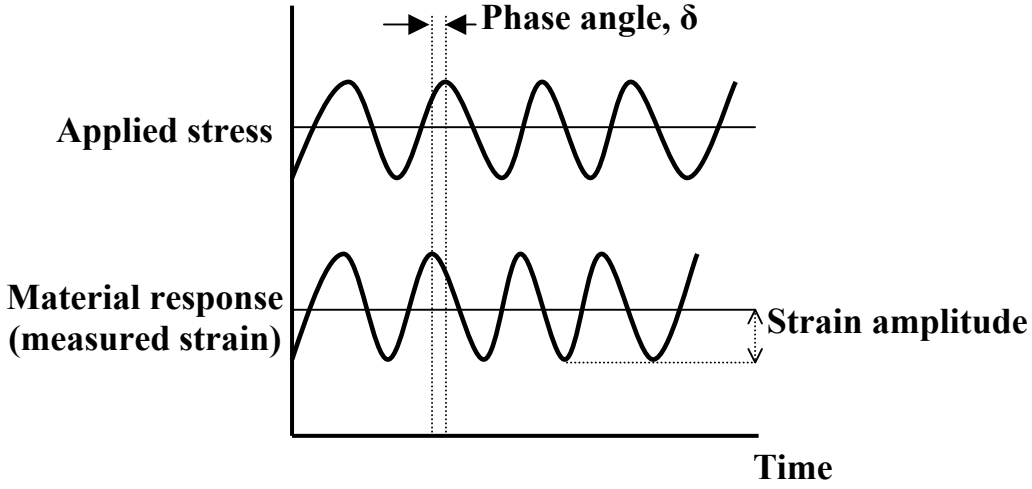

Figure 2.1 Schematic representation of dynamic stress-strain relationship of a viscoelastic material under sinusoidal deformation

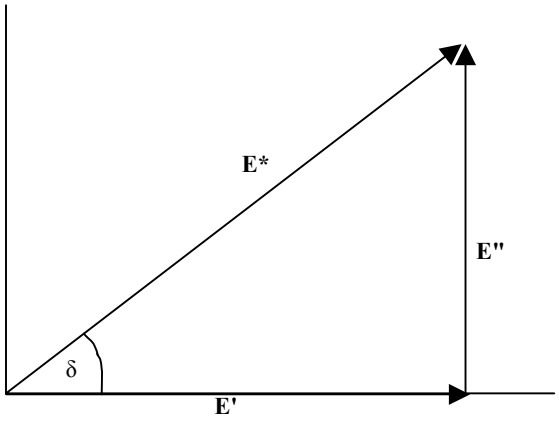

Figure 2.2 Vectorial resolution of modulus components for a viscoelastic material under sinusoidal deformation

2.2.1.3 Long Term Viscoelastic Properties – Time -Temperature Superposition (TTS)

Time-temperature superposition is an empirical technique used to predict the frequency

(time)-dependent viscoelastic properties of polymers as a function of temperature. It is based on the observation that curves representing the viscoelastic properties of a single material, determined at several temperatures, are similar in shape when plotted against a log time or log frequency axis [23]. This time-temperature equivalence therefore makes it possible to obtain exact superposition of the property-frequency (time) curves at different temperatures through horizontal curve shifting along the frequency (time) axis. The curves may be shifted with respect to a reference temperature (usually considered to be valid up to $T_g + 100^oC$ [23]) to obtain a master curve. The practical significance of TTSP as pointed out by Chartoff [23] are; a) it allows data measured over limited time scales to be used to predict viscoelastic properties over extended time scales, which otherwise cannot be accessed through experiments, and b) shift factors (the amounts of horizontal shifting) can be used to estimate viscoelastic properties at different temperatures from the master curve of a single temperature. This is done by shifting the entire master curve for the original reference temperature by an amount corresponding to the shift factor of the desired reference temperature. TTSP has been applied to natural composites such as ethyl formamide-plasticized wood [24], and synthetic composites such as glass filled phenolics (resol and novolacs) [27].

2.2.1.4 Sorption Properties

Due to the hygroscopic nature of lignocellulosics, considerable attention must be paid to the moisture absorption characteristics of lignocellulosic fiber-reinforced composites. The equilibrium moisture content of lignocellulosic fibers have been reported as ranging from 8 to 12 % at 65 % relative humidity [17]. Water interferes with fiber-matrix interaction by occupying the interfacial regions within the composite [21]. Some composite mechanical properties such as strength and impact resistance can be reduced in the presence of moisture. Moisture absorption in lignocellulosic fiber-plastic composites generally increases with increasing fiber content [22], however, it can be minimized by fiber surface treatments such as acetylation [7] and grafting with polymer chains [27].

2.3 Cellulose Fiber Options for Reinforcement in Thermoplastics

2.3.1 Fiber Sources

The lignocellulosic fibers used in thermoplastic reinforcements originate from agricultural crops (agro fibers) or woody plants (wood fibers). With respect to worldwide consumption of

cellulose fibers in composites, the use of wood fibers surpasses that of agro-based fibers, but in countries where wood supply is low or government legislation limits access to forest resources, agro-based fibers will be the primary source of fiber supply [28].

Agro fibers commonly used in thermoplastic reinforcement are classified as bast, leaf, or seed-hair fibers according to their origin in the plant [18]. Bast fibers are rigid elongated stem cells that provide support for many dicotyledonous plants. Examples include flax, hemp, ramie, jute, and kenaf. Leaf fibers originate in elongated leaves of most monocotyledonous plants, and like bast fibers serve as supporting tissue for the leaves in which they are found. Examples include sisal and abaca. Seed-hair fibers are single-celled fibers attached to some plant seeds and assist in wind dispersal e.g. cotton, milkweed, and kapok [18]. Many of the annual agro-fiber crops such as jute and kenaf are cultivated purposely for their fiber. Others such as cereal stalks and sugarcane bagasse emerge as by-products of food crops but also represent important agro-based fiber sources [18].

Much of the cellulose fibers used in thermoplastic reinforcement are products of the two main pulping processes namely chemical pulping and mechanical pulping [2]. Both wood and agro fibers can be refined by either of these processes. Chemical pulping processes such as the Kraft process involve the dissolution of lignin and usually lead to high quality pulps that are nearly pure cellulose [2]. Mechanical pulping on the other hand, involves mechanical separation of wood into fibers, sometimes with the aid of heat or chemical additives [2]. Mechanical pulp fibers retain most of their lignin and natural waxes, which result in high pulp yields (95%) as opposed to Kraft pulps yields of about 60% [2]. Other methods of fiber separation such as retting (for bast fibers e.g. jute and kenaf), [18] and steam explosion pulping [19] have also been used.

2.3.2 Regenerated Cellulose Fibers

Generally, cellulose may be chemically modified into cellulose derivatives (ethers and esters) or regenerated cellulosics, which may be processed into fibers, films, membranes, food casings, and so on [29]. Regenerated cellulose fibers are made by dissolving cellulose pulp in an appropriate solvent to form a homogenous solution, followed by spinning (or regeneration) of the cellulose out of solution. The process leads to alteration of the native cellulose (cellulose I) structure into the regenerated (cellulose II) structure. Several different regenerated cellulose processes have been developed over the years, the most popular and most utilized one being the

viscose process for the production of rayon fibers [30]. More recently, the amine oxide or lyocell process has been used to produce highly crystalline, high stiffness / strength cellulosic regenerates generically referred to as lyocell fibers [29, 31, 32].

Lyocell is produced by regeneration of dissolving pulp from an amine oxide organic solvent known as *N*-methylmorpholine-*N*-oxide (NMMO). The production process involves the dissolution of dissolving grade cellulose pulp in hot aqueous NMMO followed by spinning of the dissolved pulp into fibers by dry jet wet spinning [31]. The process leads to a greater than 99% solvent recovery and is environmentally safe due to the non-toxic nature of the solvent and effluents discharged [31]. Lyocell fibers are highly crystalline and possess superior mechanical properties compared to other regenerated cellulose fibers (Table 2.4) [30]. Lyocell fibers are mainly used in the textile industry but technical fibers have also been developed for the production of paper and non-woven textiles.

Table 2.4 Some Physical and Mechanical Properties of Viscose and Lyocell [30]

Property	Viscose	Lyocell
Water imbibition, %	90 – 100	65 – 70
Tenacity, mN / tex:		
Dry	200 – 240	400 – 440
Wet	100 – 150	340 – 380
Extensibility at break, %		
Dry	20 – 25	14 – 16
Wet	25 – 30	16 - 18
Initial wet modulus, mN/tex	400 – 500	2500 – 2700
Degree of polymerization	250 – 350	550 – 600

Up to date, very few studies have been performed on lyocell fiber-reinforced thermoplastic composites. Of these, a series of investigations on continuous lyocell fibers in (biodegradable) cellulose ester matrices undertaken at the Biobased Materials / Recycling Center of Virginia Tech represent the most comprehensive. The research involved the characterization of lyocell – thermoplastic composite mechanical properties through manipulations of the following

parameters; a) compounding methods [33], b) fiber surface chemistry and composite consolidation conditions [34], and c) cellulose ester matrices [35]. The authors reported significant increases in composites tensile strength (more than three fold at 60 wt % lyocell) and modulus (25 fold at 60 wt. % lyocell) compared with unfilled cellulose ester. Elongation at break was however observed to decrease significantly with fiber loading. The best composite properties were realized with the use of fiber impregnation in matrix solution at optimal processing conditions of 200 ^{o}C, *ca* 80 KPa, and a pressing time of 13 minutes. Neither acetylation nor matrix type were found to have significant effects on mechanical properties. The authors concluded that solution impregnation of lyocell fiber tows produced the most uniform composites. Furthermore, adequate fiber-matrix adhesion could be achieved in this class of composites with or without surface modification.

2.3.3 Steam Explosion

Steam explosion pulping is a useful method for separating lignocellulosic materials (including wood) into cellulose-rich fibers and other lignocellulosic components such as xylose and lignin. The process involves high temperature cooking of lignocellulosic material under steam pressure, followed by explosive decompression [36]. Steam under high pressure and temperature penetrates the core of the material (wood chips) and softens the cell binding material. The sudden release of steam pressure (explosion step) to atmospheric conditions causes wood defiberization due to the rapid escape of built up steam from within the wood. The explosion process is characterized by a combination of physical and chemical actions to disintegrate the lignocellulosic material. The products of steam explosion may be directly utilized, extracted by water-washing or by other solvents such as aqueous alkali solvents [37]. Steam explosion pulping has been generally described as an energy efficient, environmentally friendly and cost effective alternative to conventional pulping processes [36, 38].

Studies on SEW fiber-reinforced thermoplastic composites have yielded some conflicting results with respect to the effect of SEW on ultimate strength. Polypropylene-based composites reinforced with steam-exploded hemp [39] and softwood [40] fibers, and tested at various fiber loadings, resulted in decreases in ultimate tensile strength with increasing fiber content. This was attributed, in both cases, to poor fiber-matrix adhesion. However, with the addition of a coupling agent (maleic anhydride-grafted PP (MAPP)), ultimate strengths of steam-exploded hemp-PP

composites increased up to the maximum (30 wt. %) fiber loading whereas those of steam-exploded softwood-PP decreased initially before increasing with further fiber loading. Glasser *et al.* [6], in their studies with steam-exploded Yellow poplar *(Liriodendron tulipifera)* fiber-reinforced cellulose ester composites observed that tensile strengths of untreated, water-washed, and alkali-extracted composites declined with increasing fiber content while those of acetylated fiber composites increased with increasing fiber content. The authors attributed the strength increases in the latter to superior interfacial adhesion between acetylated fibers and matrix molecules. In contrast to the above trends, Takatani *et al*. [41], observed that ultimate bending strength of steam-exploded beech flour-reinforced PVC and PS composites increased with increasing fiber loading even without additional fiber modification. Comparing various composites at similar fiber loadings, the group observed improvements in ultimate strengths of SEW/wood flour/thermoplastic blends over those of wood flour/thermoplastic alternatives. It was concluded that steam-exploded beech flour increases strength properties of woodflour-thermoplastic composites.

With regard to moisture absorption behavior of SEW, Angles *et al.* [42] performed a series of experiments on binderless SEW panels (panels pressed without addition of polymer matrix) and showed that sorption behavior of SEW depended on the severity of steam explosion as well as panel consolidation temperature and time. They observed that moisture sorption decreased with increases in all three processing parameters, and that there exist some optimum pressing temperatures and severity factors at which moisture sorption of the binderless composites stabilizes.

2.3.4 Hybrid Composites

Composites in which two or more fibers have been used as reinforcement in a common matrix are referred to as hybrid composites [1,10]. The basis for fiber hybridization is to optimize the different contributions to composite properties from different fibers while minimizing their undesirable properties [1]. Another important driving force for hybridization is minimization of cost, which can be very substantial when high performance fibers are used alone in composites. Hybrid composites of glass and carbon fibers have been studied extensively for possible use in high performance applications where weight reduction and cost savings are desirable [1]. In such systems, carbon fibers offer stiffness, strength and weight reduction

whereas glass fibers impart toughness, deformability and cost savings. Bunsell and Harris [10] mentioned another benefit of hybridization as the ability to tailor composite properties to match specific performance requirements. Several studies on glass-carbon fiber and glass-lignocellulosic fiber hybrid composites can be found in the literature. A few cases of the latter class of composites will be briefly discussed.

Maldas and Kokta [11] investigated the effects of fiber ratio and fiber surface modification on the mechanical and sorption properties of glass / CTMP fiber-reinforced PS composites that were compounded by melt mixing and consolidated by compression molding. Poly (methylene) poly (phenyl isocyanate) (PMPPIC) and a silane were used as coupling agents. Significant interactions were observed between fiber ratio and coupling agent with respect to ultimate tensile strength, Young's modulus and elongation at break. While strength properties of PMPPIC-treated composites increased with decreasing glass fiber content, those of silane treated composites exhibited an opposite effect. Moisture absorption for all composites, however, decreased with increasing glass fiber content.

Another study [13] involving bamboo / glass fiber-reinforced PP composites showed a clear pattern of increasing mechanical properties with glass fiber content. Greater gains in mechanical properties were obtained when maleic anhydride grafted PP (MAPP) coupling agent was added to the hybrid systems.

3 Experimental

3.1 Materials

3.1.1 Lyocell fibers

Chopped lyocell fibers were supplied by Acordis, Coventry, U.K. The fibers, marketed as Tencel® and used mainly for garment manufacture have the following manufacturer-supplied properties:

Dry tenacity (strength)	4.5 – 5.0 g/denier[1] (*ca* 500 – 550) MPa
Wet tenacity	3.9 – 4.3 g/denier (*ca* 430 – 475) MPa
Extensibility at break (dry)	(14 – 16) %
Extensibility at break (wet)	(16 – 18) %
Length	10 mm
Diameter	10 μm
Water imbibition (dry fiber weight basis)	(65 – 70) %
Cellulose degree of polymerization (DP)	550 – 600
Cost per pound	$ 2.00

Figure 3.1 depicts an optical microscopic image of lyocell fibers used in this study.

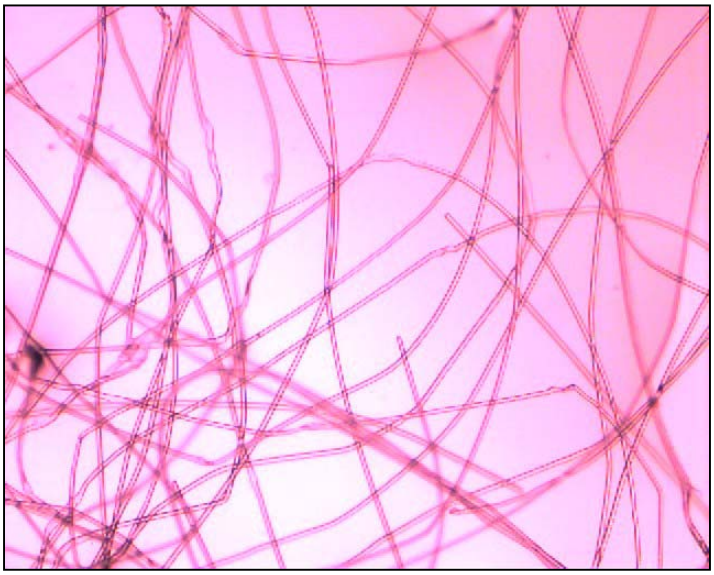

Figure 3.1 Optical microscope image of chopped lyocell fibers. Notice uniformity in fiber dimensions. Magnification = 40x.

[1] Grams per 9000 meters

3.1.2 Polypropylene

Two types of polypropylene (PP) were used in the study.

1) Commercial grade uncrimped 15 denier PP fibers, a product of average length 5 mm, diameter 4.83 μm, and melt flow index (M.I.) 40g / 10min (all manufacturer-supplied data) came from FiberVisions Incorporated (Covington, Georgia). The PP fibers were combined with lyocell fibers and used directly in the wetlay process (see section 3.2.2).
2) Laboratory grade high melt flow index (1000 g/10 min.) isotactic PP (HMiPP) granules were obtained from Aldrich Chemicals, St. Louis, Missouri. The HMiPP granules were co-steam-exploded with red oak chips (details in section 3.1.3).

3.1.3 Steam-Exploded Wood

Two types of steam-exploded materials were prepared and used for this study. The first was steam-exploded red oak fibers, designated SEW (Figure 3.2). The second was a co-steam-exploded blend of red oak and HMiPP. Co-steam explosion was used as an alternative compounding method aimed at improving fiber-matrix adhesion. The method involves the simultaneous explosion of wood and thermoplastic polymer to form a homogeneous wood-plastic mulch that can be compression molded. The process was used by S. Hunter Brooks and Associates [43] to produce a wood-plastic fiber mulch from a combination of chipped wooden pallets and post-consumer high density polyethylene (HDPE) tanks. The composite materials were successfully air-laid into mats as well as compression-molded into automobile door panels and shipping pallets. Research on the chemical characteristics of co-steam-exploded red oak and PP has already been undertaken at the Virginia Tech Department of Wood Science and Forest Products [44].

Steam explosion was performed in a two-cubic foot batch reactor (Figure 3.3) located in the Steam Explosion Pilot Laboratory at the Thomas M. Brooks Forest Products Center, Virginia Tech. Red oak chips of sizes 3.175 – 6.35 mm (1/8 – ¼ inch) were steam-exploded alone, and in combination with a high melt flow index PP (HMiPP) using equal parts by weight of wood chips and HMiPP. The use of HMiPP resulted in the best mixing of fiber and matrix after initial trials with PP fibers failed to produce a homogeneous wood-plastic blend. All materials were exploded

under fixed reactor conditions of 228°C in atmosphere (air) for 5 minutes, resulting in a steam explosion severity factor (log R_o) of 4.5. The optimal severity factor for red oak has been indicated elsewhere as 4.3 [45]. R_o is computed from the reaction temperature and retention time as follows [46]:

$$R_0 = \int_0^t \exp\left[\frac{T_r - T_b}{14.75}\right] dt \qquad (3.1)$$

where:

R_o = Steam explosion severity factor

T_r = Reaction temperature in °C

T_b = Base temperature (100°C)

t = Reaction time

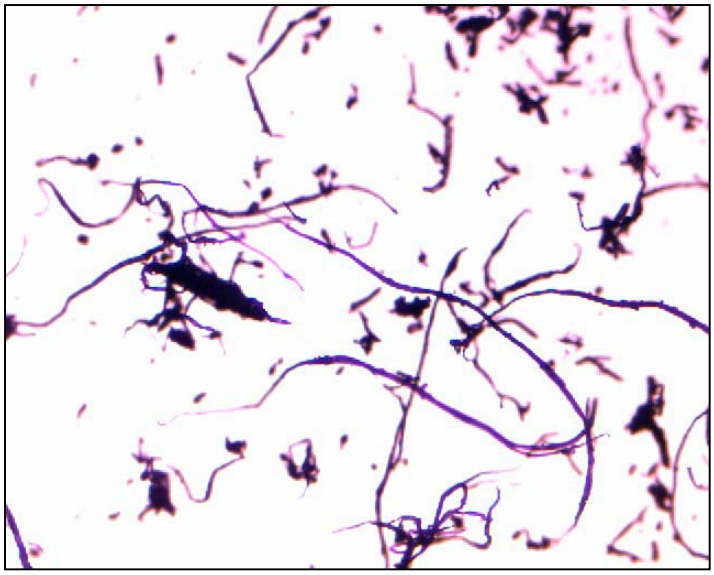

Figure 3.2 Optical microscope image of steam-exploded red oak fibers prior to wetlaying. Notice non uniformity in length and shape of fibers as well as presence of particles and fiber clumps. Magnification = 40x.

3.2 Methods

3.2.1 Solids Content Determination

Prior to compounding (by wetlaying – described under section 3.2.2), it was necessary to calculate the solids content of the steam-exploded materials since calculation of the wetlay slurry

composition was based on solid fraction. The solids content was calculated by weight difference after water solubles and moisture contents of the steam-exploded materials had been determined. Summarized below are the steps used in calculation of water solubles and moisture contents. The resulting mulch compositions are shown in Table 3.1.

Figure 3.3 Steam explosion batch reactor

1. **Reaction chamber**
2. **Steam duct from boiler**
3. **Metal pipe for transfer of steam-exploded material to collector**
4. **Cyclone**
5. **Funnel for guiding raw material into reactor**
6. **Steam vent (to atmosphere)**
7. **Collection bin**

3.2.1.1 Water Solubles Content

Water solubles content was determined by means of a simple laboratory filtration setup comprised of a Buchner funnel, filter paper, Erlenmeyer flask and aspirator. The samples were dried to constant weight (at 105^{o}C) prior to filtration. The residues were rinsed repeatedly with water until the characteristic color of the filtrate had faded significantly, indicating the removal of as much water soluble material as possible. The water solubles content was then calculated by weight difference after the residue had been redried to constant weight. Values shown represent averages of three replications per sample.

3.2.1.2 Moisture Content

Moisture content (MC) was determined after drying steam-exploded samples (~ 10g / batch) in an Ohaus MB 200 moisture balance (Figure 3.4) using a three-step temperature program (manufacturer recommended). The three-step drying program is an automated drying schedule in which the sample is heated in steps starting from the highest to the lowest temperature. The steps used here were 130-, 120-, and 115^{o}C at (10 minutes per step) to give total drying time of 30 minutes. The MC was obtained by direct reading from the instrument panel. The results shown in Table 3.1 represent averages of three replications per sample.

Table 3.1 Composition (weight %) of steam-exploded materials

Material	Solids content, %	Water solubles content, %	Moisture content, %
SEW	18.60	3.90	77.60
Co-SEW / iPP	40.35	3.25	56.40

3.2.2 Compounding – The Random Wetlay Process

The random wetlay (papermaking) process, patented by Geary and Weeks [47] and assigned to the DuPont Company was employed for compounding. The process achieves intimate mixing of reinforcing and matrix (thermoplastic) fibers to form a wet sheet that is subsequently transformed into a rigid self-supporting sheet after melting of the matrix fibers.

The wetlay process starts with a dilute aqueous slurry of reinforcing and matrix fibers. The slurry is fed at controlled rates into a highly specialized headbox where the composite sheet formation begins. In the headbox, the fiber mixture is dispersed onto a wire screen (wetlaying) to form a continuous mat of randomly oriented fibers. The wet mat is drained of excess water while

being transported over a series of vacuum extractors. The dewatered mat is then conveyed into a convection oven (heated above the melting temperature (T_m) of the matrix) where the matrix fibers fuse into numerous tiny beads and bind the reinforcing fibers together. The resulting nonwoven sheet is then rolled onto a spool for storage and subsequent use. Advantages of the random wetlay process include efficient fiber dispersion, absence of fiber attrition, and indefinite shelf (storage) life of preimpregnated thermoplastic sheets [48]. The materials for this study were wetlaid at the Virginia Tech – DuPont Random Wetlay Composites Laboratory, Virginia Tech. A general wetlay process has been described in Figure 3.5 below. Also shown in Figure 3.6 is a scanning electron microscopic image of a wetlaid sheet from this study.

Figure 3.4 Ohaus MB 200 moisture balance

a. Pulper: Vigorous agitation of aqueous suspension (slurry) of reinforcing & matrix fibers (≤ 0.5% by volume). Viscosity modifier (thickener) is added to maintain fiber suspension. Surfactant or antifoam may be added to improve fiber dispersion.

b. Stock tanks. Slurry is pumped from pulper into stock tanks and continuously agitated to maintain fiber suspension until ready to use.

c. **Whitewater tank.** Holds whitewater (water + viscosity modifier) for controlled release (by gravity) into headbox. Essential for maintaining uniform mat properties.

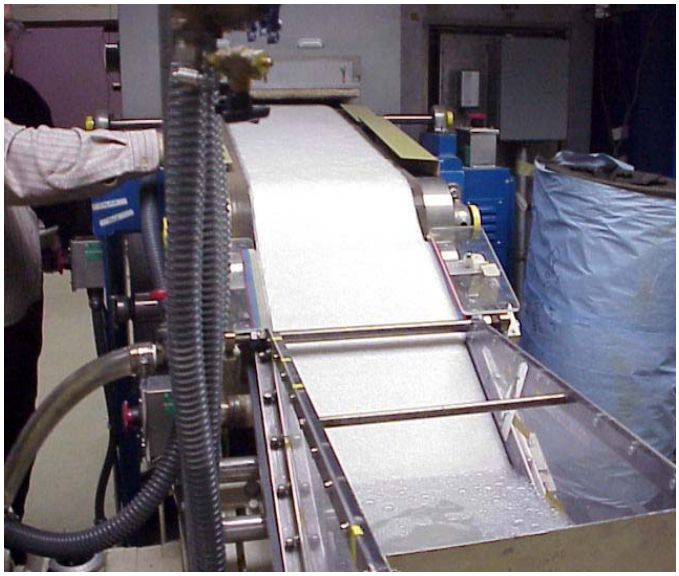

d. **Inclined wire wetlay machine:** Produces randomly oriented mat of reinforcing and matrix fibers from aqueous slurry. The mat is rapidly de-watered with a vacuum pumping system (whitewater filtered through wire mesh via vacuum extraction) leading to mat formation.

e. **Convection dryer**: Ten-foot-long convection dryer heated above polymer T_m fuses polymer fibers into tiny beads that hold reinforcing fibers together in the mat

f. **Storage core.** Finished product is rolled up onto a spool.

Figure 3.5 a – f Summary of Random Wetlay Process at the Va Tech – DuPont Random Wetlay Composites Laboratory [48]. Images were posted by the lab manager, Joseph Price O'Brien

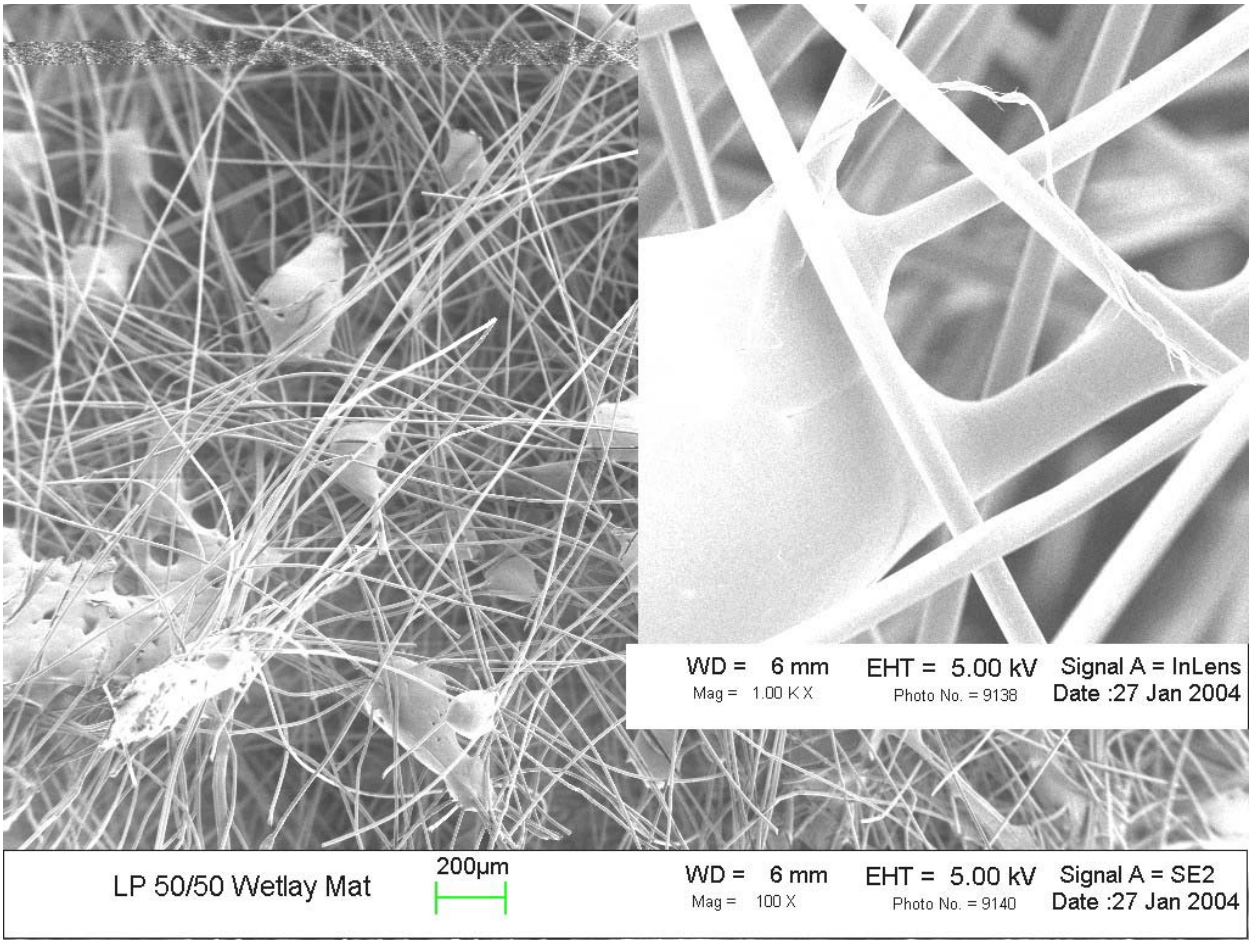

Figure 3.6 Scanning electron micrograph of LP 50 wetlaid sheet. Notice retention of fiber lengths and wetting of fibers by matrix (highlighted in insert by low fiber-matrix contact angles)

3.2.3 Wetlay Composition Calculations

Slurry compositions were varied as needed to obtain the required reinforcement / matrix ratios for wetlaying. Each of the fiber / matrix combinations used for the study was wetlaid in a single batch having a total solids content of 500 grams. For each composition, the weight percent of each component was adjusted for the total and measured accordingly. For example, a one to one ratio of lyocell fibers to PP fibers required 250 g of each material.

In the case of co-steam-exploded material, initial attempts at wetlaying were unsuccessful due to the presence of wood-plastic clumps that could not be easily defiberized in the slurry. The clump sizes were reduced after blending the co-steam exploded mulch in a laboratory blender for 5 minutes, prior to wetlaying. To ensure the formation of a continuous sheet, 10 wt. % of lyocell

fibers were added to the co-steam exploded material before wetlaying. The added lyocell served as carrier fibers because the mulch fibers alone were not long enough to form the web necessary to generate a continuous sheet.

Table 3.2 shows weight fractions of the fiber-matrix compositions used for this study. (The actual measured weights are shown in the Appendix).

Table 3.2 Weight fractions and compositions of materials studied

Label	Constituent Materials		
	Steam-exploded wood (SEW) content (wt. %)	Lyocell content (wt. %)	Polypropylene content (wt. %)
PP	-	-	100
SP 50	50	-	50
LP 25	-	25	75
LP 35	-	35	65
LP 50	-	50	50
LP 65	-	65	35
SLP 45/5	45	5	50
SLP 40/10	40	10	50
SLP 35/15	35	15	50
SLP 30/20	30	20	50
COSLP	45	10	45

PP: Polypropylene
SP: SEW / PP
LP: Lyocell / PP
SLP: Lyocell / SEW / PP
COSLP: Co-(SEW / PP) / Lyocell

3.2.4 Sample Preparation

Wetlaid sheets were compression molded into plaques from which test specimens were cut. The procedures for plaque pressing and test specimen preparation are described below.

3.2.4.1 Compression Molding

Wetlaid sheets were cut to fit in a square steel mold of dimensions 152.4 mm * 152.4 mm (6 inch * 6 inch). To ensure balance of plaque properties, adjacent sheets were rotated through a 90^{o} angle during lay-up. The laid up sheets were compression-molded (under heat) in a Carver Laboratory Press Model C using a consolidation temperature of 180 ± 2ºC (to ensure complete

melting of the matrix) and a pressure of 4.65 MPa, which was the maximum pressure possible with the press. Enough material was used to obtain a consolidated plaque thickness of *ca* 3.2 mm (1/8 inch), which was the ASTM [49] recommended specimen thickness for thermoplastic and thermosetting polymer materials.

A steel plunger was then inserted in the mold (loaded with sheets) and mounted in the press at room temperature. Samples were heated at a controlled rate (with the help of variacs) to ensure uniform heat transfer from platens to all parts of the mold. A minimum amount of pressure (just enough for the composite to maintain contact with the mold) was applied during the heating step. Once the consolidation temperature was reached, the pressure was increased to the maximum and held there while a combination of air and water- cooling was applied to bring the sample down to room temperature. An initial air-cooling that was applied prior to water-cooling was to minimize excessive vaporization of water going through the hot platens at the high consolidation temperatures. Samples for dynamic mechanical analysis were consolidated under rigorous temperature control to obtain identical thermal histories.

3.2.4.2 Specimen Cutting

Specimens for stress-strain testing were cut with a diamond saw to minimize specimen variation. All specimens were cut in accordance with recommended ASTM standards dimensions (see section 3.2.5.1). Six tensile and seven flexural specimens were obtained from each plaque.

Dynamic mechanical test specimens were cut with a fine band saw since a diamond saw was unavailable at the time. To obtain uniform specimen dimensions, specimen edges were sanded with a smooth sandpaper after rough sawing.

3.2.5 Testing

Stress-strain (tensile and flexural) tests were first performed on all composites according to ASTM standards (see section 3.2.5.1). Dynamic mechanical analysis was performed on selected hybrid composites and non-hybrid controls. Also measured were sorption properties of all composites using a 24 hour-water soaking test. Details of testing procedures are described in the following sections.

3.2.5.1 Stress-Strain Testing

Flexural and tensile properties tests followed ASTM D790 (Standard Test Methods for Flexural Properties of Reinforced and Unreinforced Plastics and Insulating Materials) [49] and

ASTM standards D 3039C 3039M 95a (Standard Test Methods for Tensile Properties of Polymer Matrix Materials) [50] respectively. Tensile testing was performed on a United Calibration Corporation Model SFM-100KN testing machine equipped with a 20,000 N load cell and a computer for data acquisition. The constant head-speed option was used at a crosshead speed of 2 mm / minute. Strain was measured with an extensometer attached to the sample midsection. Average dimensions of tensile specimens were (152.4 * 12.7 * 3.175) mm. (6 * 0.5 * 0.125) in. Flexural tests were performed at a strain rate of 0.01 mm/mm/min (according to procedure A in the standard) on an MTS testing machine. Average dimensions for flexural specimens were (50 * 12.7 * 3.175) mm. (1.97 * 0.5 * 0.125) in. Prior to testing, all specimens were conditioned in a humidity chamber at 50 ± 10 % relative humidity and 23 ± 3°C in accordance with ASTM recommendations [49]. The tensile and flexural properties were computed using equations (3.2) to (3.6) below.

Tensile modulus of elasticity :

$$E = \frac{\Delta \delta}{\Delta \varepsilon} \qquad [3.2]$$

where: E = Elastic modulus (MPa),

$\Delta\delta$ = change in stress,

$\Delta\varepsilon$ = change in strain.

Elongation at break :

$$\varepsilon_f = \frac{\Delta_f}{L_g} \qquad [3.3]$$

where: ε_f = final strain (mm/mm),

Δ_f = extensometer displacement (mm),

L_g = extensometer gauge length (mm).

Ultimate tensile strength :

$$\sigma_f = \frac{P_f}{A} \qquad [3.4]$$

where: σ_f = final stress (MPa),

P_f = max load (N),

A = cross sectional area (mm^2).

Ultimate Flexual Strength :

$$\sigma_f = \frac{3PL}{2bd^2} \qquad [3.5]$$

where: σ_f = final stress in the outer fibers at midpoint, MPa

P = load at a given point on the load-deflection curve, N,

L = support span, mm (in),

b = width of specimen tested, mm (in), and

d = depth of specimen tested, mm (in).

Flexural modulus :

$$E_B = \frac{L^3 m}{4bd^3} \qquad [3.6]$$

where: E_B = modulus of elasticity in bending,

L = support span,

b = width of specimen tested,

d = depth of the specimen tested and

m = slope of the tangent to the initial straight line portion of the deflection curve

3.2.5.2 Dynamic Mechanical Analysis (DMA)

A TA Q800/2980 Dynamic Mechanical Analyzer was used to measure the dynamic mechanical properties (storage modulus, loss modulus, and loss factor) of unfilled PP and five selected composites namely LP 50, SLP 40/10, SLP 30/20, SP 50 and COSLP. The samples were selected to allow comparisons between hybrid and non-hybrid composites as well as to evaluate the effects of co-steam explosion on storage modulus and damping. To accomplish these goals, thermal scans from -70 to 70^{o}C (assumed to cover the most probable use temperature range for the materials) were performed on the samples at a rate of 5^{o}C / minute and a fixed frequency of 1 Hz. Based on the rigidity of the test specimens, the single cantilever clamp was selected.

In a typical scan, the TA Q800/2980 applies a constant strain to the sample and measures the material response (force as a function of temperature) and the phase angle, δ. The measured force and strain amplitude (see Figure 2.1) are used to calculate the sample stiffness, K as follows:

$$K = F / A \quad (3.7)$$

where:

F = Force

A = Strain amplitude

The stiffness (complex) is further resolved into storage (K') and loss (K'') siffnesses as follows:

$$K' = K \cos \delta \quad (3.8)$$

$$K'' = K \sin \delta \quad (3.9)$$

$$\text{Tan } \delta = K'' / K' \quad (3.10)$$

The storage and loss moduli are then calculated as products of stiffnesses (K′ and K″ respectively) and a correction factor. The correction factor is a combination of clamping corrections and adjustments for sample geometry [51]. Modulus values for the single cantilever setup are calculated by the analyzer according to equation 3.11 below.

$$E = \frac{K_s}{F_c} \times \frac{L^3}{12\ I} \times \left(1 + \frac{12}{5} \times (1+\nu) \times \left(\frac{t}{L}\right)^2\right) \qquad (3.11)$$

$$F_c = 0.7616\ - 0.02713\ \times \sqrt{\frac{L}{t} + 0.1083\ \ln\left(\frac{L}{t}\right)}$$

where:

E = Dynamic modulus (storage or loss)

L = Sample length

t = Sample thickness

I = Sample moment of inertia

ν = Poisson's ratio

K_s = Measured stiffness

F_c = Clamping correction factor

In addition to thermal scans, TTS was performed on unfilled PP and selected composites (LP 50, SLP 30/20, SLP 40/10, SP 50, COSLP) using frequency scans of 0.5 to 100 Hz and a temperature range of –10 to 70°C. Plots of storage modulus versus frequency curves, obtained at different temperatures, were used to construct master curves for each material. Shift factor versus temperature plots were also used to assess the effects of fiber reinforcement on stress relaxation behavior of PP. A reference temperature of 10°C was chosen due to its closeness to the T_g (7.85°C) of neat PP.

3.2.5.3 Sorption

Sorption tests (24 hours immersion in water) were performed to assess composite water absorption behavior. Due to the water repelling nature of the matrix, small specimen sizes of 12.7 mm (1/2 inch) square were used to ensure complete specimen soaking within the 24-hour period. First, all specimens were dried at 70°C for 24 hours and weighed. The specimens were then immersed in distilled water for 24 hours, after which they were removed, immediately wiped of excess water, and reweighed. Weight gain (water absorption) after 24 hours was calculated according to equation 3.12 below.

$$Weight\ gain\ (\%) = \frac{W_f - W_i}{W_{fib}} \times 100 \qquad (3.12)$$

where:

W_f represents the final specimen weight, W_i the initial specimen weight, and W_{fib} the dry weight of fiber in the specimen. Note that weight of matrix was not included in the denominator since moisture absorption of PP is assumed to be negligible compared to that of cellulose. Sorption tests were performed on selected hybrid composites (SLP 30/20, SLP 35/15, SLP 40/10) and non-hybrid controls (LP 50 and SP 50).

3.2.6 Scanning Electron Microscopy

The nature of fiber-matrix interaction was examined by means of scanning electron microscopy (SEM). Fracture surfaces of tensile test specimens were observed with a LEO 1550 Scanning Electron Microscope. Specimens were coated with a 10 nanometer gold sputter.

4 Results and Discussions

Chopped lyocell fibers were used exclusively and in combination with SEW fibers to reinforce a commercial grade PP at different fiber concentrations. Compounding was accomplished by means of the random wetlay process (described in chapter 3). Wetlaid sheets were compression-molded and tested for mechanical (stress-strain) and dynamic mechanical properties as well as sorption characteristics. Fiber-matrix interactions were visually assessed from SEM images of wetlaid sheets and fracture surfaces of tensile specimens. An alternative compounding method aimed at improving fiber-matrix adhesion is the co-steam explosion process. Co-steam exploded wood / PP composites were also produced and investigated in the same manner as described above. In this chapter, a summary of results has been presented and the effects of fiber hybridization on the mechanical and sorption properties of composites have been evaluated.

All statistical comparisons are based on t-tests (Fisher's least significant differences) performed at a 95 % confidence limit (C.L).

A summary of materials tested is shown below (see Table 3.2 for complete list).

Composite type (Designation)	**Composition, wt. %**
• Lyocell / PP (LP)	25 / 65 to 65 / 25
• SEW / PP (SP)	50 / 50
• (SEW / lyocell)/ PP (SLP)	(45 / 5 to 30 / 20) / 50
• (SEW / PP) / lyocell (COSLP)	(45 / 45) / 10

4.1 Mechanical Properties

4.1.1 LP Composites – Effects of Lyocell Concentration

4.1.1.1 Tensile and Flexural Properties

Table 4.1 shows tensile properties of unfilled PP and LP composites. The data have also been graphically presented in Figures 4.1 and 4.2. The data shows that both strength and modulus increase with fiber loading up to a maximum and then start to decline with further fiber addition. A similar trend was observed by Lu [52] in his study with wetlaid short glass / short carbon fiber-reinforced thermoplastic (PP and polyethylene terephthalate [PET]) composites with no fiber hybridization. Maximum tensile/flexural properties were observed between 20 and 30 vol.

Table 4.1 Tensile Properties of LP Composites (Values in parenthesis represent standard deviations). Materials belonging to the same letter group (shaded) are not significantly different.

Material	Modulus (GPa)	t-grouping[1]	Strength (MPa)	t-grouping	EAB (%)	t-grouping	Density (g/cm^3)
PP	1.21 (0.08)	D	27.0 (0.3)	**E**	12.61 (3.03)	**A**	0.91
LP-25	2.71 (0.16)	**C**	52.7 (0.70)	**D**	5.92 (0.26)	**C**	1.01
LP-35	3.29 (0.15)	**B**	59.4 (0.60)	**C**	4.97 (0.27)	**C**	1.04
LP-50	3.60 (0.19)	**A**	70.2 (2.3)	**A**	7.87 (0.23)	**B**	1.07
LP-65	2.55 (0.16)	**C**	63.7 (3.4)	**B**	7.76 (0.41)	**B**	1.06

% glass fiber content for composites loaded with 5 to 50 vol. % glass fibers. According to Nando and Gupta [53], addition of very low concentrations of short fibers to a polymer matrix causes an initial decline in strength properties due to the creation of localized strains by the few fibers present. With addition of more fibers, a critical concentration is reached at which the fibers' reinforcing effect begins to show. Then at very high fiber loadings, mechanical properties decline once again as a result of reduced matrix volume fraction and increased fiber to fiber interactions [53]. Data from the present study show that optimum reinforcement in tension for lyocell/PP composites occur at or around 50 wt. % fiber content. Since very low fiber concentrations were not used in this study, the initial decline in strength was not observed.

Table 4.2 shows flexural properties of LP composites (also presented in Figures 4.3 and 4.4). Flexural properties display similar trends as tensile properties except that peak flexural strength was observed at a lower fiber loading (35 wt. %). A similar reasoning as previously discussed under tensile properties apply to flexural properties as well.

4.1.1.2 Elongation at Break

Elongation at break under tensile testing was measured as change (in percent) to original length of a specimen at failure. The EAB values were directly measured by an extensometer attached

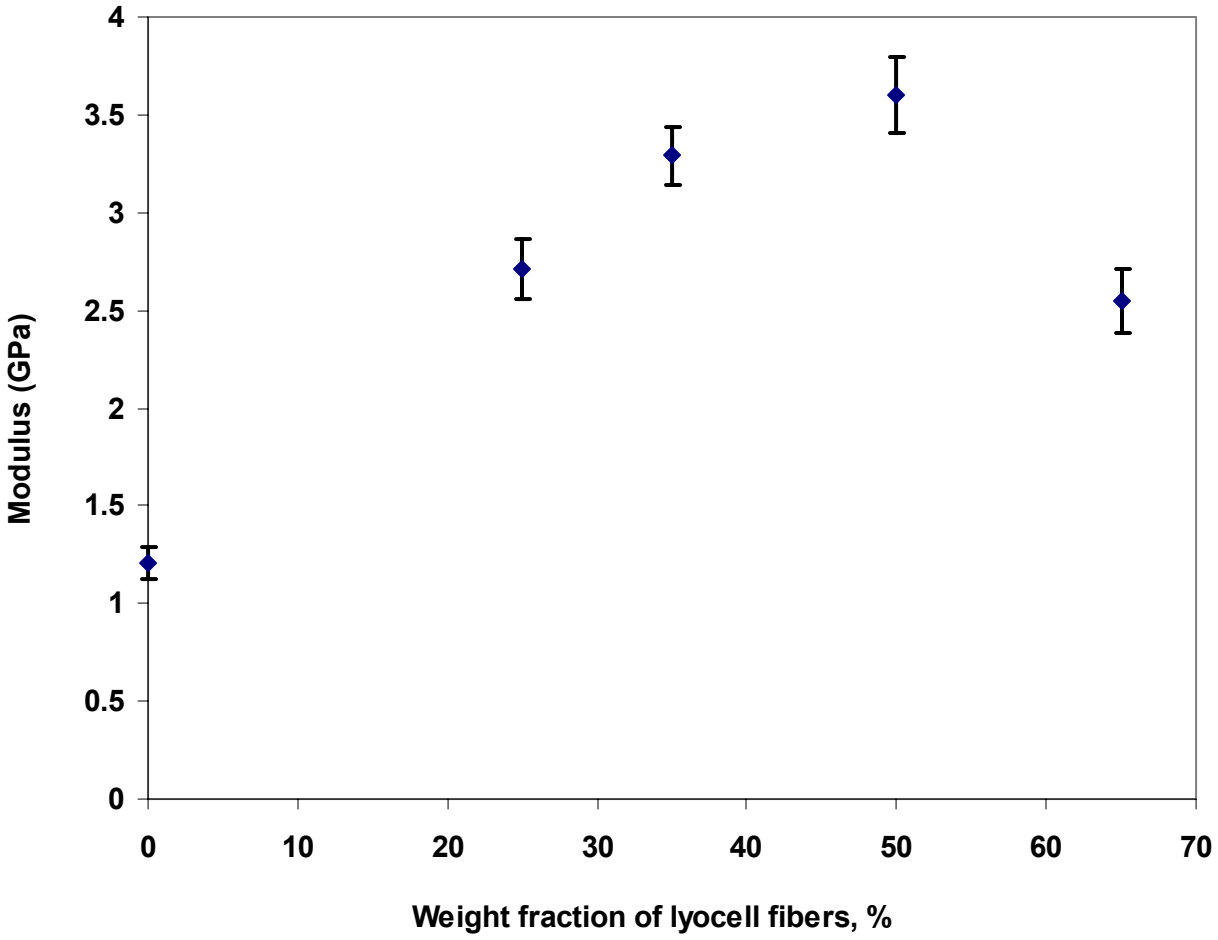

Figure 4.1 Tensile modulus of LP composites as a function of lyocell concentration. Error bars represent ± standard deviation.

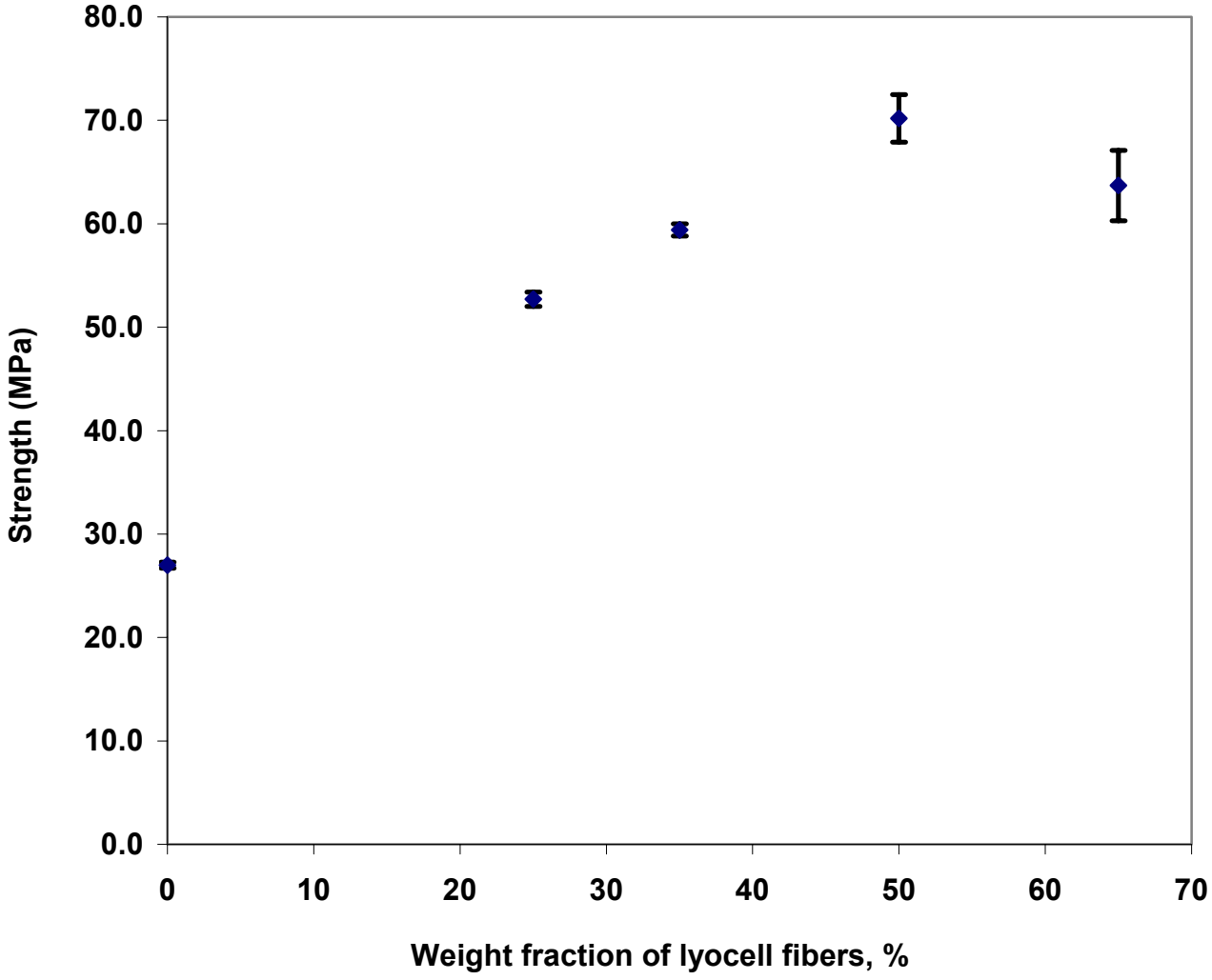

Figure 4.2 Tensile strength of LP composites as a function of lyocell concentration. Error bars represent ± standard deviation.

Table 4.2 Flexural Properties of LP Composites (Values in parenthesis represent standard deviations) Materials belonging to the same letter group (shaded) are not significantly different.

Material	Modulus (GPa)	t-grouping	Strength (MPa)	t-grouping
PP	1.32 (0.06)	**E**	48.6 (4.2)	**D**
LP-25	2.97 (0.14)	**D**	76.1 (4.8)	**B**
LP-35	3.57 (0.05)	**B**	86.2 (4.7)	**A**
LP-50	4.39 (0.37)	**A**	84.8 (3.7)	**A**
LP-65	3.27 (0.25)	**C**	68.8 (2.9)	**C**

to the sample midsection. The results in Table 4.1 reveal that increasing lyocell fiber concentration decreases EAB for all composites compared to unfilled PP. Among the composites, the lowest EAB is observed for LP 35 while the highest is observed for LP 50. The increase in EAB with increasing lyocell concentration appears to result from the inherent extensibility of lyocell fibers (14 – 16)%. The ability of lyocell to undergo large strains under tension has also been observed in a previous study on continuous lyocell fiber-reinforced thermoplastic composites where brittle matrix (cellulose acetate butyrate) failure occurred ahead of lyocell fiber rupture [33].

4.1.2 Comparison of LP 50 With Cellulose Fiber-Reinforced Composites from Other Studies

Table 4.3 compares tensile properties of LP 50 (from the present study) with other fiber-reinforced composites. Also included for contrast are the tensile properties of a continuous lyocell reinforced thermoplastic composite. Among the short fiber reinforced composites, LP 50 ranks third in strength after Cordenka® (high strength rayon) and glass-reinforced PP composites. Strength performance of LP 50 is notable given that most of the other composites were treated with coupling agents. (See remarks column of Table 4.3). The high strength performance of LP composites stems from high aspect ratio and uniformity of lyocell fibers, in addition to good fiber dispersion and fiber length retention from the wetlay process. At this stage, no deductions could be made about the influence of fiber-matrix adhesion, however, evidence from DMA studies (discussed later) suggested the existence of interactions between

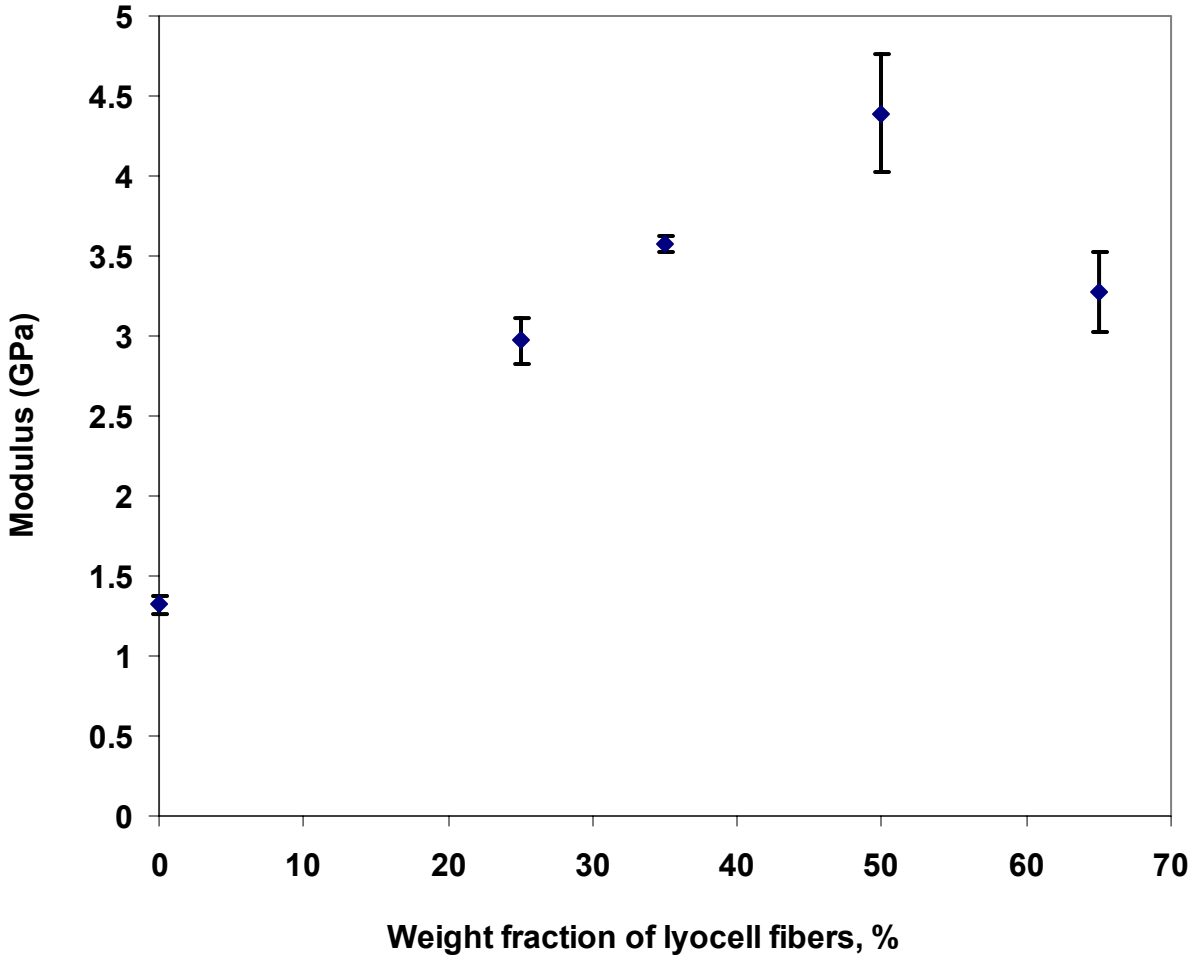

Figure 4.3 Flexural modulus of LP composites as a function of lyocell concentration. Error bars represent ± standard deviation.

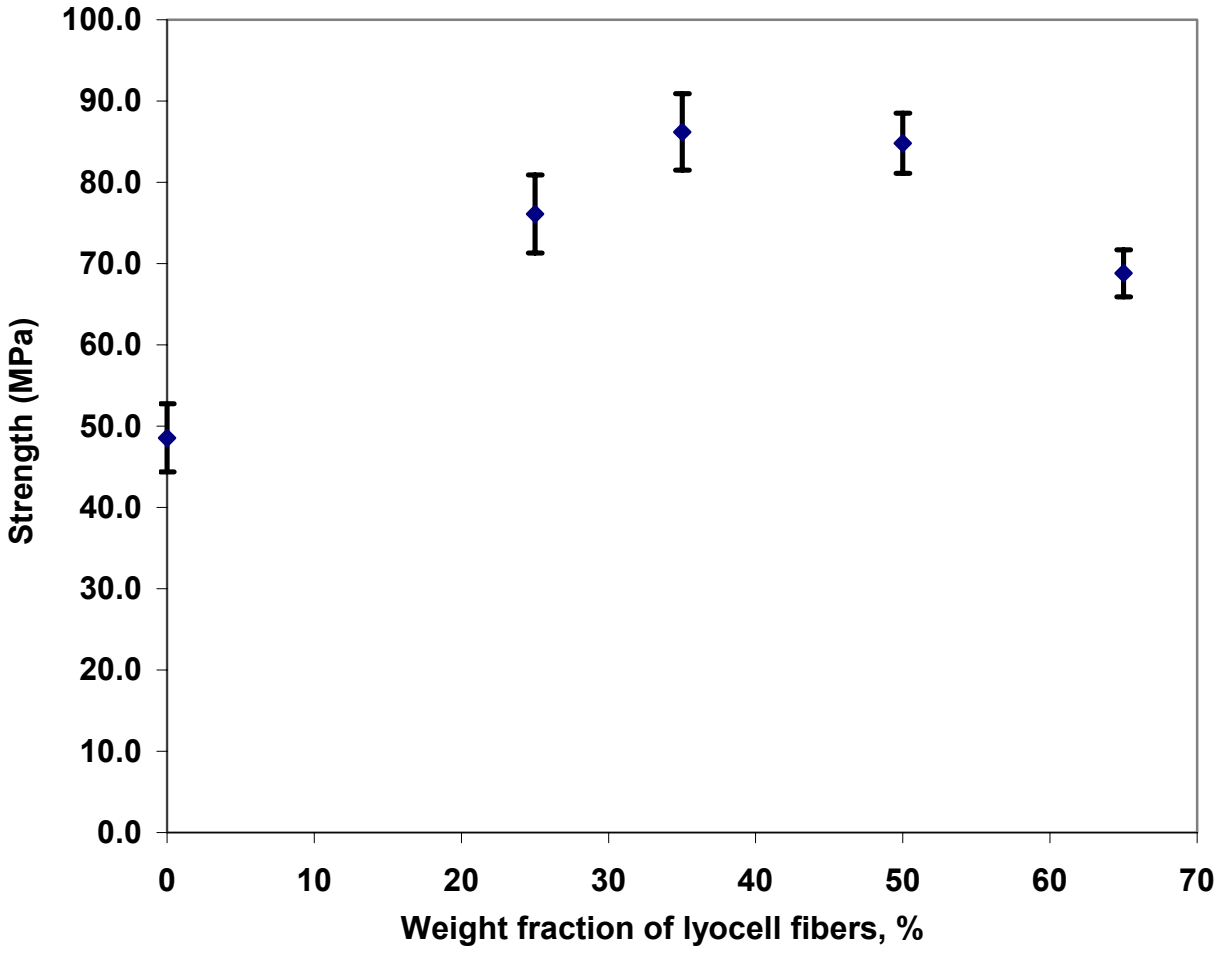

Figure 4.4 Flexural strength of LP composites as a function of lyocell concentration. Error bars represent ± standard deviation.

Table 4.3 Tensile Properties of Selected Fiber – Reinforced Thermoplastic Composites. (All composites have PP matrices except where indicated).

Fiber type (wt. %)	Tensile modulus, GPa	Tensile strength, MPa	Elongation at break, %	Remarks	Source
Lyocell (50)	3.6	70.2	7.9	Fiber preimpregnation by random wetlay process, followed by compression molding of prepreg sheets	Present study
Continuous lyocell (69 to 74) / cellulose acetate butyrate matrix	19.9 – 21.5	250.3 – 264.1	3.3 – 2.8	Pre-impregnation of fibers in matrix solution followed by compression molding of prepregged fibers	Seavey *et al*,.[33]
Cordenka®[1] (42)	4.1	90.0		Compounding by extrusion, followed by injection molding. PP-MAPP (3 wt. % MAPP) used as matrix	Weigel *et al*, [54]
Glass (49)	7	81.7	1.83	Fiber preimpregnation by random wetlay process, followed by compression molding of prepreg sheets	Lu, [52]
Kraft pulp fiber (60)	3.01	32.7		Fiber preimpregnation by random wetlay process, followed by compression molding of prepreg sheets	Bullions *et al.* [55]
Kraft pulp fiber (60)	4.35	44.9		Fiber preimpregnation by random wetlay process (8 wt. % MAPP added), followed by compression molding	Bullions *et al*. [55]
Kraft pulp fiber (40)	4.60	43		Melt mixing in a Brabender mixer with 2 wt. % (by pulp weight) stearic acid dispersing agent	Woodhams *et al*, [2]
Kenaf (50)	7.7	62.0	2.2	High intensity mixing in kinetic mixer, followed by injection molding. (2wt. % MAPP by weight of PP included)	Sanadi *et al.*, [21]

1. High strength rayon fibers from Acordis, Obernburg, Germany

lyocell fibers and PP.

Inspite of their high strength performance, lyocell fibers do not seem to influence composite modulus significantly. This may be due to their high extensibility (14 – 16 %) that makes the resulting composites more compliant than those of other less extensible natural fibers such as kenaf (with extensibility of 2.7 % [17]).

4.1.3 SLP Composites – Effects of Fiber Hybridization

4.1.3.1 Tensile and Flexural Properties

The results for SLP composites have been summarized in Tables 4.4 and 4.5 (also in Figures 4.5 to 4.8. SP 50 and LP 50 were included to serves as non-hybrid controls.. Total fiber concentration for SLP composites was fixed at 50 wt. % based on the previous observations of peak stiffness/strength performance (of LP composites) at 50 wt. % fiber concentration.

Figures 4.5 and 4.7 reveal general increases in composite moduli with increasing lyocell concentration up to the maximum fiber loading. A slight decline in tensile modulus can however be seen in SLP 45/5, which may be due to its low lyocell fiber content. At that low a concentration, lyocell fibers are insufficient to produce a stiffening effect. Instead, they serve as stress concentration points in the otherwise homogeneous composite of SEW fibers and thereby lower the modulus.

Figures 4.6 and 4.8 show a decline in matrix strength with the exclusive use of SEW (SP 50). This observation agrees with other SEW studies [6, 39, 40] where composite strengths were observed to decline with increasing SEW fiber loading (up to 40 wt. %). However, incorporation of lyocell fibers, even at low concentrations (SLP 45/5) reverses the direction of change in strength (Figures 4.6 and 4.8). The dependence of hybrid composite strengths on lyocell concentration appear to follow a linear pattern except for a deviation observed for the tensile strength of SLP 40/10. This anomaly is suspected to result from poor fiber dispersion in SLP 40/10. An initial plan to wetlay without the use of dispersants was abandoned after segregation between reinforcing and PP fibers was noticed while wetlaying SLP 40/10. It therefore became necessary to add dispersants to later runs involving SLP 35/15 and SLP 30/20. Evidence of poor fiber dispersion in SLP 40/10 is seen from comparing SEM images of tensile failure surfaces of SLP 40/10 and SLP 30/20 (Figure 4.9).

Comparing the reinforcing effects of SLP 30/20 with LP 50 (Figures 4.5 to 4.8), it is evident that the two materials compare favorably in moduli and flexural strength properties but not in tensile strength. Given that both composites possess similar fiber dispersion and orientation characteristics, and that the same testing conditions were used, the much lower tensile strength of SLP 30/20 can be readily attributed to the larger proportion of weaker, shorter, and less-uniform SEW fibers.

Table 4.4 Tensile Properties of Hybrid (SLP) Composites. Values in parenthesis represent standard deviations Materials belonging to the same letter group (shaded) are not significantly different.

Material	Modulus (GPa)	t-grouping	Strength (MPa)	t-grouping	EAB (%)	t-grouping	Density (g/cm^3)
SP-50	2.59 (0.12)	**E**	21.6 (0.8)	**E**	2.24 (0.24)	**E**	1.03
SLP-45/5	2.50 (0.07)	**E**	27.6 (0.8)	**D**	3.09 (0.48)	**D**	1.03
SLP-40/10	2.87 (0.16)	**D**	27.4 (1.8)	**D**	3.78 (0.86)	**C**	1.05
SLP-35/15	3.23 (0.06)	**C**	41.9 (0.4)	**C**	3.84 (0.24)	**C**	1.04
SLP-30/20	3.53 (0.09)	**A B**	47.1 (1.2)	**B**	4.61 (0.55)	**B**	1.05
LP-50	3.60 (0.19)	**A**	70.2 (2.3)	**A**	7.87 (0.23)	**A**	1.07
COSLP	3.43 (0.14)	**B**	26.7 (0.5)	**D**	2.29 (0.62)	**E**	1.06

Table 4.5 Flexural Properties of Hybrid (SLP) Composites. Values in parenthesis represent standard deviations Materials belonging to the same letter group (shaded) are not significantly different.

Material	Modulus (GPa)	t-grouping	Strength (MPa)	t-grouping
SP-0	2.19 (0.07)	**E**	36.7 (0.5)	**F**
SLP-45/5	2.37 (0.16)	**E**	49.3 (3.65)	**E**
SLP-40/10	2.79 (0.12)	**D**	57.7 (2.5)	**D**
SLP-35/15	3.16 (0.12)	**C**	71.5 (3.5)	**C**
SLP-30/20	3.43 (0.13)	**B**	76.7 (2.5)	**B**
LP-50	4.39 (0.37)	**A**	84.8 (3.7)	**A**
COSLP	3.40 (0.21)	**B**	55.0 (1.1)	**D**

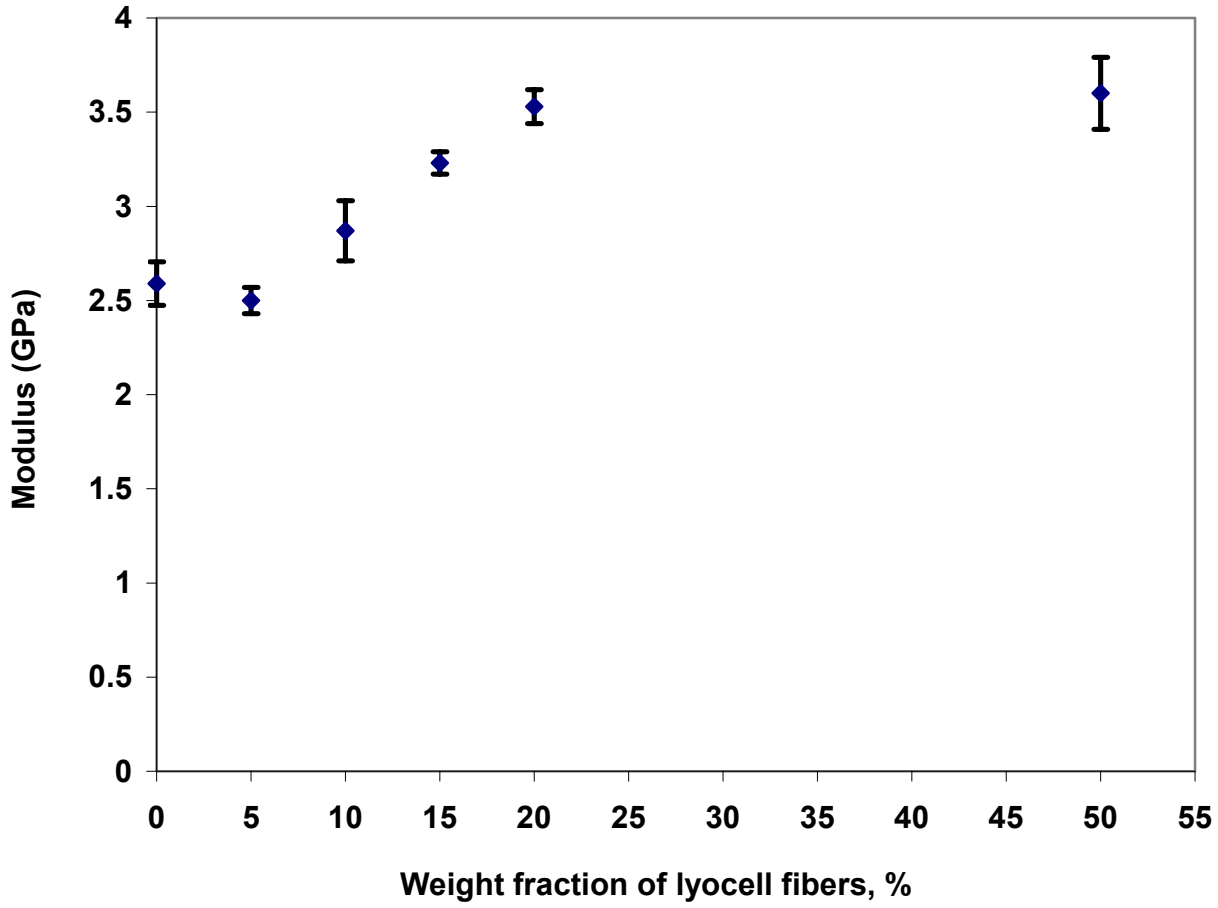

Figure 4.5 Tensile modulus of SLP composites as a function of lyocell concentration. Error bars represent ± standard deviation. Note: 0% lyocell = 50% SEW

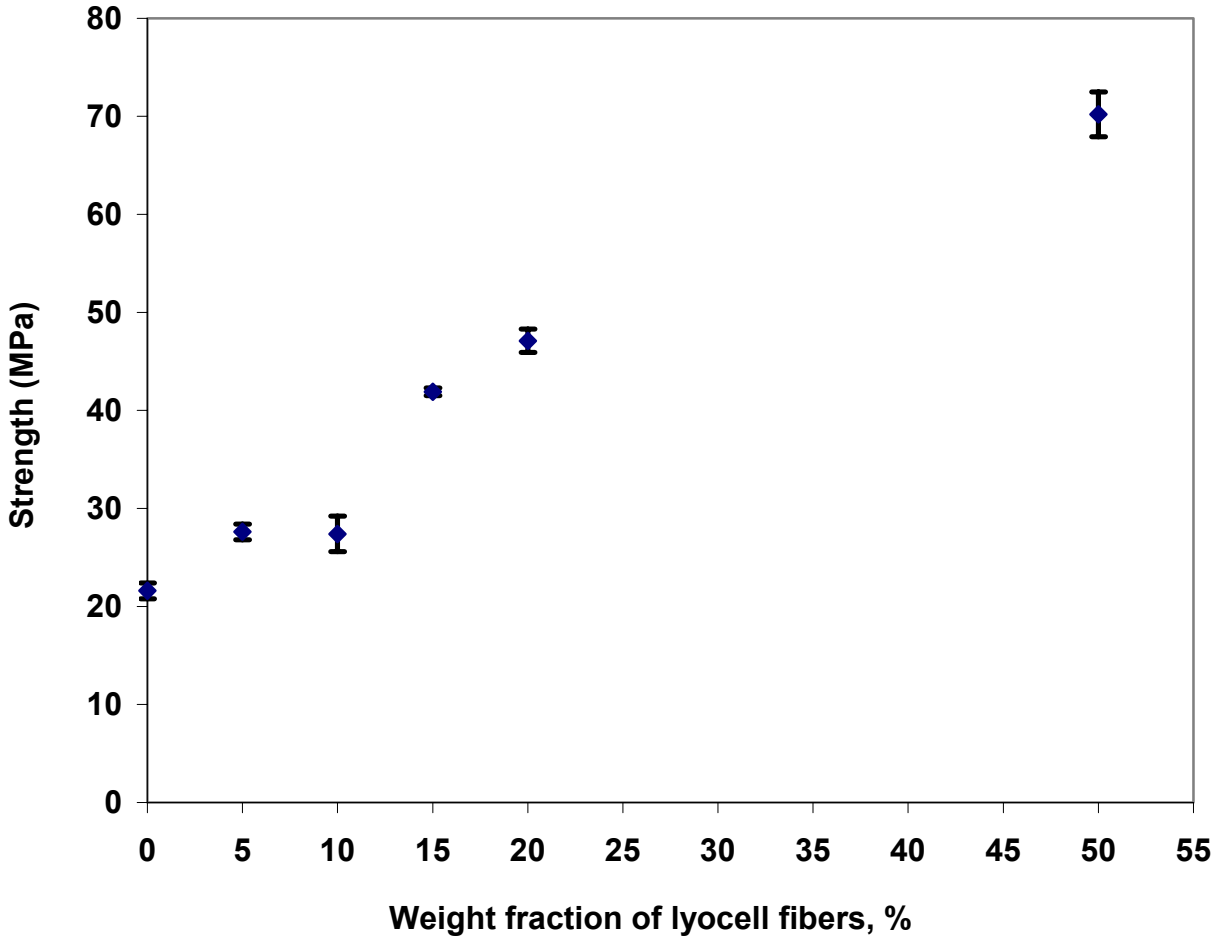

Figure 4.6 Tensile strength of SLP composites as a function of lyocell concentration. Error bars represent ± standard deviation. Note: 0% lyocell = 50% SEW

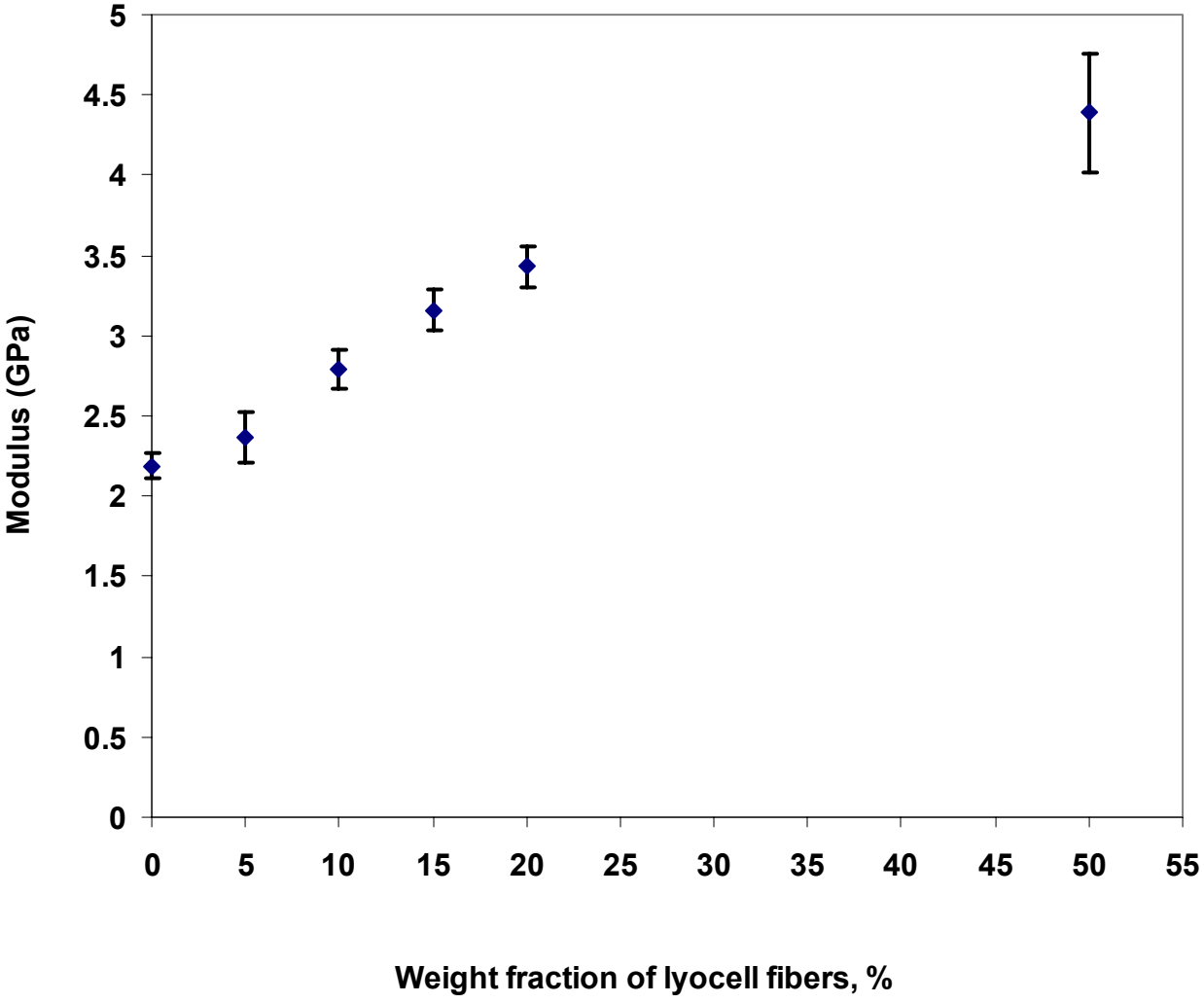

Figure 4.7 Flexural modulus of SLP composites as a function of lyocell concentration. Error bars represent ± standard deviation. Note: 0% lyocell = 50% SEW

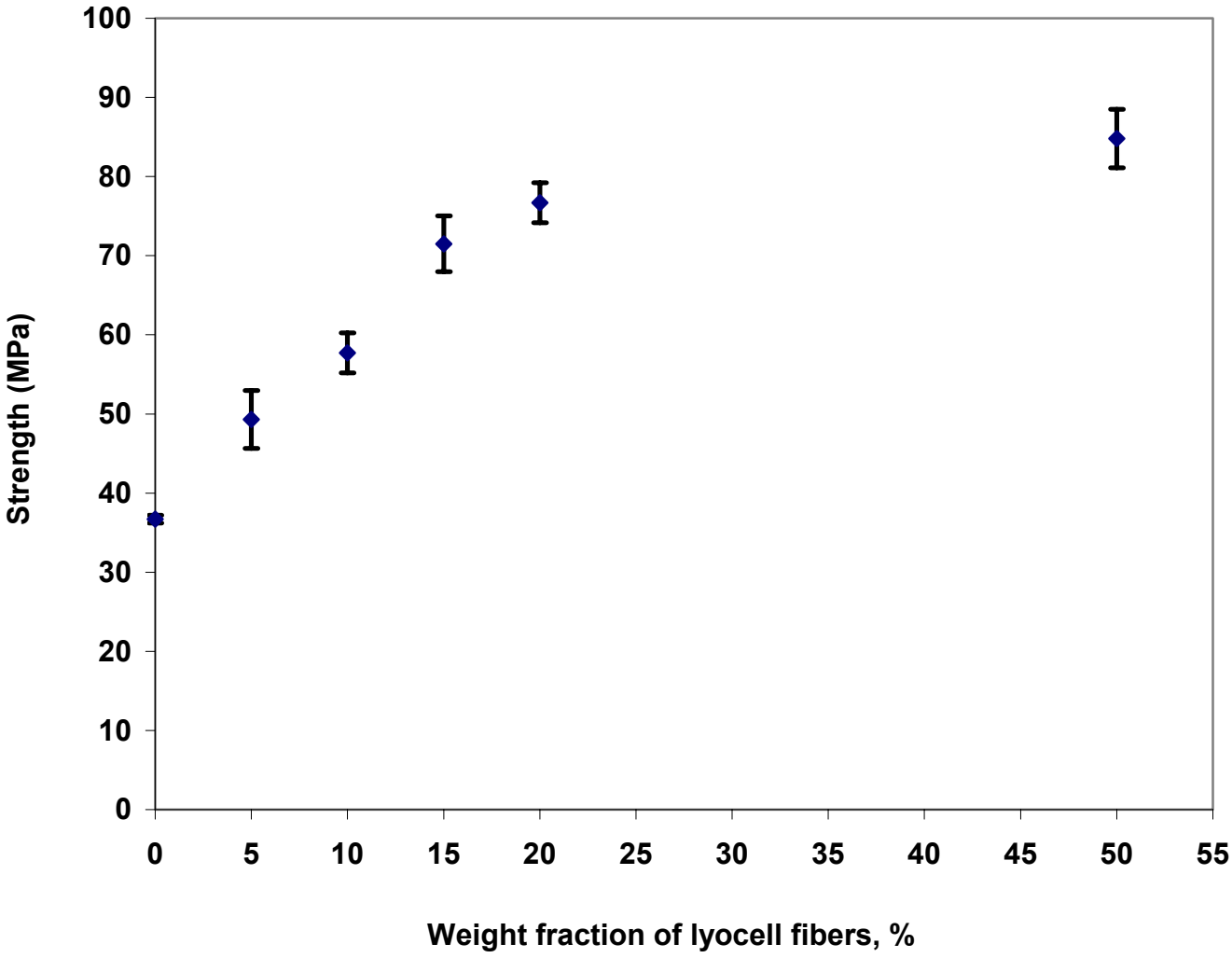

Figure 4.8 Flexural strength of SLP composites as a function of lyocell concentration Error bars represent ± standard deviation. Note: 0% lyocell = 50% SEW

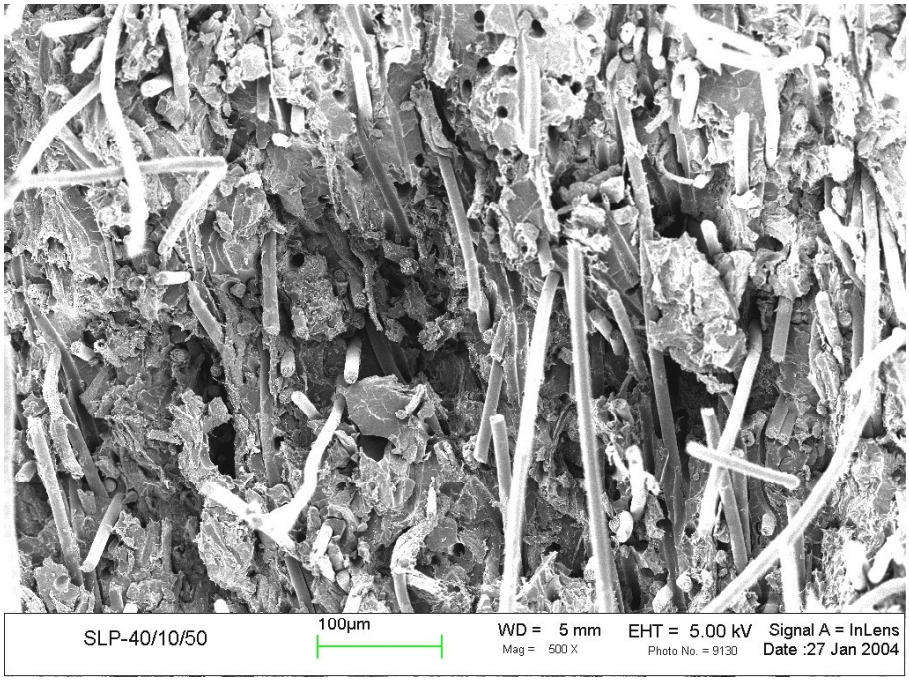

a

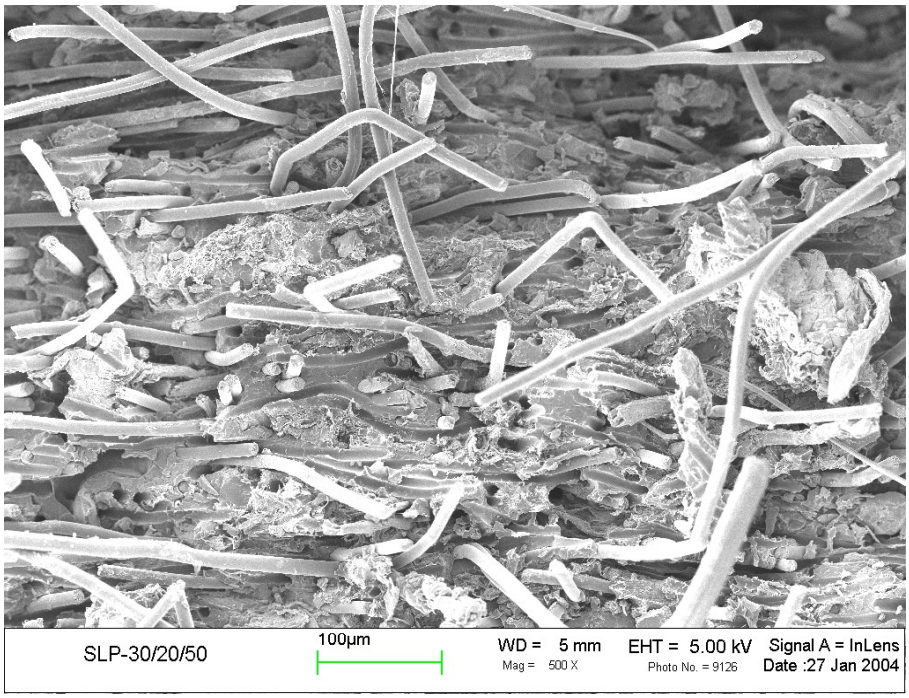

b

Figure 4.9 Tensile fracture surface of a) SLP 40/10.and b) SLP 30/20 at 500x magnification. Contact between fibers and matrix appears to be better in LP 30/20. than SLP 40/10, which appears to have many large voids.

Unlike bending stresses, which are distributed more uniformly across the length of a sample, tensile stresses are concentrated at all points in the material cross section with equal intensity. It seems obvious therefore, that increases in tensile strength for the hybrid composites are a direct consequence of increases in concentration of the stronger lyocell fibers. Tensile fracture surfaces of LP 50 and LSP 30/20 (Figure 4.10) show greater fiber delamination / pullout in the latter.

4.1.3.2 Elongation at Break

As expected, EAB for the SLP composites increased with increasing lyocell concentration. (Table 4.4) but did so to a lesser extent than in the LP composites. An obvious reason is the overall reduction in lyocell content for the SLP composites. An equally important contribution must have come from the high content of relatively short and inflexible SEW fibers.

4.1.4 Effect of Co-steam Explosion on Mechanical Properties

Red oak chips and a high melt flow index PP (HMiPP) were co-steam-exploded and wetlaid together with lyocell as earlier described. Due to the addition of 10 wt. % lyocell, the total fiber concentration of COSLP became 55 wt. % as opposed to 50 wt. % for all other hybrid composites. In addition, COSLP was prepared with a different PP matrix than that used for the other composites (see 3.1.3 for reasons). In spite of the stated differences, it is possible to compare COSLP directly with SLP 40/10 due to their nearly identical fiber compositions. The following discussion should therefore be regarded with these distinctions in mind.

Clearly, modulus properties of COSLP composites are significantly higher than those of SLP 40/10 (Tables 4.4 and 4.5). Indeed, the modulus data rather show statistical equivalence between COSLP and SLP 30/20. The high stiffness shown by COSLP may have originated from HMiPP, which is highly brittle, probably due to its relatively low molecular weight (high melt index). Lower molecular weight, semicrystalline polymers tend to be stiffer than their higher molecular weight counterparts due to the low amorphous content of the former. Attempts to fabricate test plaques out of HMiPP for stress-strain testing resulted in the development of cracks within the plaques that made extraction of test specimens impossible.

Strength results of COSLP, on the other hand, were equivalent to those of SLP 40/10 (see t-groupings). Considering the similarity in composition between the two materials, the evidence

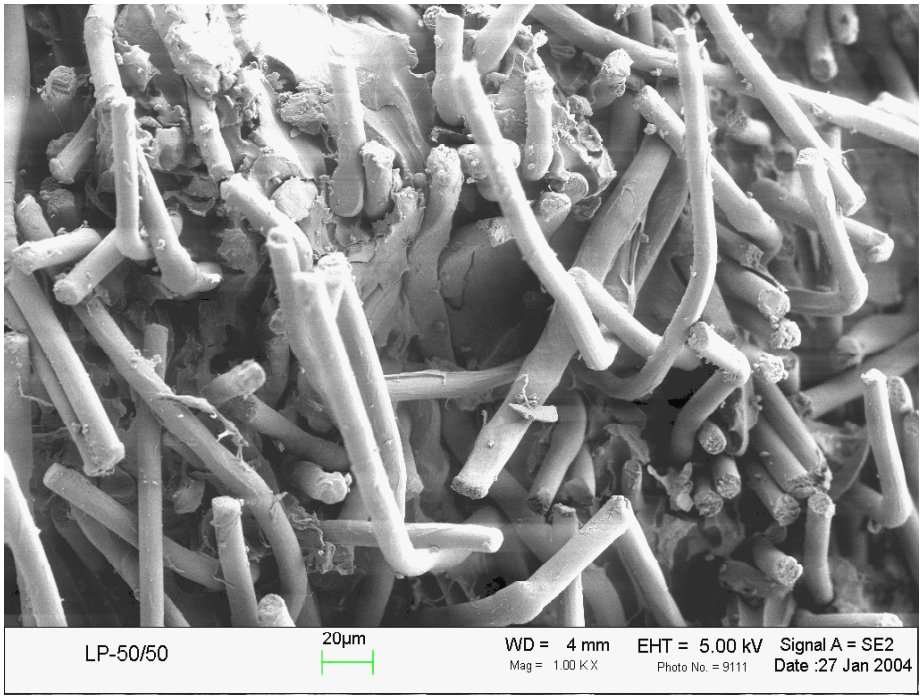

(a)

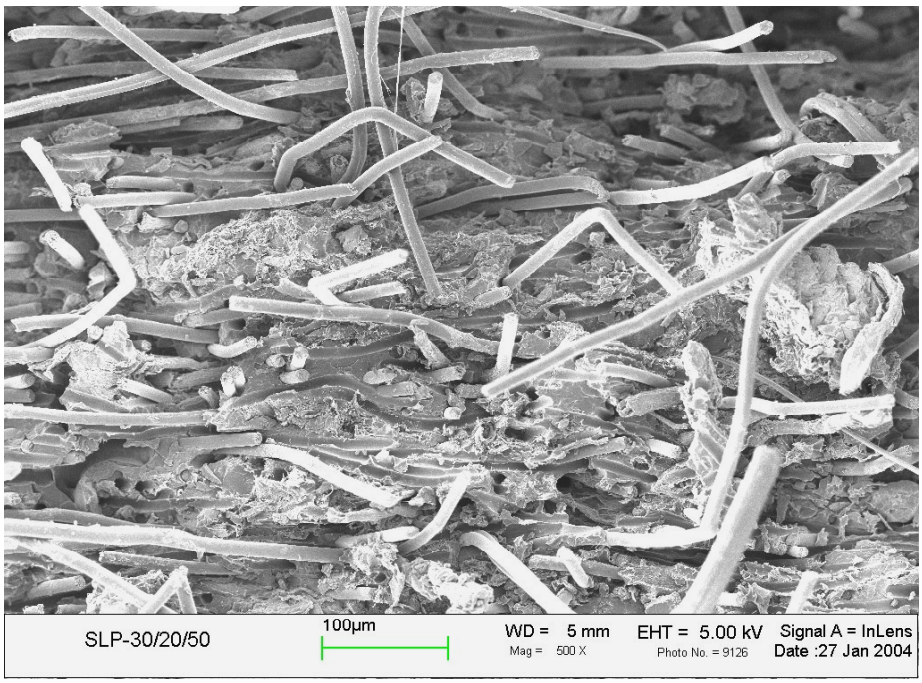

(b)

Figure 4.10 SEM images of a) LP 50 and b) SLP 30/20. Significant fiber delamination / pullout is evident in (b)

does not seem to indicate added improvement in fiber-matrix interactions as a result of co-steam explosion.

4.1.5 Estimation of Lyocell Fiber Reinforcement Efficiency in Hybrid versus Non-Hybrid Composites

In the preceding sections on mechanical properties of LP and SLP composites, it was observed that composite strengths and moduli generally increased with increasing lyocell fiber concentration. Steam exploded wood fibers on the other hand, were found to increase moduli but decrease strengths when used alone as reinforcements. In this section, the efficiency of lyocell as a modulus/strength-building fiber has been evaluated for hybrid (SLP) and non-hybrid (LP) composites. This has been done by comparing the rates at which mechanical properties of hybrid (SLP) and non-hybrid (LP) composites increase as a function of lyocell fiber content. In addition, property gain as a function of fiber cost has been determined for the two composite types.

4.1.5.1 Efficiency of Lyocell in Hybrid versus Non-Hybrid systems – Regression Analysis of Mechanical Properties

Regression plots showing property change as a function of lyocell concentration were made for both composite types (Figures 4.11 – 4.14) based on an assumption of linearity between mechanical properties and lyocell concentration. Table 4.6 summarizes relative dependencies of hybrid and non-hybrid composites on lyocell concentration. Lyocell reinforcement efficiency was taken as slope ratio of the fitted regression line for SLP to that of LP composites (see last column in Table 4.6). A value >1 indicates higher lyocell efficiency in SLP than in LP composites and vice versa.

Table 4.6 shows that with the exception of tensile modulus, for which there is no apparent difference between the two composite types, efficiency of lyocell is greater in SLP than in LP composites for all other properties. Notice also that higher efficiencies were obtained for strength than for modulus, signifying a superior strength-building ability of lyocell in hybrid composites. The observation points to possible synergistic effects from lyocell and SEW fibers blends, which results in composites with more favorable balance of properties than can be achieved for either fiber alone. This assertion is further justified by the property gain versus fiber cost analyses presented in section 4.1.5.2. The greater impact of synergism on strength properties is an indication of more rapid improvements in stress transfer for blends than for LP composites.

Stress transfer in hybrid composites may have been enhanced by the lignin on SEW forming linkages between SEW and lyocell fibers. Another likely contribution comes from the increased retention of solids content with increasing lyocell concentration. It was observed that the amount of SEW fibers and particles that fell through the screen (at the headbox) during wetlaying decreased with increasing lyocell concentration. This was attributed to the formation of webs by lyocell fibers that prevented the smaller wood fibers and particles from falling through. Thus, it is suspected that as lyocell concentration is increased, the wetlay sheet tends to retain more solid matter, which contributes to stiffness / strength improvements.

4.1.5.2 Cost Analysis

As already indicated, the primary goals of fiber hybridization include optimization of composite properties and minimization of production costs. Plots of mechanical property versus fiber cost have been presented in Figures 4.15 – 4.18. Fiber cost was obtained by summing up the costs of SEW and lyocell fibers in a given composite, based on the respective weight fraction of each fiber type present. It is evident from each of the figures that hybrid composites (SLP 45/5 to SLP 30/20) properties increase at a faster rate than fiber cost. Between SLP 30/20 and LP 50, the curves tend to flatten out indicating that fiber cost increases at a faster rate than composite properties in going from a hybrid (SLP) to a non-hybrid (LP) system. This change appears most significant for tensile modulus.

4.2 Dynamic Mechanical Analysis

Two types of DMA studies were performed; 1) Thermal scans, to evaluate the temperature dependencies of viscoelastic properties of unfilled PP and composites, and 2) Time-temperature superposition to estimate storage moduli of PP and composites over extended frequencies (times) and to evaluate the effects of reinforcement type on relaxation times of PP (by comparing shift factor plots).

In this study, samples were deformed at constant strain and the stress response as a function of temperature (thermal scans) and or frequency (time-temperature studies) were recorded. Appropriate test strains were obtained by performing strain sweeps and estimating the linear viscoelastic regions (LVR) of the materials from strain sweep results. The procedure for LVR estimation has been summarized in the next section.

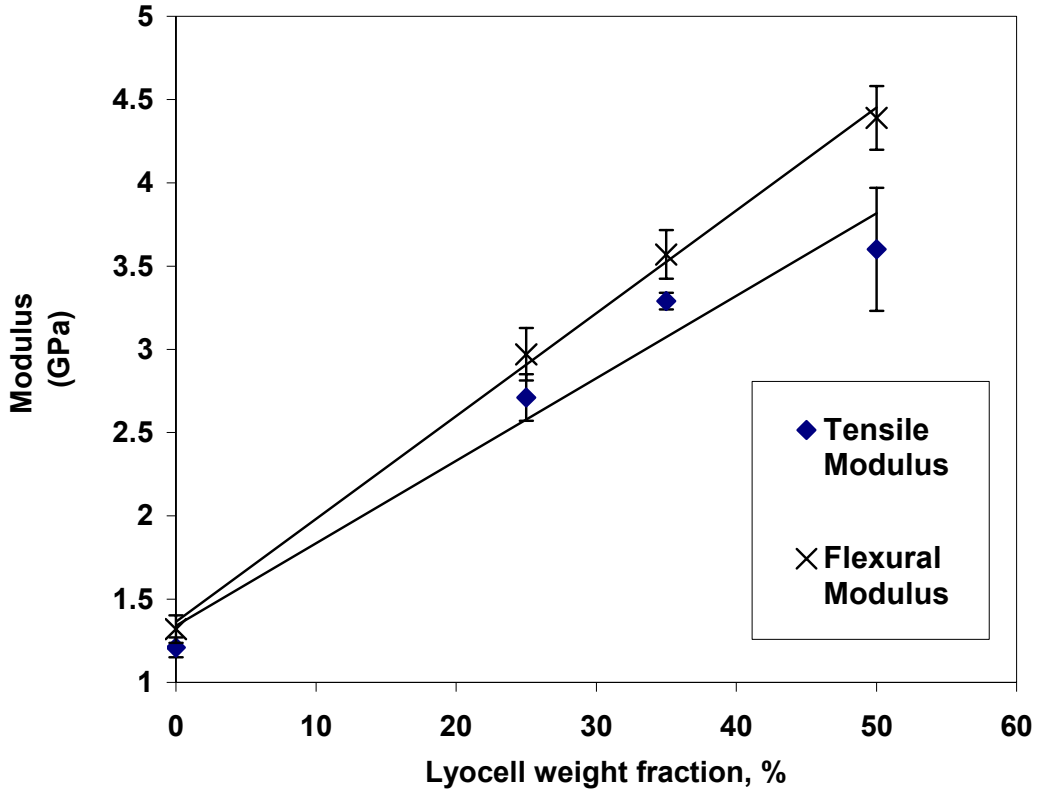

Figure 4.11 Simple linear regression plots for LP composites moduli. Error bars represent ± standard deviation. See Table 4.6 for slopes and R^2 values.

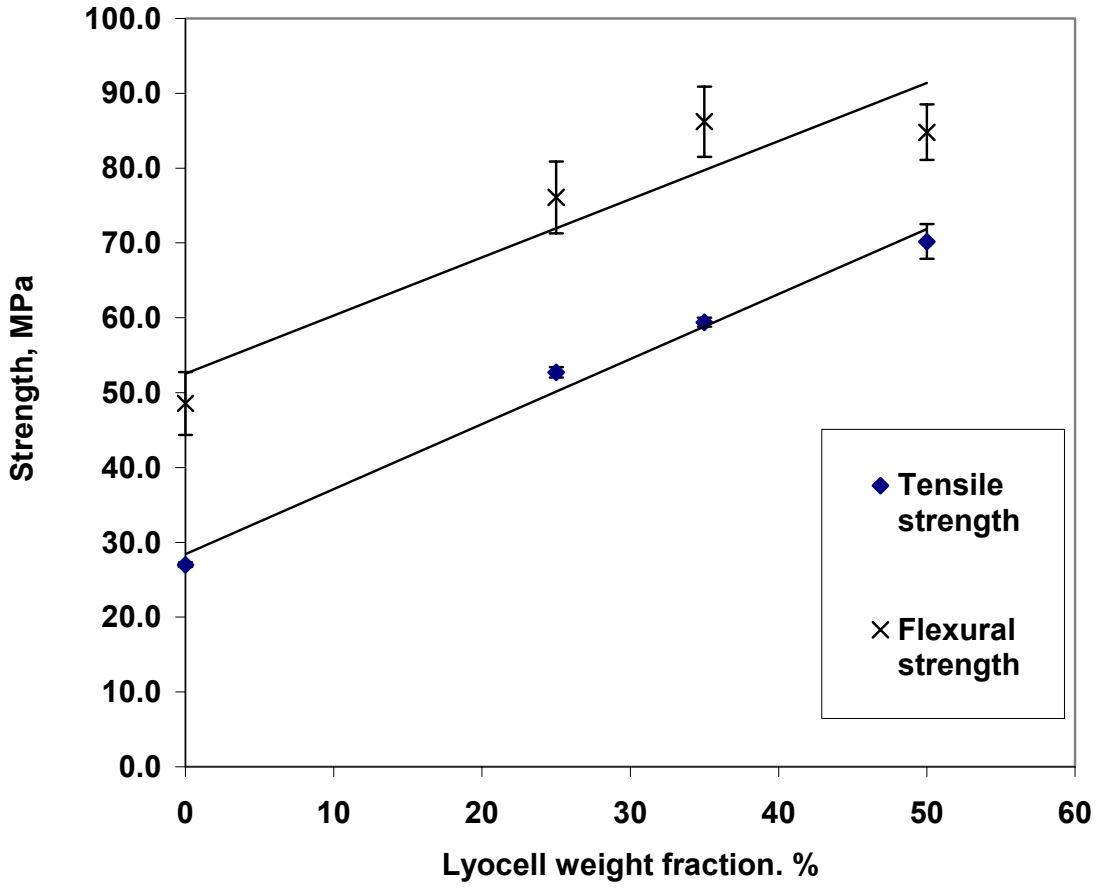

Figure 4.12 Simple linear regression plots for LP composites strengths. Error bars represent ± standard deviation. See Table 4.6 for slopes and R^2 values.

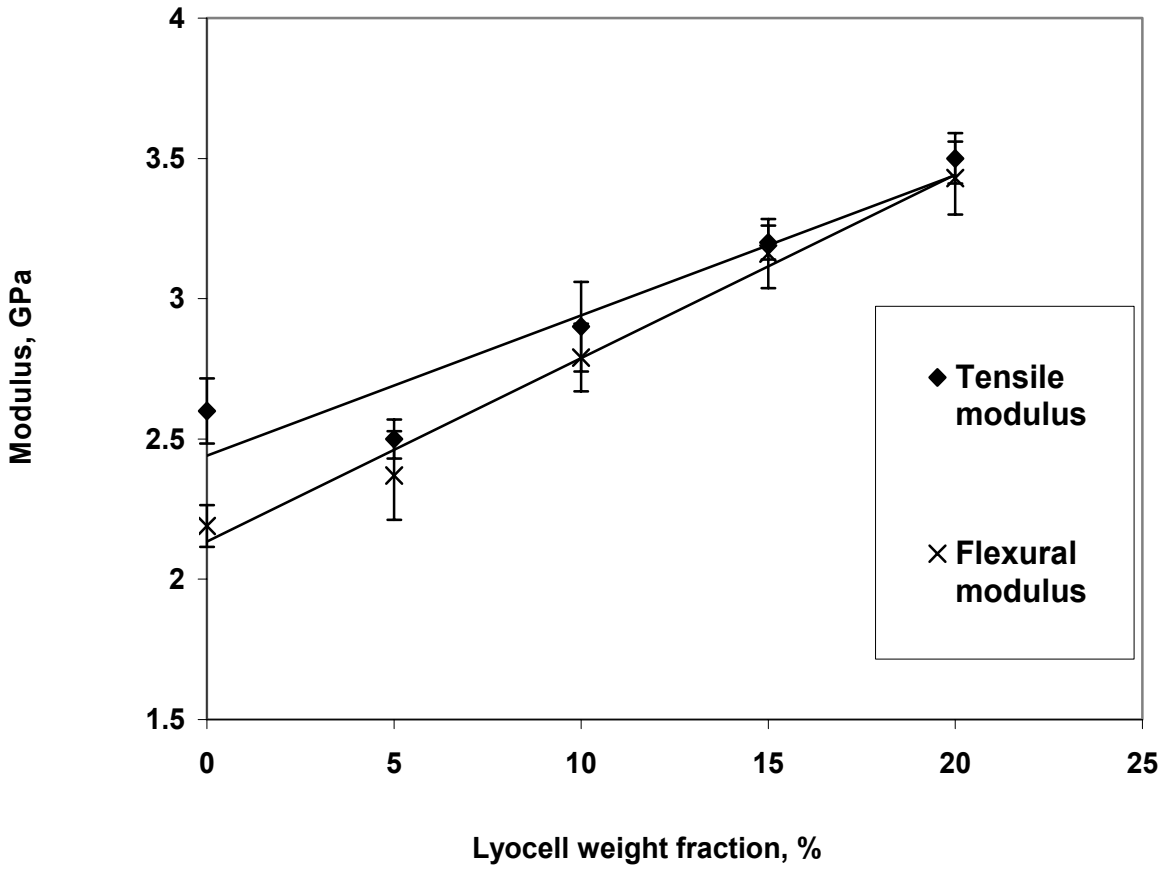

Figure 4.13 Simple linear regression plots for SLP composites moduli. Error bars represent ± standard deviation. Note that all composites carry 50 wt. % total fiber (lyocell + SEW). See Table 4.6 for slopes and R^2 values.

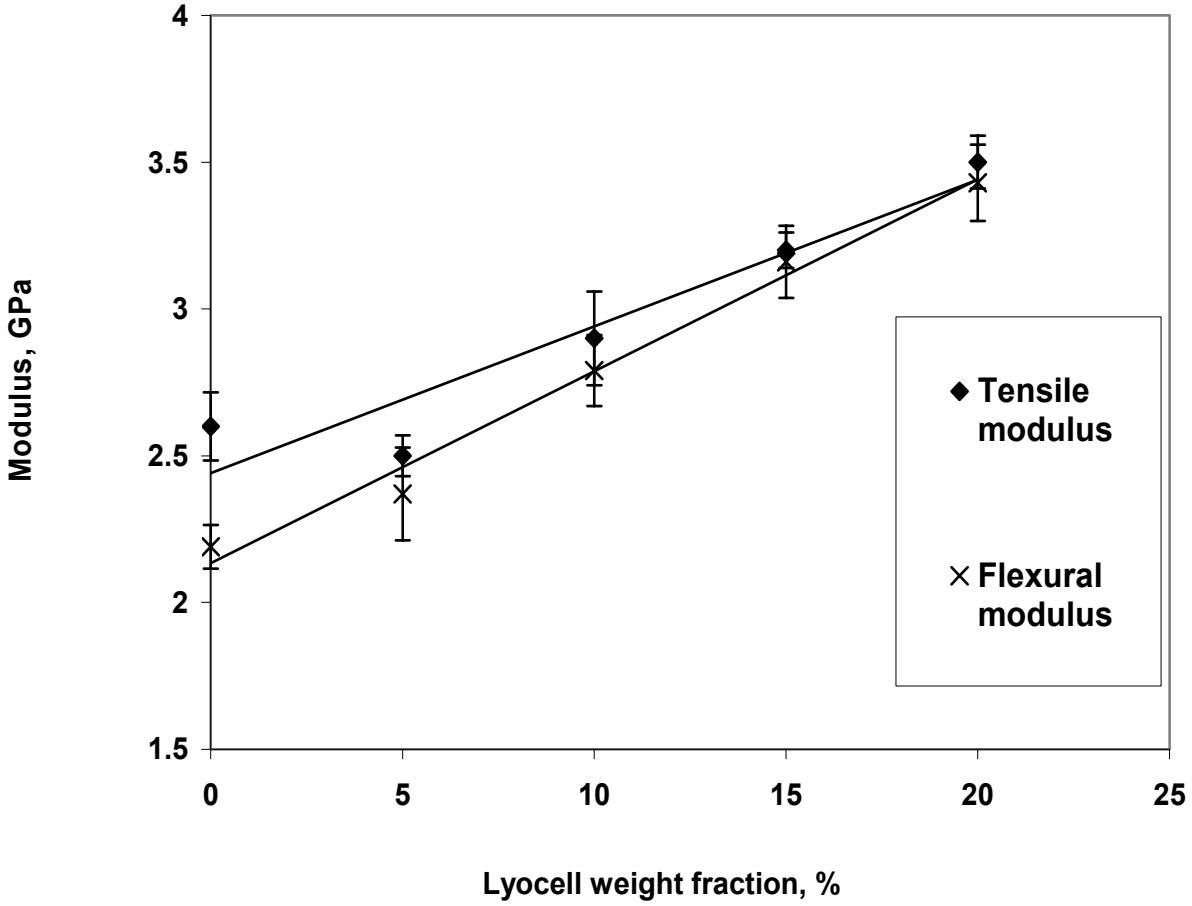

Figure 4.14 Simple linear regression plots for SLP composites strengths. Error bars represent ± standard deviation. Note that all composites carry 50 wt. % total fiber (lyocell + SEW). See Table 4.6 for slopes and R^2 values.

Table 4.6 Estimated Reinforcement Efficiencies of Lyocell in Hybrid (SLP) versus Non-Hybrid (LP) Composites.

Property	LP		SLP		Reinforcement efficiency ($Slope_{SLP}$ / $Slope_{LP}$)
	Property change per unit change in lyocell concentration ($Slope_{LP}$)[1]	R^2	Property change per unit change in lyocell concentration ($Slope_{SLP}$)[1]	R^2	
Tensile modulus (GPa)	0.05	0.96	0.05	0.90	1
Tensile strength (MPa)	0.87	0.99	1.31	0.91	1.51
Flexural modulus (GPa)	0.06	1.00	0.07	0.99	1.17
Flexural strength (MPa)	0.78	0.87	2.04	0.98	2.62

1. Slopes of best fit lines from simple linear regression analyses (See Figures 4.11 – 4.14).

4.2.1 Thermal Scans

4.2.1.1 Linear Viscoelastic Region

The LVR of the test specimens were first determined to allow for an appropriate strain to be chosen for the tests. To ensure that material response to the applied strain is linear throughout the experiment, it is vital during dynamic experiments that material deformation is maintained within its LVR. The maximum limit for linear viscoelasticity was taken as the strain corresponding to a 5 % change in storage modulus measured in a strain sweep test. This approach is a suggested convention by the manufacturers of the DMA Q800 / 2980, which was used for this study [56].

Based on an assumption of similarities in material characteristics, the results of strain sweeps performed on unfilled PP and LP 50 (Figures 4.19 and 4.20) were extended to represent HMiPP the other composites respectively. From the strain sweep data, a 25 μm amplitude was considered appropriate for all materials based on the above-mentioned criteria for selection. Two sweeps per specimen were performed at –70- and 70^{o}C since these were the temperature limits selected for dynamic testing.

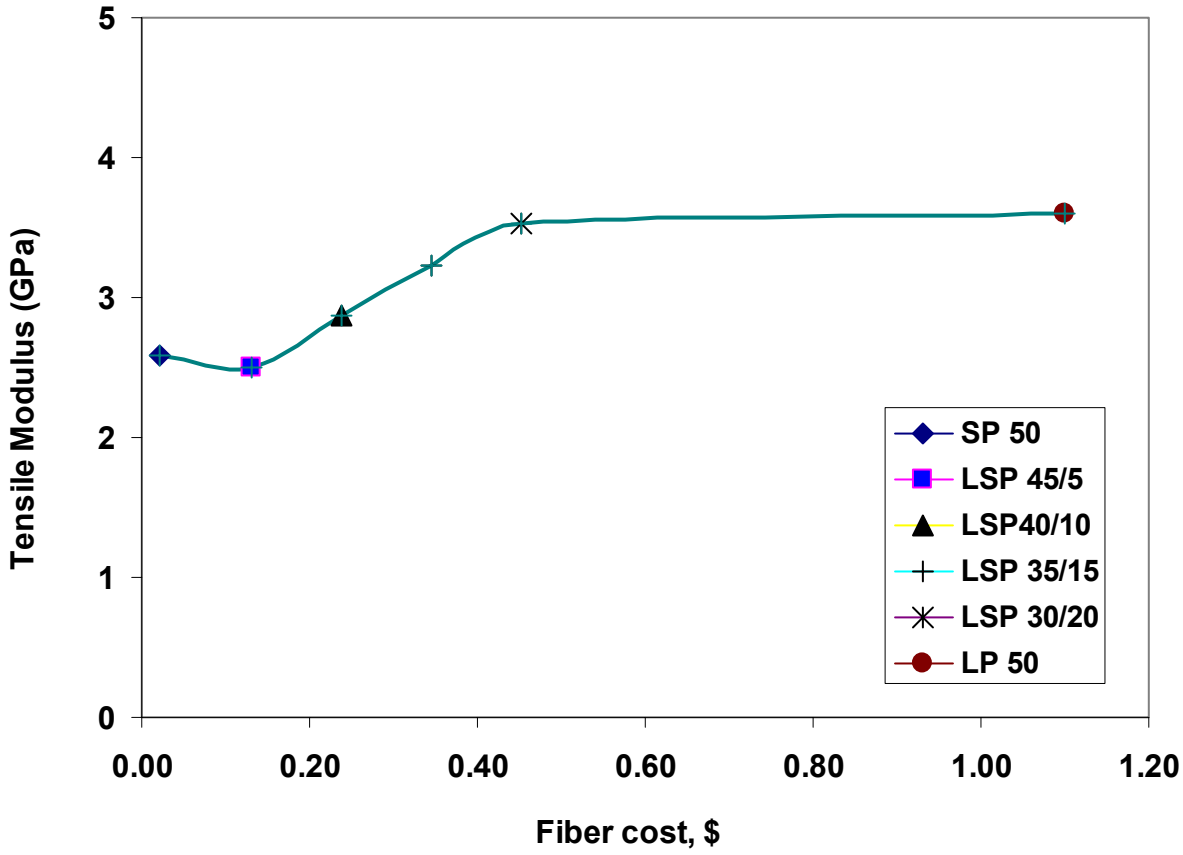

Figure 4.15 Tensile modulus versus fiber cost for hybrid (SLP) composites and non-hybrid (SP 50 and LP 50) controls. Fiber cost is obtained by summation of costs of respective SEW and lyocell weight fractions in the composite.

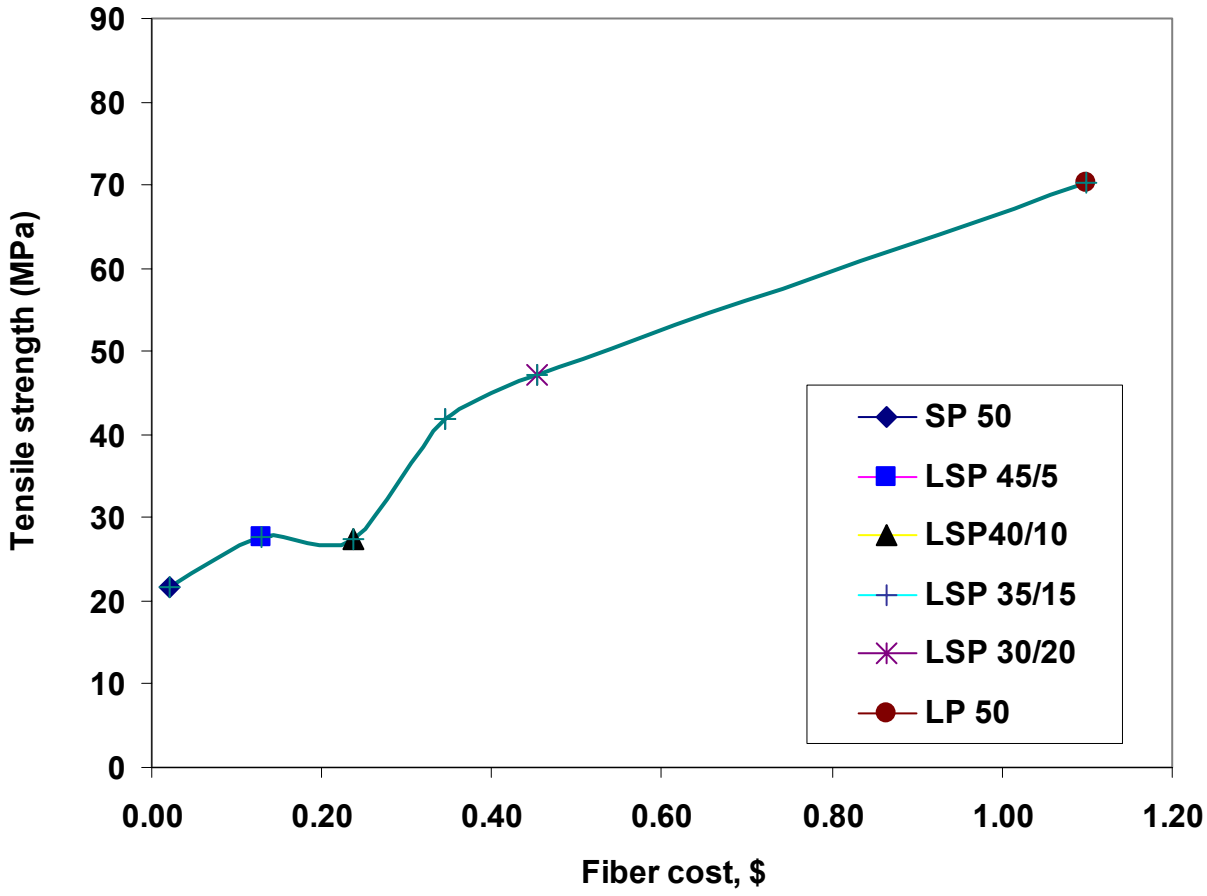

Figure 4.16 Tensile strength versus fiber cost for hybrid (SLP) composites and non-hybrid (SP 50 and LP 50) controls. See Figure 4.15 for fiber cost calculation procedure.

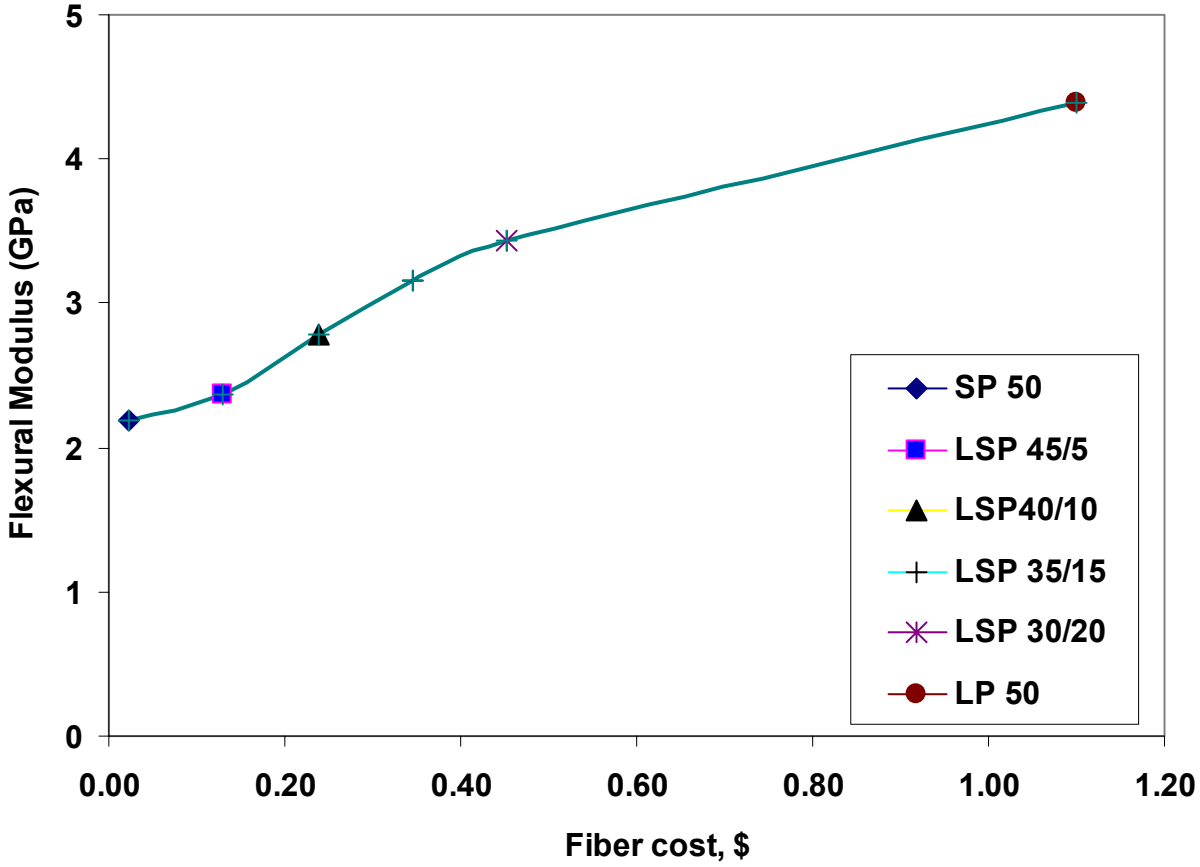

Figure 4.17 Flexural modulus versus fiber cost for hybrid (SLP) composites and non-hybrid (SP 50 and LP 50) controls. See Figure 4.15 for fiber cost calculation procedure.

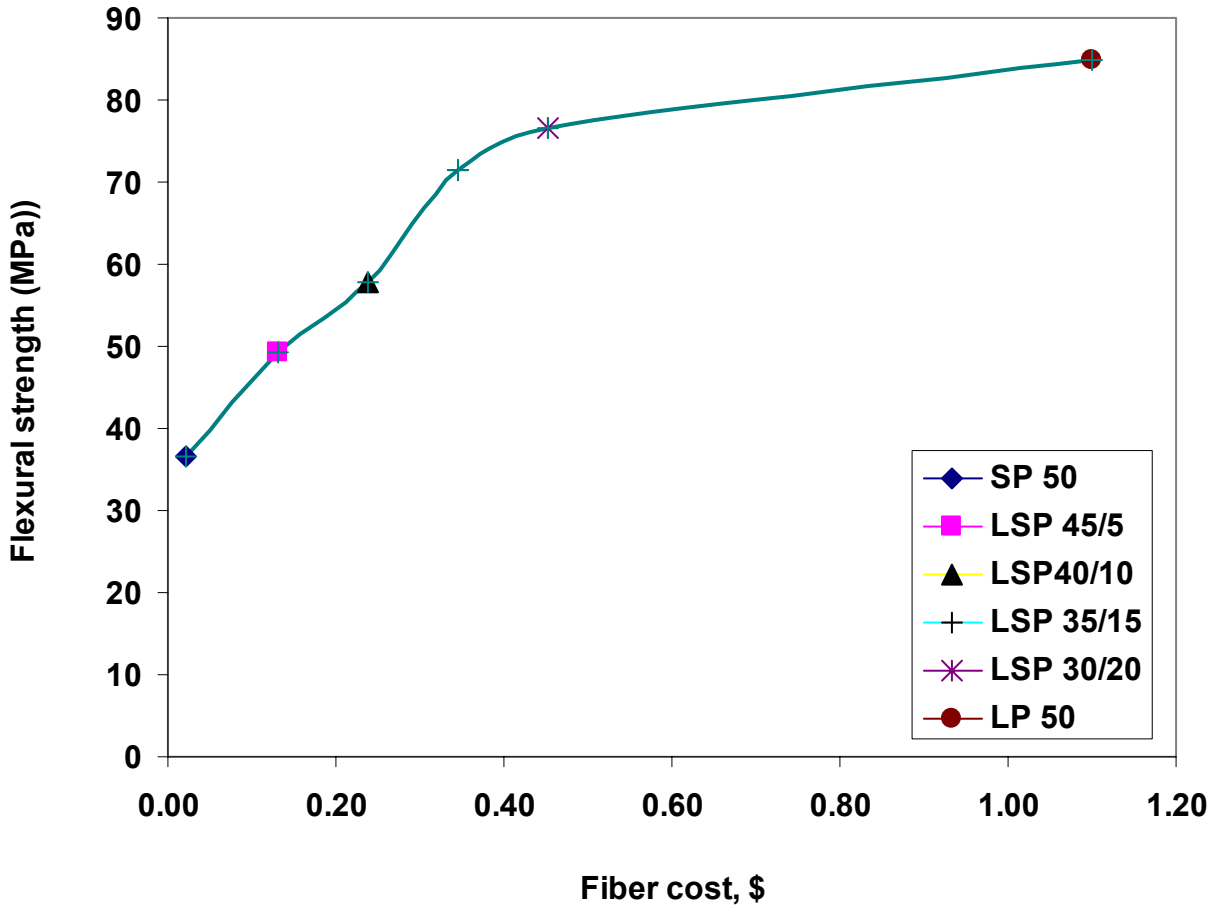

Figure 4.18 Flexural strength versus fiber cost for hybrid (SLP) composites and non-hybrid (SP 50 and LP 50) controls. See Figure 4.15 for fiber cost calculation procedure.

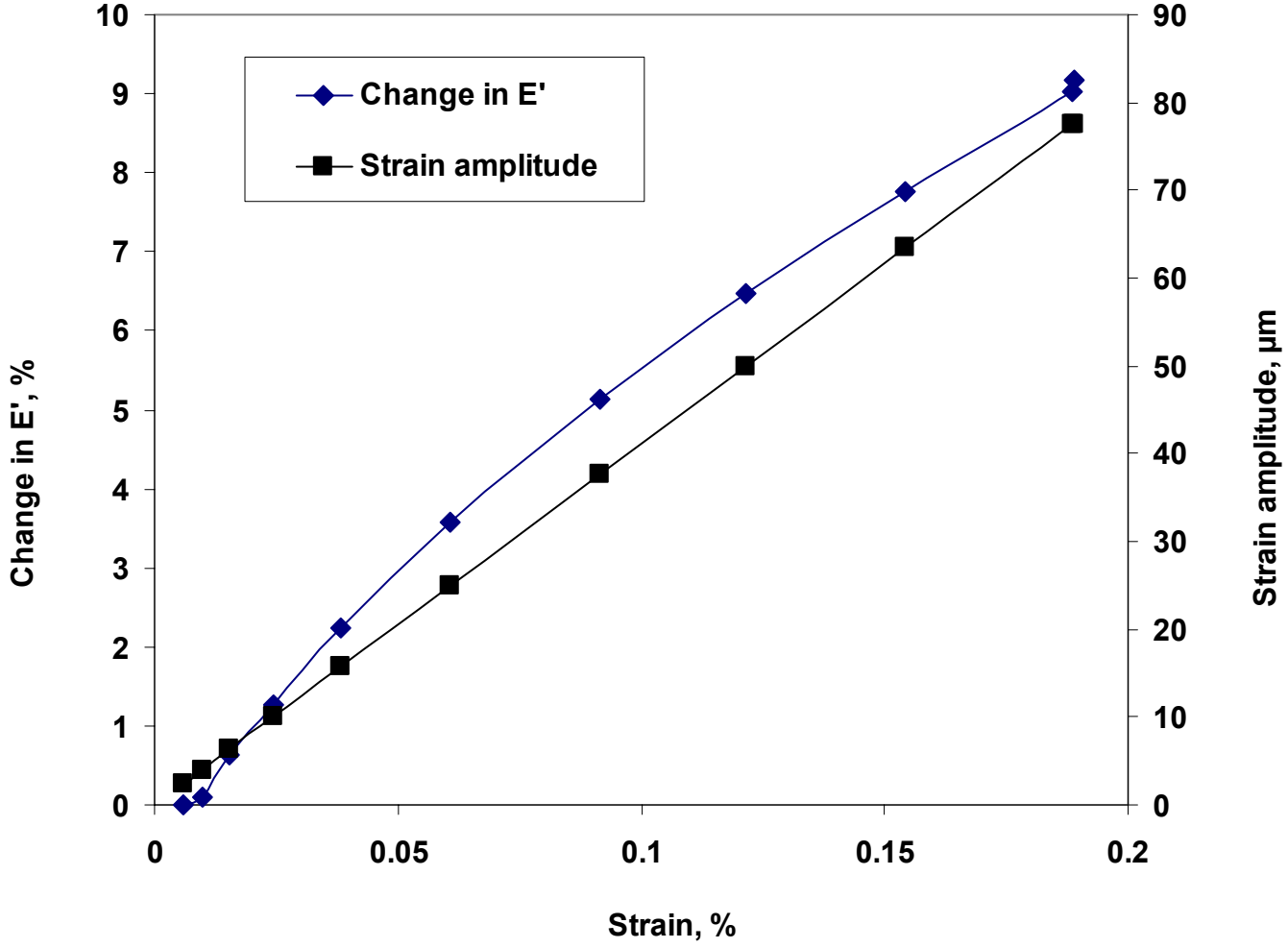

Figure 4.19 Storage modulus change and amplitude as a function of strain for LP 50. Data represents a typical isothermal strain sweep at –70°C.

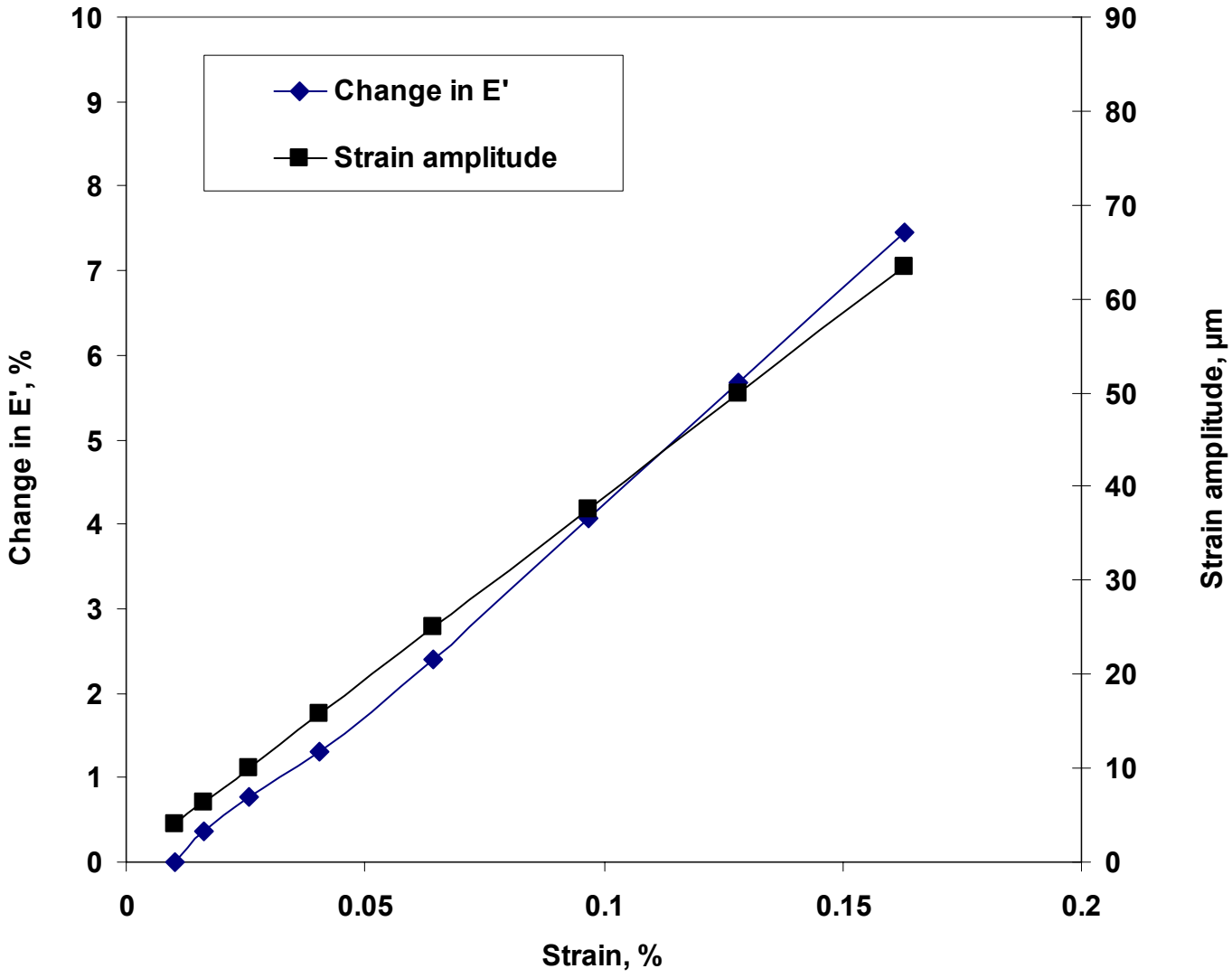

Figure 4.20 Storage modulus change as a function of strain for LP 50. Data represents a typical isothermal strain sweep at 70°C.

4.2.1.2 Linear Viscoelastic Properties

Figures 4.21 to 4.23 show the temperature dependencies of viscoelastic properties (storage modulus, loss modulus, and tan δ respectively) of unfilled PP, selected hybrid (SLP 30/20 and SLP 40/10) composites, and non-hybrid (SP 50 and LP 50) controls. The data shown are representative plots selected from among three replications for each material type.

The shapes of all E' plots (Figure 4.21) are representative of a semicrystalline polymer showing three distinct regions; a fairly flat glassy region, a rapidly declining glass transition zone, and a slowly declining rubbery region. It can be seen from Figure 4.21 that E' for all lyocell-containing composites exceed that of unfilled PP, with those of SLP 30/20 and LP 50 showing the greatest increases. The curve positions clearly show increasing E' with increasing lyocell concentration. It may be recalled that a similar trend was observed under transient (stress-strain) testing (see section 4.1.3.1). The dependence of storage modulus on lyocell concentration can be attributed to the same fiber- and processing-related factors earlier cited under section 4.1.2. Another study by Amash and Zugenmaier [57] on Cordenka® (high strength rayon fibers), wood microfibers, and Xylan fillers (in PP matrix) resulted in Cordenka® exhibiting the highest E'. At room temperature, the E' of Cordenka® exceeded those of unfilled PP and wood microfibers by 1040 MPa and 470 MPa respectively. Figure 4.21 also reveals a less drastic decline in E' for composites than for unfilled PP in the transition zone. This is accompanied by peak broadening of E'' (Figure 4.22) and tan δ (Figure 4.23) curves of the composites. Similar effects have been observed in several DMA studies on reinforced thermoplastics [57, 58, 59, 60] and have been attributed to mechanical restraint on the amorphous fraction of the matrix. Furthermore, the curve flattening (or peak broadening) effect gives an indication of the strength of fiber-matrix interactions. Stronger fiber-matrix interactions are associated with weaker transitions as appear to be the case in composites with high lyocell fiber loadings. To compare the fiber reinforcing effects of hybrid and non-hybrid composites, differences in storage modulus at the two temperature extremes (-70- and 70ºC) were determined and compared for SLP 30/20, LP 50, and PP (Table 4.7). T-test results (Table 4.7) reveal that the E' change for SLP

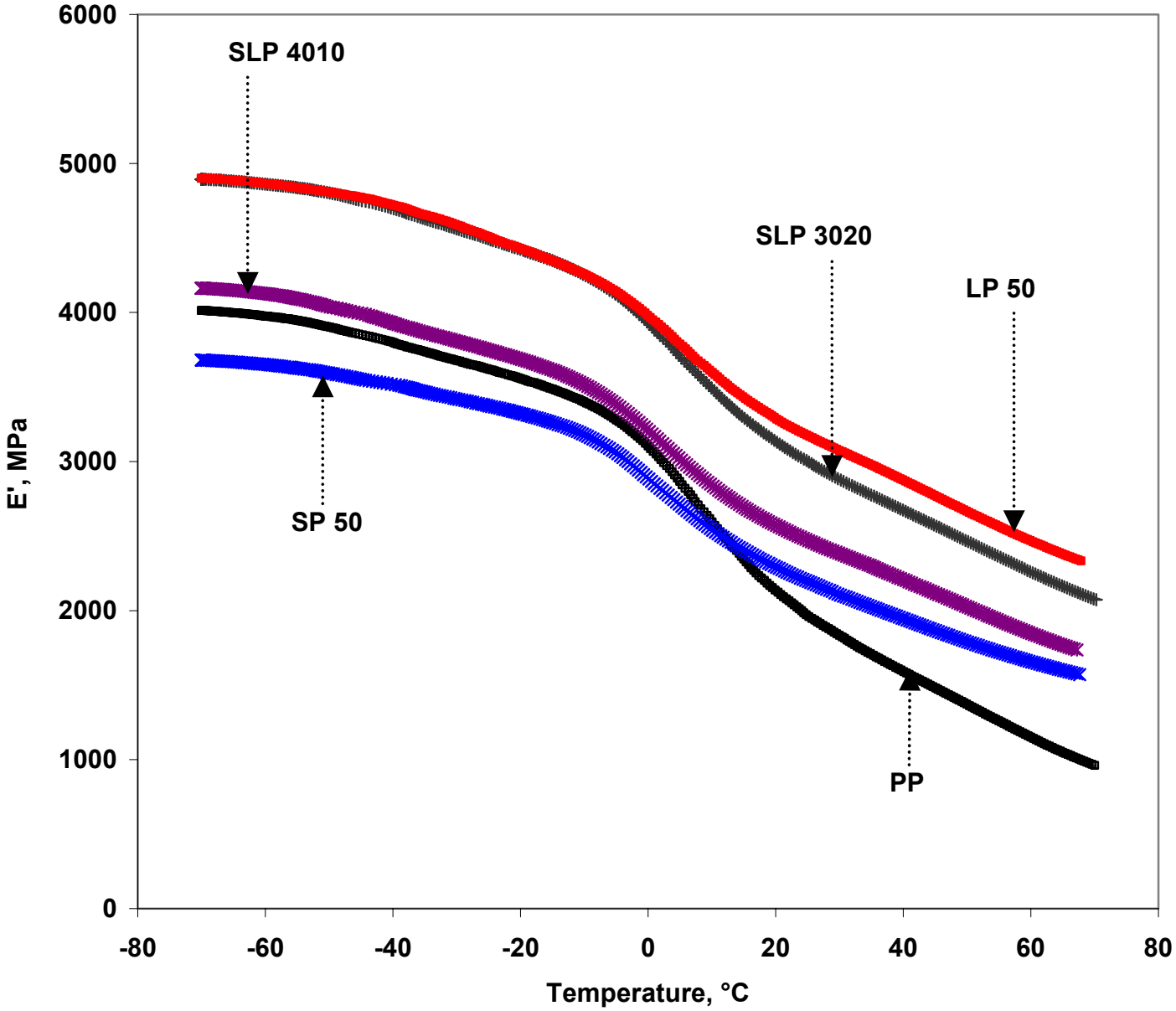

Figure 4.21 Dynamic mechanical spectrum of PP and selected composites. Storage modulus versus temperature (–70ºC to 70ºC)

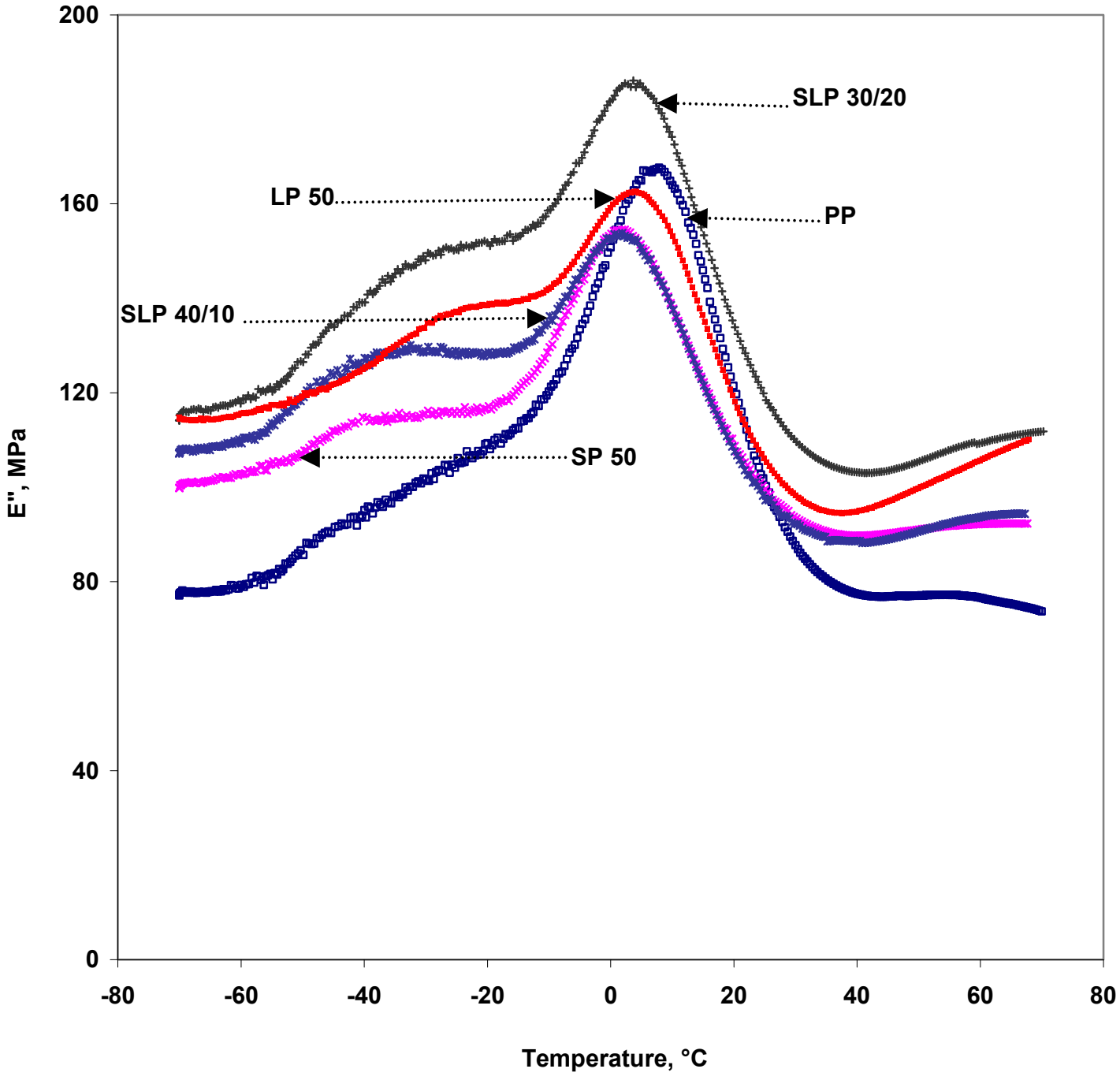

Figure 4.22 Dynamic mechanical spectrum of PP and selected composites. Loss modulus versus temperature (–70ºC to 70ºC). Tg values, taken from E'' peak maxima have been summarized in Table 4.8.

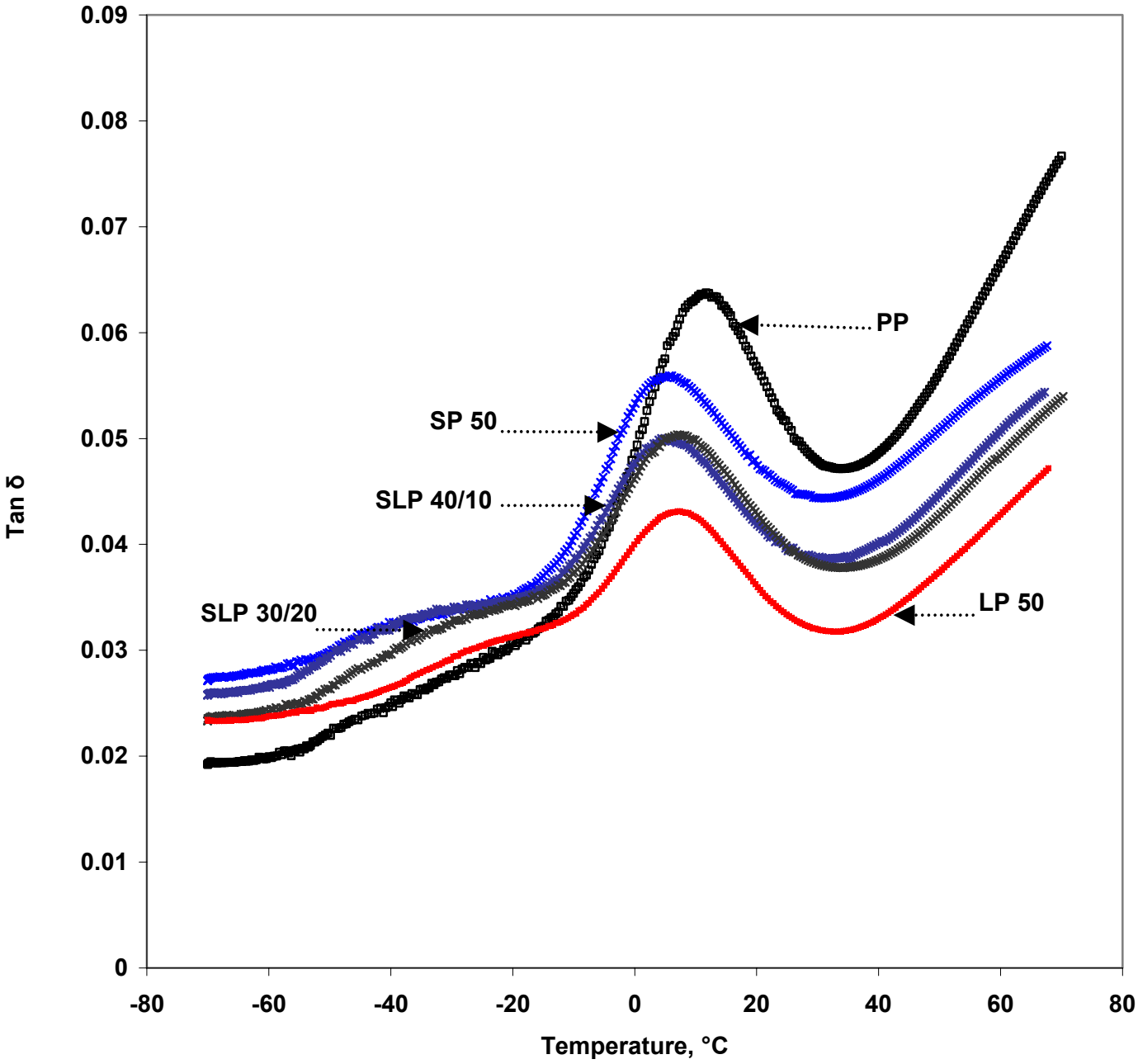

Figure 4.23 Dynamic mechanical spectrum of PP and selected composites. Tan δ versus temperature (–70ºC to 70ºC).

30/20 is not significantly different from that of LP 50. This observation can be likened to the synergistic effect earlier described under section 4.1.5.1 and is also supported by the property gain versus fiber cost analyses (section 4.1.5.2).

Glass transition temperatures were assigned to the peak maxima of E'' plots. The data, which have been presented in Table 4.8 for all materials reveal shifts of composite T_gs to lower temperatures (*ca.* 4 to 6°C compared to unfilled PP). Among the composites however, fiber composition did not appear to have any significant effect on T_g (shown by only slight differences of < 2°C). The effect of fiber reinforcement on the T_g of PP has been characterized by conflicting reports. Some researchers have reported no change [57], some have reported increases [61], while others have reported decreases [59, 62, 63]. These differences have been partly attributed to changes in crystallization behavior of PP because of fiber addition. The effects of crystallinity changes on T_g of semicrystalline polymers have been well-described by Chartoff [23].

The origin of a weak low-temperature transition (between ~ [-50 to -15^{o}C]), which can be clearly observed in E'' and tan δ curves was not known. To the author's knowledge, other DMA studies on PP and its composites over similar temperature ranges have not reported on the existence of such a peak. No further investigations were however made in the present study with respect to its identity.

Figure 4.23 shows tan δ plots for the various materials. The intensities and sizes of tan δ peaks for the composites reflect the effects of reinforcement types on matrix damping. These effects have been compared for SLP 30/20 and LP 50 composites by considering the area under their respective tan δ peaks (Table 4.9). Peak sizes were measured with the aid of the DMA instrument software from –20 to 35°C, which were observed to be the approximate tan δ peak inflection temperatures for the selected materials. T-groupings in Table 4.9 show significant differences in damping between the neat polymer and the composites and also between the hybrid and non-hybrid composites. It has been reported that damping in composites increases when flaws (weak fiber-matrix adhesion and or cracks at the fiber-matrix interphase) are present [25]. This is because flaws within the composite act as energy dissipation regions [25]. This probably explains why SLP 30/20, with high concentration of SEW that has been observed as having poor interactions with PP, exhibits higher damping than LP 50.

The E', E'', and tan δ curves for COSLP have also been presented in Figures 4.24 to 4.26. The behavior of COSLP under DMA testing is comparable to those of the hybrid composites in

the previous discussions. However, the shapes of both HMiPP and COSLP curves appear more flattened than those of PP and its composites. This is also shown by the smaller area under tan δ plot for COSLP. Two reasons may account for this difference. The first is a possible improvement in fiber matrix interaction as a result of co-steam explosion. The second is a possible increase in composite stiffness coming from the 5 wt % increase in fiber content for COSLP. The relative contributions of these two factors to the viscoelastic properties of COSLP could however, not be ascertained.

Table 4.7 Comparisons of E' changes for PP and composites from –70- to 70°C. Values in parentheses represent ± standard deviation. Materials belonging to the same letter group (shaded) are not significantly different.

Material	Average change in storage modulus[1], MPa	t-grouping
PP	3129 (265)	A
SLP 30/20	2820 (113)	B A
LP 50	2517 (66)	B

Table 4.8 T_g of unfilled PP and composites taken from peak maxima of E'' curves

Material	T_g, °C
PP	7.9
SP 50	2.3
SLP 40/10	2.3
SLP 30/20	3.7
LP 50	4.1

Table 4 9 Comparisons of damping abilities for PP and selected composites. Values represent averages of 3 replications for each material type. Standard deviations are shown in parentheses.

Material	Damping ability[1]	t-grouping
PP	0.11 (0.006)	A
SLP 30/20	0.07 (0.005)	B
LP 50	0.04 (0.006)	C

[1]Damping abilities were obtained from measuring areas under the tan peaks for each material. The higher the value, the greater the ability of the material to dissipate energy under dynamic stress. The procedure for measuring damping has been explained in the text.

4.2.2 Time-Temperature Superposition (TTS)

The time-temperature superposition principle was employed to examine the effect of reinforcement type (hybrid versus non-hybrid) on viscoelastic properties of PP over extended frequencies (times). Storage modulus was chosen as the viscoelastic function to be examined and the resulting master curves for PP, LP 50, and SLP 40/10 have been shown in Figure 4.27. The master curve for SLP 30/20 was found to overlay that of LP 50 exactly and was therefore excluded from Figure 4.27 for purpose of clarity. The experiments were performed from –10 to 70^{o}C in steps of 10^{o}C for composites and 5^{o}C for unfilled PP. Shorter temperature steps were used for unfilled PP because its frequency scan plots from 10°C steps failed to overlap after shifting. This observation was attributed to the higher sensitivity of unfilled PP properties to temperature changes. A reference temperature of 10 ^{o}C was used due to its closeness to the T_g (7.9^{o}C) of PP. The insert in Figure 4.27 shows examples of frequency scan plots prior to shifting.

As expected, E's for all materials increase from left to right in response to higher frequencies (shorter times) and lower temperatures. The effect of fiber reinforcement on E' is also shown by the elevation of composite master curves to higher moduli and the reduction in their overall slope intensities in comparison to those of unfilled PP. It is also evident from the positions of the composite master curves (the reader is reminded that the curve for SLP 30/20 overlays that of LP 50 exactly) that frequency (or time) sensitivity of viscoelastic properties decreases at a faster rate in hybrid than in non-hybrid composites. This observation agrees with thermal scan results where the temperature sensitivity of hybrid composites was found to decrease with increasing lyocell concentration.

Figure 4.28 shows shift factor versus temperature curves for PP and composites. The value "a_T", is the ratio of stress relaxation times of a polymer at different temperatures and is defined mathematically by equation 4.1 [23, 64].

$$a_T = \tau_T / \tau_0 \qquad (4.1)$$

where:

a_T = Shift factor

τ_T = Polymer stress relaxation time at temperature, T

τ_0 = Polymer stress relaxation time at reference temperature, T_o

According to Chartoff [23], equation 4.1 assumes that a change in temperature from T_o to T and vice versa multiplies by the same factor all of the relaxation times that characterize polymer behavior. The relaxation times are related to the molecular diffusional motions responsible for viscoelastic behavior. It can be seen from the Figure 4.28 that shift factor curves of the composites occupy a narrower range than that of unfilled PP indicating lower values of relaxation time ratios for the composites. This effect can be attributed to fiber-matrix interactions, which suppress the temperature-dependence of PP relaxation in the composites.

HMiPP and COSLP (Figures 4.29 and 4.30) exhibited responses similar to those observed for PP and its hybrid composites.

4.3 Sorption Properties

4.3.1 Effects of Fiber Blending

The effects of fiber blending on the sorption properties of hybrid composites were measured and compared with those of non-hybrid controls as well as with COSLP. Samples were immersed in water and weight gains after 24 hours were measured. Ten samples per specimen were tested. Results are shown in Table 4.10 and Figure 4.31 below.

The data reveals significant differences in moisture sorption between LP 50 to SP 50 (t-groupings in Table 4.10). This is not surprising considering that SEW contains substantial amounts of lignin while lyocell is more or less pure cellulose. The surprising observation is with the sorption behavior of the hybrid composites. All hybrid composites absorbed significantly less moisture than both LP 50 and SP 50, which is contrary to the more obvious expectation of some intermediate sorption characteristics between those of the two controls. The synergistic effects observed between lyocell and SEW under previous characterizations (mechanical and dynamic

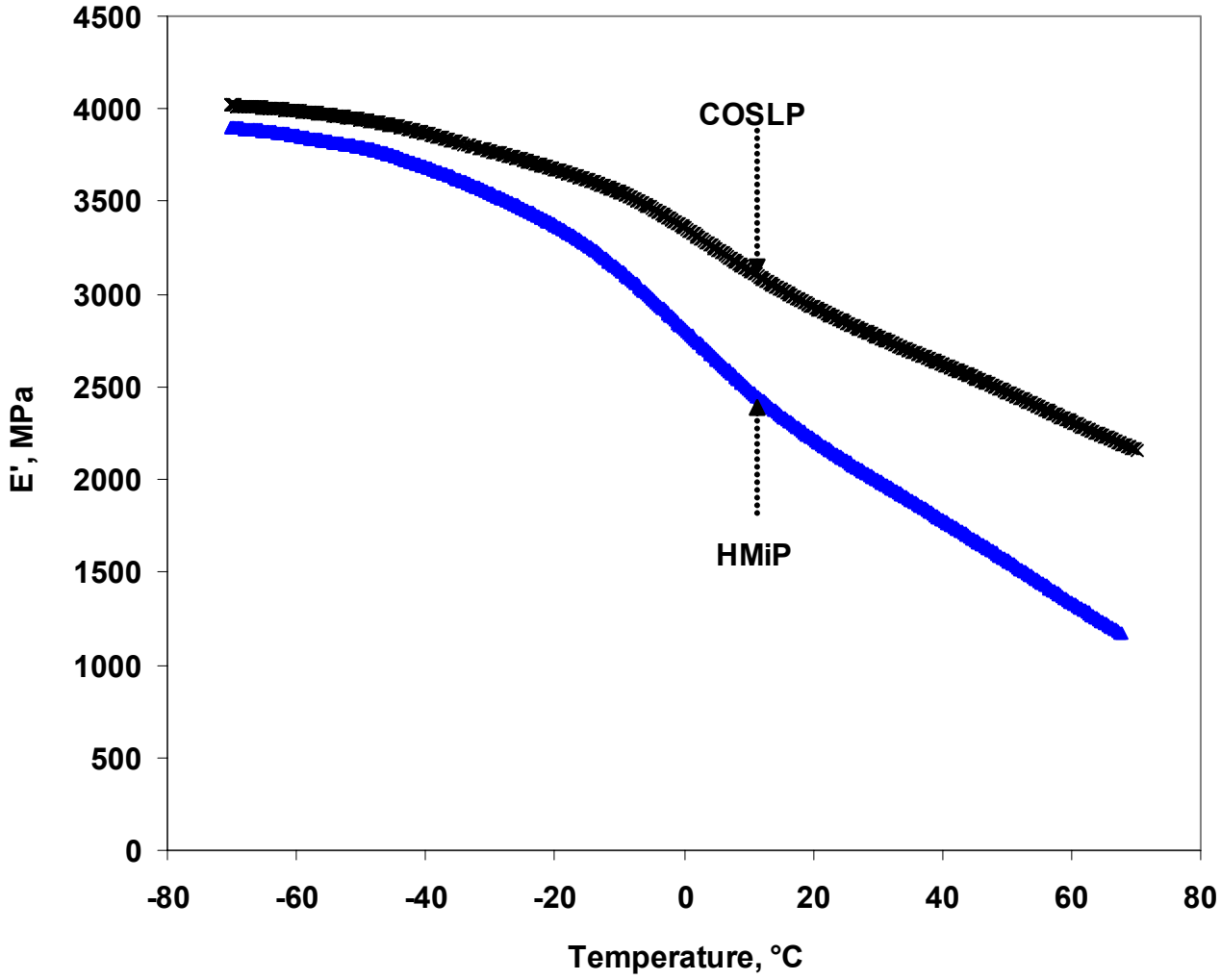

Figure 4.24 Dynamic mechanical spectrum of HMiPP and COSLP. Storage modulus versus temperature. (–70ºC to 70ºC).

.

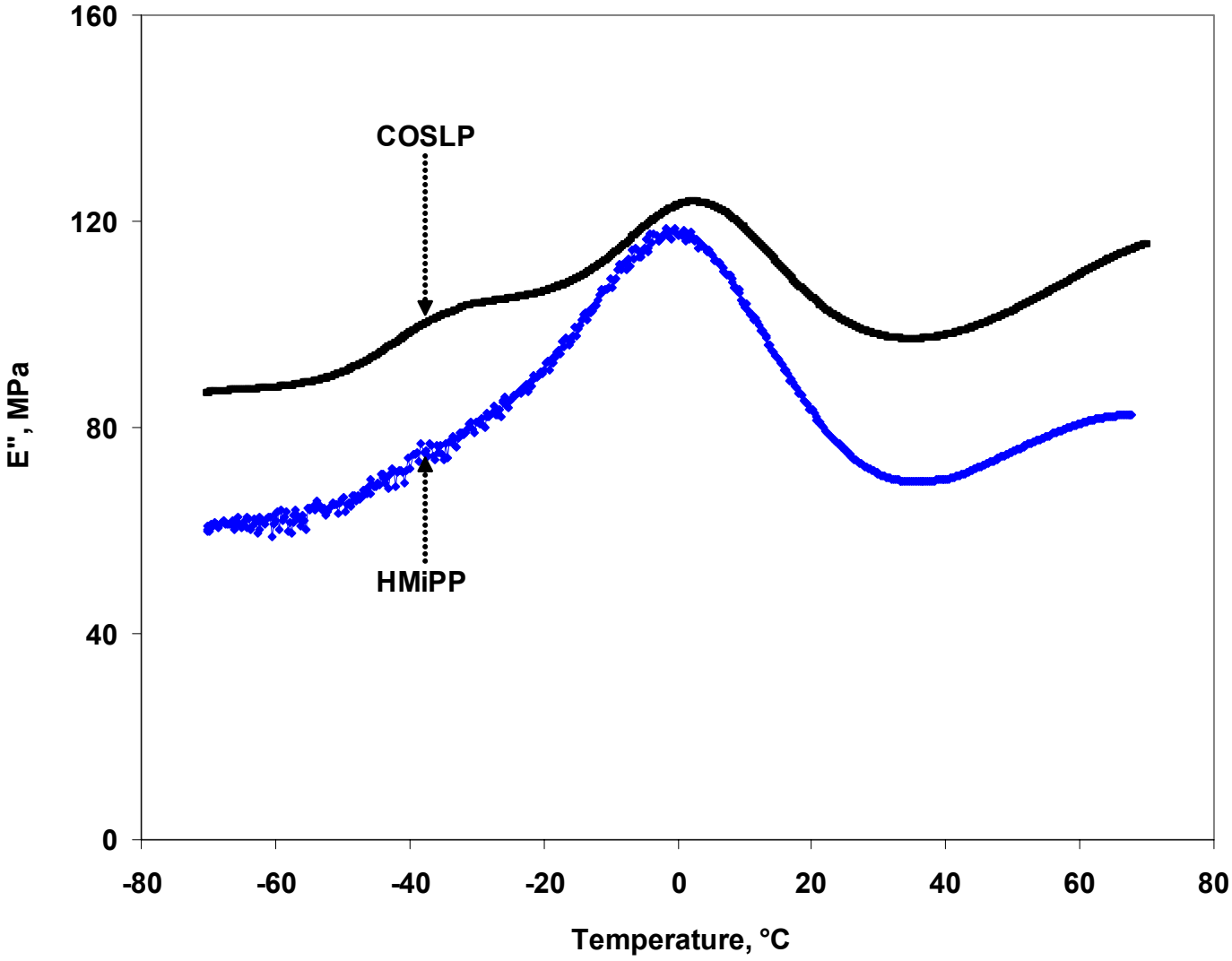

Figure 4.25 Dynamic mechanical spectrum of HMiPP and COSLP. Loss modulus versus temperature. (–70ºC to 70ºC).

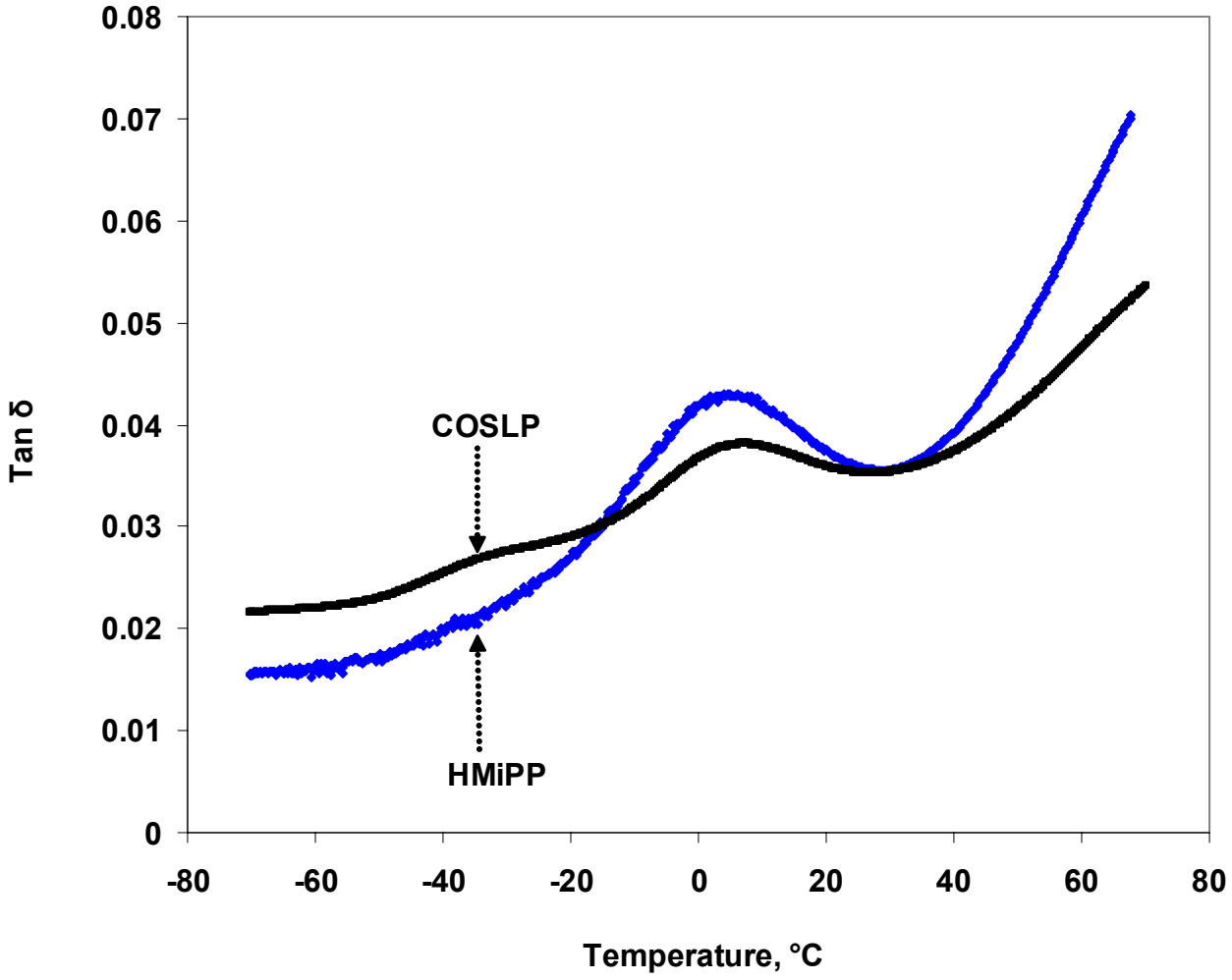

Figure 4.26 Dynamic mechanical spectrum of HMiPP and COSLP. Tan δ versus temperature. (–70ºC to 70ºC).

mechanical studies) appear to influence moisture sorption behavior as well. It is, however, not obvious as to which specific interactions among the components of the hybrid composites are responsible for the sorption decline. Possible causes may be changes to moisture transport mechanism induced by hybridization or differences in porosity of hybrid versus non-hybrid composites.

Table 4.10 Sorption Properties of Hybrid and Non-Hybrid Composites. (Values in parentheses represent standard deviations. Materials belonging to the same letter group (shaded) are not significantly different.

Material	Average weight gain sorption (%)	t-grouping
COSLP	8.94 (0.95)	A
LP 50	7.74 (0.21)	B
SP 50	6.76 (1.01)	C
SLP 30/20	5.76 (0.23)	D
SLP 35/15	4.80 (0.28)	E
SLP 40/10	4.72 (0.39)	E

4.3.2 Effect of Co-steam Explosion on Sorption Properties

It has been observed that co-steam exploding wood and PP produces fibers with reduced sorption characteristics due to coating of wood fibers by PP [44]. The effect of co-steam explosion on the sorption properties of COSLP was also studied.

Sorption test results (Table 4.10) reveal higher moisture absorption in COSLP compared to SLP 40/10 (having similar fiber content as COSLP but without co-explosion). The different sorption characteristics may be the result of differences in level of fiber coating by matrix between the two systems. Possible degradation of the low molecular weight HMiPP under steam explosion could account for its inadequacy in resisting moisture sorption by the wood fibers.

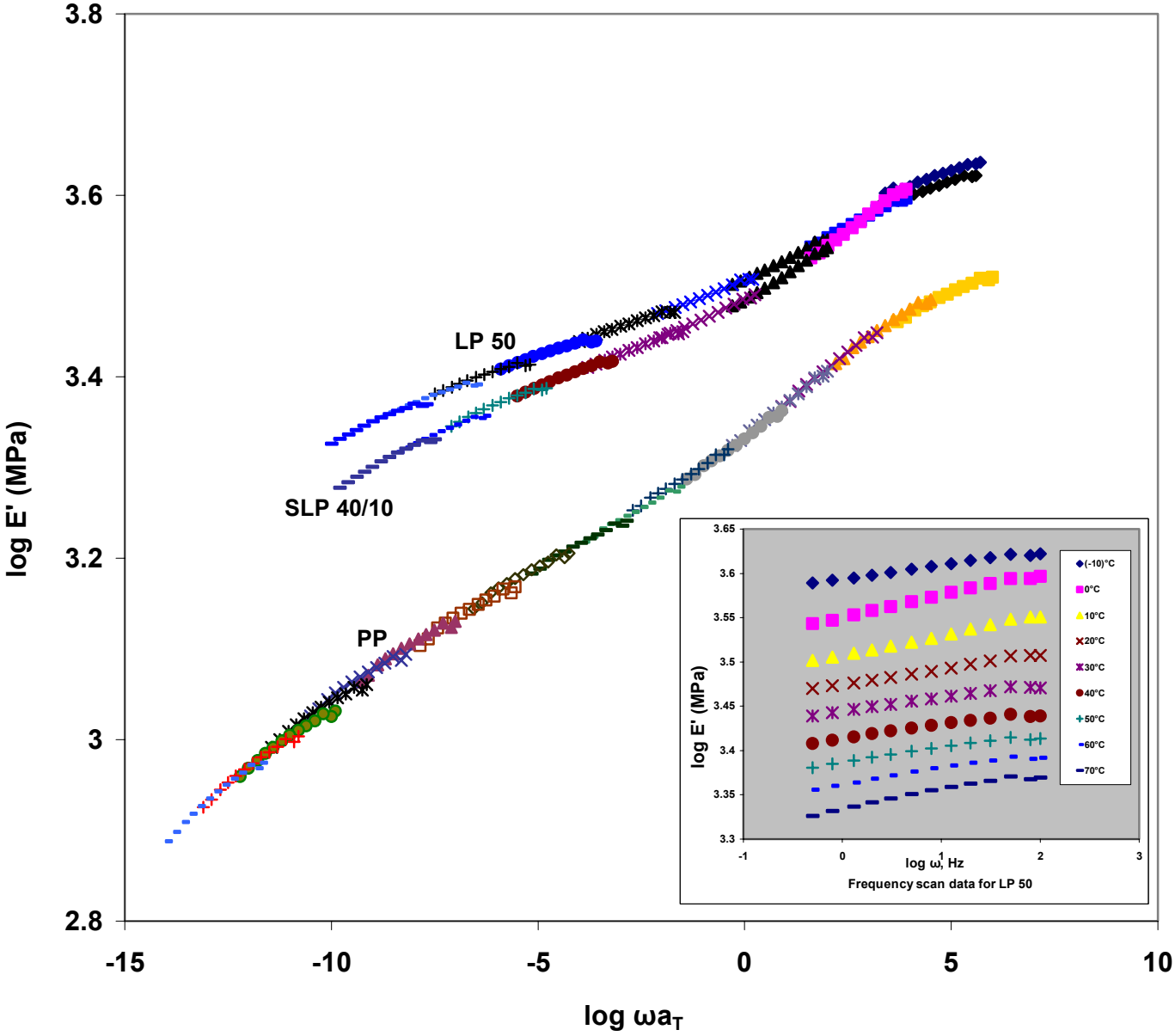

Figure 4.27 Master curves for PP and selected composites from –10- to 70°C. Data has been shifted to a reference temperature of 10°C. Insert is an example of log frequency (ω) scans prior to shifting.

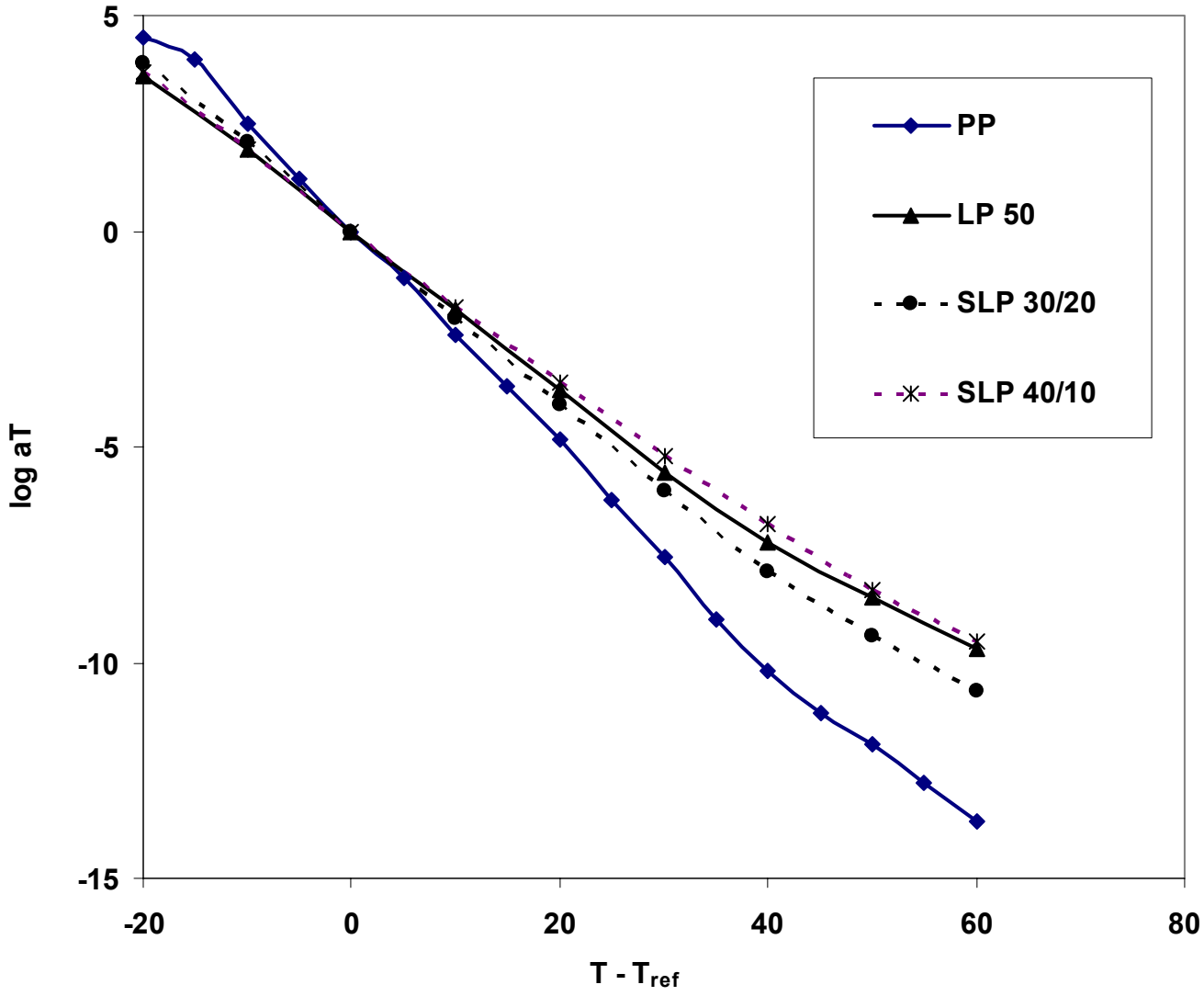

Figure 4.28 Shift factor versus temperature for PP and composites. Reference temperature is 10°C. The shift factor values used in plotting the curves were obtained from empirical (horizontal) shifting of frequency scan plots. See Figure 4.25 for corresponding master curves.

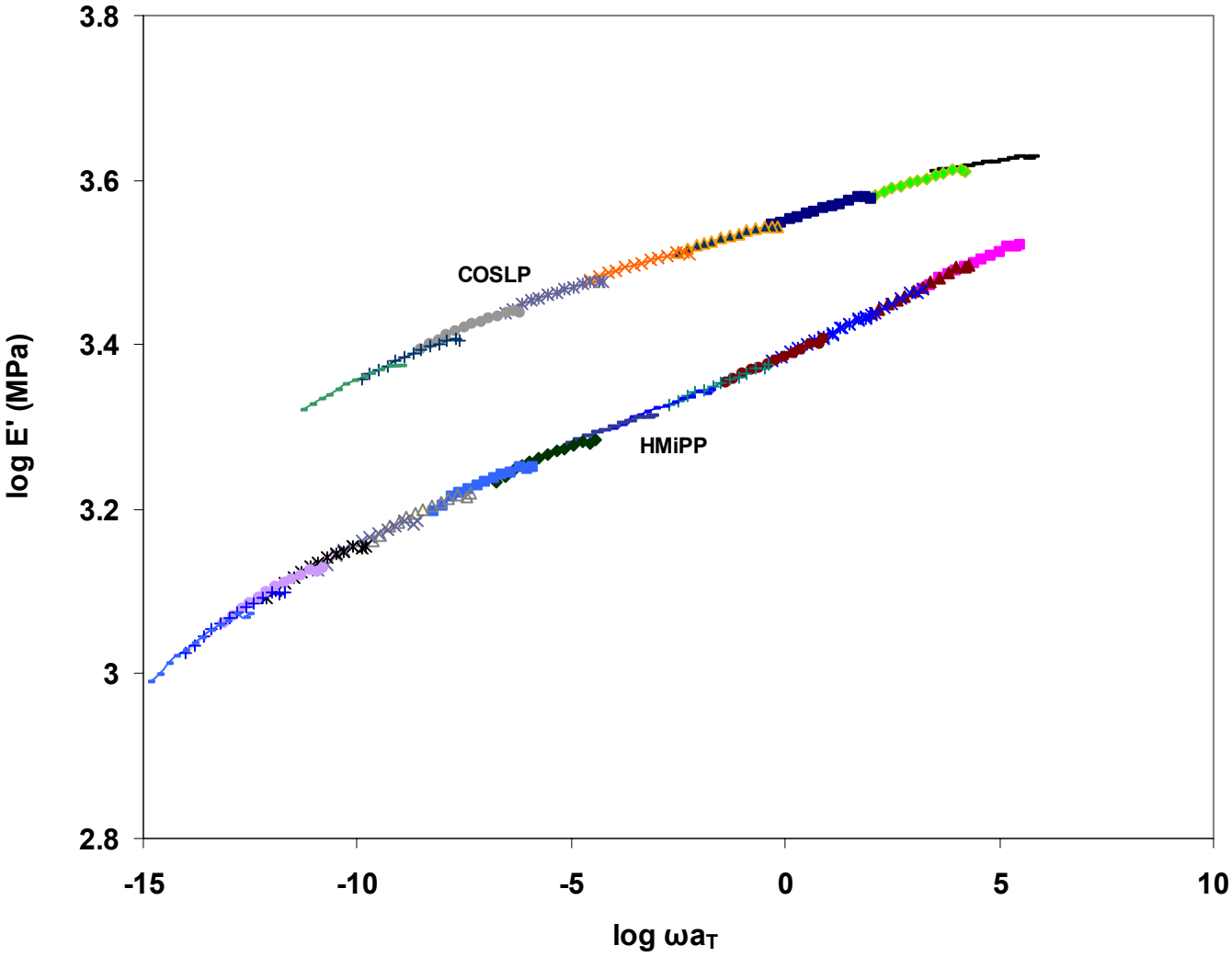

Figure 4.29 Master curves for HMiPP and COSLP from –10- to 70°C. Data has been shifted to a reference temperature of 10°C.

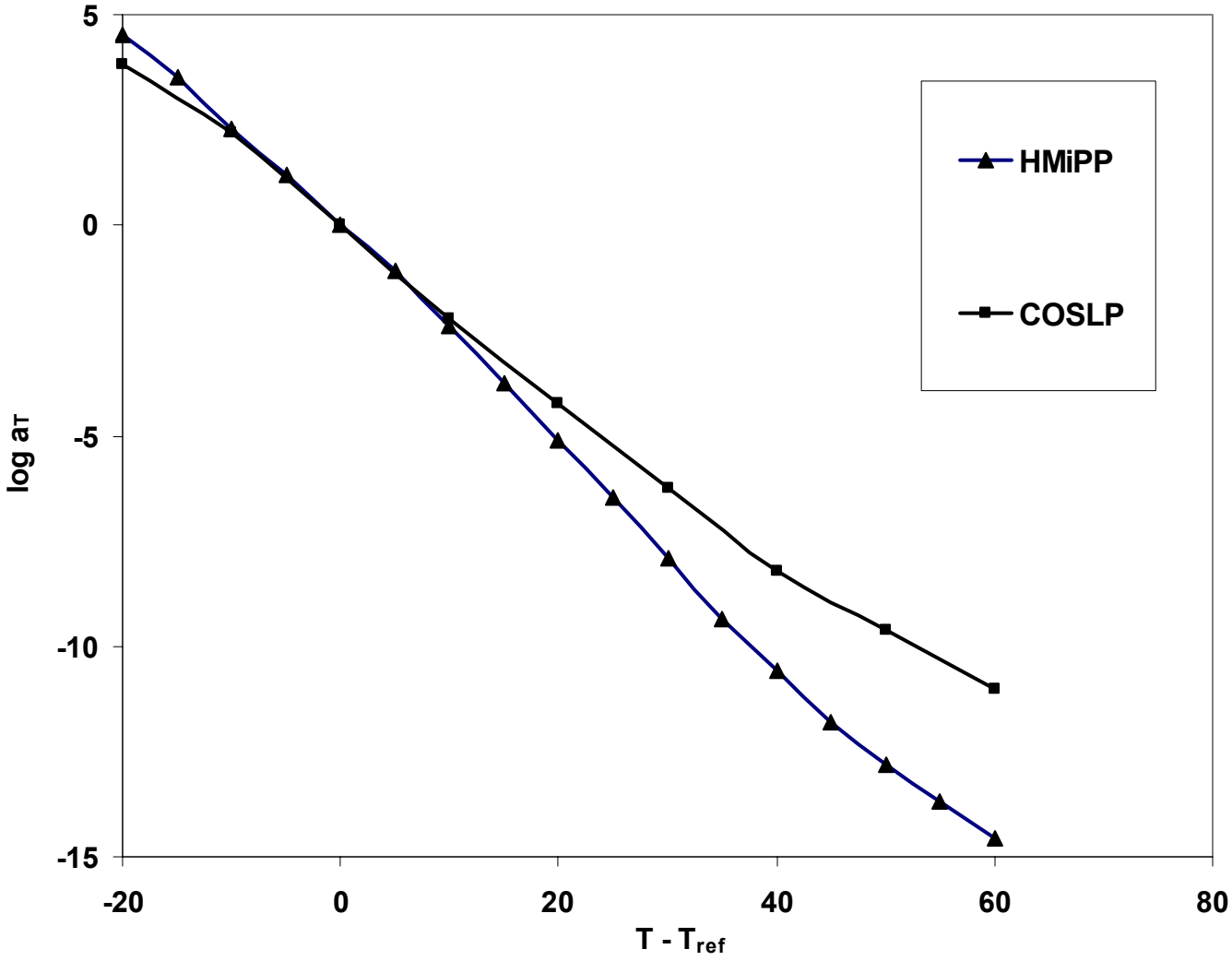

Figure 4.30 Shift factor versus temperature for HMiPP and COSLP. Reference temperature is 10°C. The shift factor values used in plotting the curves were obtained from empirical (horizontal) shifting of frequency scan plots. See Figure 4.27 for corresponding master curves.

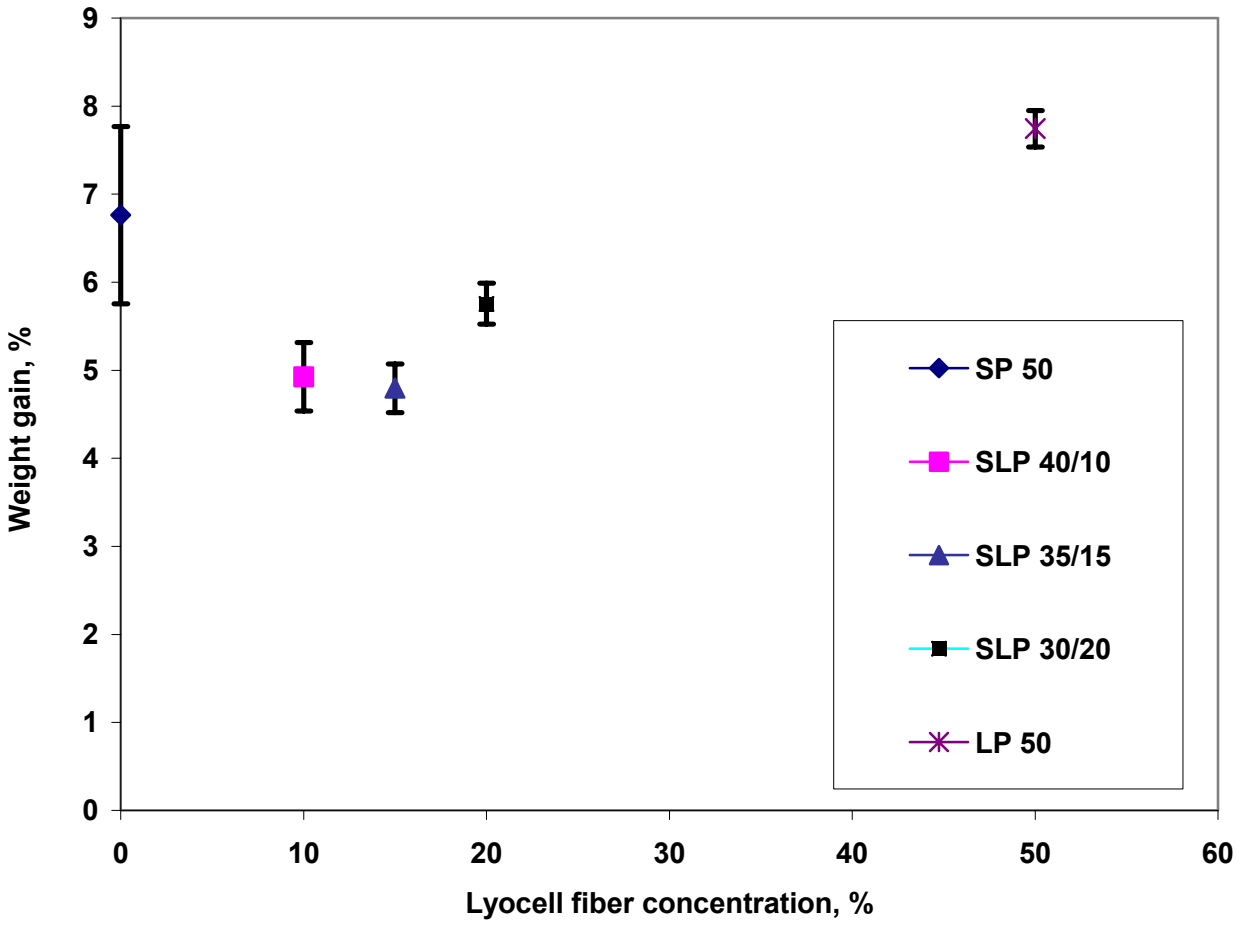

Figure 4.31 Weight gain in composites after 24 hours immersion in water plotted as a function of lyocell fiber content. SP 50 and LP 50 represent non-hybrid SEW and lyocell controls respectively.

5 Summary, Conclusions, and Recommendations

5.1 Summary and Conclusions

In this study, attempts were made to explore the potential benefits of blending high and low performance cellulose fibers in PP matrices to generate low-cost hybrid composites of desirable properties. Hybrid composites were characterized and compared with non-hybrid controls for tensile / flexural, dynamic mechanical, and moisture sorption properties. It was consistently observed under each of the characterization methods that hybrid composites outperformed non-hybrid counterparts from a viewpoint of overall material property balance in relation to cost benefits.

Summarized below are specific conclusions drawn from the study.

1. Modulus and strength properties of composites were found to vary in the same direction as lyocell fiber concentration. The positive interaction was attributed to high strength/stiffness and high aspect ratio of lyocell fibers as well as efficient fiber dispersion and fiber length retention from the wetlay process.

2. Property increase with lyocell concentration was found to be greater (up to 2.6 times) in hybrid (SLP) than non-hybrid (LP) composites. The difference was attributed to synergism between lyocell and SEW fibers.

3. Cost analyses of mechanical property variation as a function of fiber cost yielded higher property increases per unit fiber cost in hybrid than non-hybrid composites of equal fiber loading. The difference was found to be most significant for tensile modulus.

4. Storage moduli of composites generally increased with increasing lyocell concentration. However, the storage modulus of SLP 30/20 (hybrid composite with 20 wt. % lyocell/30 wt. % SEW fiber loading) showed statistical equivalence (at 95 % C.L.) to LP 50 (non-hybrid composite with 50 wt. % lyocell loading). This observation represented further evidence of synergism between lyocell and SEW fibers.

5. Damping (tan δ) was found to be significantly greater (at 95 % C. L.) in hybrid than in

non-hybrid composites. This was attributed to increased proportion of flaws that must have originated from weak interactions between SEW fibers and PP matrix.

6. At equal fiber concentrations of 50 wt. %, moisture sorption values of all hybrid composites were found to be lower compared to those of non-hybrid counterparts (LP 50 and SP 50). The cause of sorption decline in hybrid composites was not known.

7. The quantitative effects of co-steam explosion on tensile and flexural as well as sorption properties could not be evaluated and compared with ordinarily blended counterparts. This was due to differences in matrix properties whose contributions could not be isolated from those of compounding methods.

5.2 Recommendations

Hybridization of lyocell and SEW fibers in PP composites have been shown to have substantial property gain to fiber cost advantages over non-hybrid systems. These advantages notwithstanding, the potential for future growth will also depend on the practicability of compounding and consolidation processes. Therefore, alternative compounding (melt mixing, solution impregnation) and consolidation (extrusion, injection molding) methods should be evaluated and compared with those from the present study.

Further investigations are necessary to determine the causes of synergism in hybrid composites. Investigations should include matrix crystallization behavior, which has been found to contribute significantly to properties of semicrystalline polymer composites.

Compounding by co-steam explosion appears to be a cost-effective approach to achieving excellent, ready-to-use raw materials for composite production. However, optimum material and processing conditions for achieving best results have not yet been found. Key material and consolidation parameters such as wood chip condition (species and sizes), matrix properties (molecular weight and molecular weight distribution), and steam-explosion severity should be manipulated for best results and if possible, modeled in the interest of process optimization.

Moisture sorption behavior should be further investigated to determine the causes of sorption reduction in hybrid composites.

References

1. Sheldon, R. P.; Composite Polymeric Materials. Applied Science Publishers. England, 1982 pp 45, 58, 196.

2. Woodhams, R. T.; Thomas, G.; Rodgers, D. K. Woodfibers as Reinforcing Fillers for Polyolefins. *Polymer Engineering and Science* **1984** 24 (15) 1166 – 1171.

3. Morton, J.; Quarmley, J.; Rossi, L. Current and Emerging Applications for Natural and Wood-Fiber Composites In *7th International Conference on Woodfiber-Plastic Composites.* Forest Products Society, Madison, WI, 2003.

4. Kardos, J. L. Short-Fiber-Reinforced Polymeric Composites, Structure-Property Relations. In *Handbook of Composites Reinforcement;* Lee, S. M. Ed.; VCH Publishers, Inc. New York, 1993; pp 590 – 601.

5. Kokta, B. V.; Chen, R.; Deneault, C.; Valade, J. L. Use of Woodfibers in Thermoplastic Composites. *Polymer Composites.* **1983** 4 (4) pp 229 – 232.

6. Glasser, W. G.; Taib, R.; Jain, R. K.; Kander, R. Fiber-Reinforced Cellulosic Thermoplastic Composites. In *Journal of Applied Science* **1999** 73 (7) pp 1329 – 1340.

7. Rowell, R. M.; Cleary, B. A.; Rowell, J. S.; Clemons, C.; Young, R. A. Results of Chemical Modification of Lignocellulosic Fibers for Use in Composites. In *Wood-Fiber / Polymer Composites: Fundamental Concepts, Processes, and Material Options,* Wolcott, M. P. Ed.; Forest Products Society, Madison, WI, 1993, pp 121 – 127.

8. Kokta, B. V.; Raj, R. G.; Maldas, D. Use of Wood in Thermoplastic Composites. In *Lignocellulosics Science, Technology, Development, and Use.* Kennedy, J. F.; Phillips, O.; Williams P. A. Eds. Ellis Harwood Ltd. England, 1992, pp 747 – 762.

9. Bledzki, A. K.; Gassan, J. Composites Reinforced with Cellulose Based Fibers. In *Program in Polymer Science* **1999** 24 (2) pp 221 – 274.

10. Bunsell, A. R.; Harris, B. Hybrid Carbon and Glass Fiber Composites. In *Composites* **1974** 5 pp 157 – 164

11. Maldas, D; Kokta, B. V. Performance of Treated Hybrid Fiber-Reinforced Thermoplastic Composites under Extreme Conditions II Use of Glass and Wood Pulp as Hybrid Fiber. In *Holzforschung* **1991** 45 (2) pp 131 – 135.

12. Maldas, D; Kokta, B. V. Performance of Treated Hybrid Fiber-Reinforced Thermoplastic Composites under Extreme Conditions IV. Use of Glass Fiber and Sawdust as Hybrid Fiber. In Journal In *Journal of Applied Science* **1991** 42 (5) pp 1443 – 1450.

13. Thwe, M. M.; Liao, K. Characterization of Bamboo-Glass Fiber Reinforced Polymer Matrix Hybrid Composite. In *Journal of Materials Science Letters* **2000** 19 (20) pp 1873

– 1876.

14. Suddell, B. C.; Evans, W. J. The Increasing Use and Application of Natural Fiber Composite Materials Within the Automotive Industry. In *7th International Conference on Woodfiber-Plastic Composites.* Forest Products Society, Madison, WI, 2003.

15. Sjöström, E.; Wood Chemistry Fundamentals and Applications 2nd Edition. Academic Press Incorporated, San Diego, 1993. p 54 – 73.

16. Haygreen, J. G.; Bowyer, J. L. Forest Products and Wood Science, An Introduction 2nd Edition. Iowa State University Press, Ames, 1989. pp 42 – 44.

17. Rials, T. G.; Wolcott, M. P. Physical and Mechanical Properties of Agro-Based Fibers. In *Paper and Composites from Agro-Based Resources.* Rowell, R. M.; Young, R. A.; Rowell, J. K. Eds. Lewis Publishers, Boca Raton. 1997. p 63 – 81.

18. English, B.; Chow, P.; Bajwa, D. S.; Processing Into Composites. In *Paper and Composites from Agro-Based Resources* Rowell, R. M.; Young, R. A.; Rowell, J. K. Eds. Lewis Publishers, Boca Raton. 1997. pp 269 – 299.

19. Ulrich, R.; Nickel, J.; Biocomposites: State-of-the-Art and Future Perspectives. In *7th International Conference on Woodfiber-Plastic Composites.* Forest Products Society, Madison, WI, 2003.

20. Cruz-Ramos, C. A. Natural Fiber Reinforced Thermoplastics. In *Mechanical Properties of Reinforced Thermoplastics.* Clegg, D. W.; Collyer, A. A. Eds. Elsevier Applied Science Publishers, London, 1986. pp 73 – 74.

21. Sanadi, A. R.; Caulfield, D. F.; Jacobson, R. E. Agro-Fiber Thermoplastic Composites. In *Paper and Composites from Agro-Based Resources.* Rowell, R. M.; Young, R. A.; Rowell, J. K. Eds. Lewis Publishers, Boca Raton. 1997. p 378.

22. Ichazo, M. N.; Albano, C.; Gonzalez, J.; Perera, R.; Candal, M. V.; Polypropylene / Wood Flour Composites: Treatments and Properties. In *Composites Structures.* **2001** 54 (2 – 3) 207 – 214.

23. Chartoff, R. P. Thermoplastic Polymers. In *Thermal Characterization of Polymeric Materials* 2nd Edition. Turi E. A. Ed. Academic Press, San Diego, 1997. pp 488 – 519

24. Kelly, S. S.; Rials, T. G.; Glasser, W. G. Relaxation Behavior of the Amorphous Components of Wood. *Journal of Materials Science.* 22 (2) 617 – 624.

25. Nielsen, L. E.; Landel, R. F. Mechanical Properties of Polymers and Composites 2nd Edition. Marcel Dekker Incorporated, New York, 1994. p 10, 492.

26. Menard, K. P. Dynamic Mechanical Analysis A Practical Introduction. CRC Press, Boca

Raton, 1999. p 100.

27. Maldas, D; Kokta, B. V. Role of Coupling Agents and Treatments on the Performance of Wood Fiber-Thermoplastic Composites. In *Wood-Fiber / Polymer Composites: Fundamental Concepts, Processes, and Material Options,* Wolcott, M. P. Ed.; Forest Products Society, Madison, WI, 1993, pp 112 – 119.

28. Rowell, R. M. Opportunities for Composites from Agro-Based Resources. In *Paper and Composites from Agro-Based Resources.* Rowell, R. M.; Young, R. A.; Rowell, J. K. Eds. Lewis Publishers, Boca Raton. 1997. pp 250 – 251.

29. Fink, H.-P.; Weigel, H. J.; Ganster, P. J. Structure Formation of Regenerated Cellulose Materials from NMMO-solutions. *Prog. Polym. Sci.* **2001** *26* (9) 1473-1524.

30. Hearle, J. W. S. Physical Structure and Fiber Properties. In *Regenerated Cellulose Fibers;* Woodings, C. Ed.; Woodhead Publishing Limited Series in association with The Textile Institute; CRC Press: Washington DC, 2001; pp 199 – 234.

31. Mbe, P. W. Lyocell: The Production Process and Market Development. In *Regenerated Cellulose Fibers;* Woodings, C. Ed.; Woodhead Publishing Limited Series in association with The Textile Institute; CRC Press: Washington DC, 2001; pp 62-86.

32. Woodings, C. A Brief History of Regenerated Cellulosic Fibers. In *Regenerated Cellulose Fibers;* Woodings, C. Ed.; Woodhead Publishing Limited Series in association with The Textile Institute; CRC Press: Washington DC, 2001; pp 1-21.

33. Seavey, K. C.; Ghosh, I.; Davis, R. M.; Glasser, W. G. Continuous Cellulose Fiber-Reinforced Cellulose Ester Composites I. Manufacturing Options. In. *Cellulose* **2001** 8 (2) 149-159.

34. Seavey, K. C.; Glasser, W. G. Continuous Cellulose Fiber-Reinforced Cellulose Ester Composites II. Fiber Surface Modification and Consolidation Conditions. In *Cellulose* **2001** 8 (2) 161-169.

35. Franco, A.; Seavey, K. C.; Gumaer, J.; Glasser, W. G. Continuous Cellulose Fiber-Reinforced Cellulose Ester Composites III. Commercial Matrix and Fiber Options. In *Cellulose* **2001** 8 (2) 111-179.

36. Kokta, B. V.; Ahmed, Aziz. Steam Explosion Pulping. In. *Environmentally Friendly Technologies for the Pulp and Paper Industry;* Young R. A.; Akhtar, M. Eds.; John Wiley and Sons Incorporated, New York, 1998. pp 191 – 213.

37. Young, R. A. Processing of Agro-Based Resources into Pulp and Paper. In *Paper and Composites from Agro-Based Resources.* Rowell, R. M.; Young, R. A.; Rowell, J. K. Eds. Lewis Publishers, Boca Raton. 1997. pp 138 – 245.

38. Avellar B. K.; Glasser, W. G. Steam-Exploded Biomass Fractionation. I. Process Considerations and Economic Evaluation. *Biomass and Bioenergy* **1998** 14 (3) pp 205 – 218.

39. Vignon, M. R.; Dupeyre, D.; Jaldon-Garcia, C. Morphological Characterization of Steam-Exploded Hemp Fibers and Their Utilization in Polypropylene-Based Composites. In *Bioresource Technology* **1996** 58(2) 203 – 215.

40. Anglès, M. N.; Ferrando, F.; Farriol, X.; Salvadó, J.; Dufrense, A. Suitability of Steam Exploded Residual Softwood for the Production of Binderless Panels. Effect of the Pre-Treatment Severity and Lignin Addition. In *Biomass and Bioenergy.* **2001** 21 (3) 211 – 224.

41. Takatani, M.; Ito, H.; Ohsugi, S.; Kitayama, T.; Saegusa, M.; Kawai, S.; Okamoto, T. Effect of Lignocellulosic Materials on the Properties of Thermoplastic Polymer/Wood Composites. In *Holzforschung* **2000** 54 (2) pp 197 – 200.

42. Anglès, M. N.; Salvadó, J.; Dufrense, A. Steam-Exploded Residual Softwood-Filled Polypropylene Composites. In *Journal of Applied Polymer Science.* **1999** 74 (8) 1962 – 1977.

43 Brooks, H. W.; Duranceau, C. M.; Gallmayer, W. W.; Williams, R. L.; Winslow, G. R. Stake Digester Process for HDPE Fuel Tank Recycling. Research Project. Society of Automotive Engineers Incorporated, 2002.

44 Renneckar, S. Modification of Wood Fiber with Thermoplastics by Reactive Steam Explosion Processes. PhD. Dissertation. Virginia Polytechnic Institute and State University, 2004.

45 United States Department of Agriculture Cooperative State Research, Education, and Extension Service National Research Initiative Competitive Grants Program. *Engineering The Wood Fiber-Plastic Interface by Steam Explosion* Project Proposal by Glasser, W. G.; Wright R. S.; Zink-Sharp A. p 10.

46 Chornet, E.; Overend, R. P. Phenomenological Kinetics and Reaction Engineering Aspects of Steam/Aqueous Treatments. In *Steam Explosion Techniques: Fundamentals and Industrial Applications*, Focher, B., Marzetti A.; Crescenzi, V. Eds., Gordan and Breach Science Publishers, Philadelphia, 1991. pp 21-58.

47 Week, G. P. US Patent No. 5409573, 1993.

48 Virginia Tech-DuPont Random Wetlay Composites Laboratory website www.wetlay.vt.edu. Cited June 2004

49 ASTM D 790 – 98 Standard Test Method for Flexural Properties of Unreinforced and Reinforced Plastics and Electrical Insulating Materials.

50 ASTM D 3039/D 3039M – 95a Standard Test Method for Tensile Properties of Polymer Matrix Composite Materials.

51 DMA 2980 Operators Manual Chapter 6, p.25.

52 Lu, Yunkai. Mechanical Properties of Random Discontinuous Fiber Composites Manufactured from the Wetlay Process. Masters Thesis. Virginia Polytechnic Institute and State University, 2002. p 52.

53 Nando, G. B.; Gupta, B. R. Short Fiber-Thermoplastic Elastomer Composites. In *Short Fiber-Polymer Composites;* De, S. K.; White, J. R. Eds. Woodhead Publishing Ltd. England 1996 p 95.

54 Weigel, P; Ganster, J; Fink, H-P. Man-Made Cellulosic Fiber-Reinforced Polypropylene Compounds for Injection Molding. In *Abstracts of Papers, 225th ACS National Meeting,* New Orleans LA, USA. **2003** March 23 – 27.

55 Bullions, T. A.; Gillespie, R. A.; O'Brien, J. P.; Loos, A. C. The Effect of Maleic Anhydride Modified Polypropylene on the Mechanical Properties of Feather Fiber, Kraft Pulp, Polypropylene Composites. *Journal of Applied Polymer Science*, **2004** 92 (6) pp 3771 – 3783.

56 TA Instruments Website. http://www.tainst.com/support/TS61.PDF Cited June 2004.

57 Amash, A.; Zugenmaier, P. Study on Cellulose and Xylan Filled Polypropylene Composites. In *Polymer Bulletin* **1998** 40 (2-3) 251 – 258.

58 Wielage, B.; Lampke, T.; Utschick, H.; Soergel, F. Processing of Natural Fiber Reinforced Polymers and the Resulting Dynamic Mechanical Properties. In *Journal of Materials Processing Technology* **2003** 139 (1-3) 140 – 146.

59 Nunez, A. J.; Kenny, M. J.; Reboredo, M. M.; Aranguren, M. I.; Marcovich, N. E. Thermal and Dynamic Mechanical Characterization of Polypropylene-Woodflour Composites. In *Polymer Engineering and Science* **2002** 42 (4) 733 – 742.

60 Joseph, P. V.; Mathew, G.; Joseph, K.; Groeninckx, G.; Thomas, S. Dynamic Mechanical Properties of Short Sisal Fiber Reinforced Polypropylene Composites. In *Composites Part A: Applied Science and Manufacturing* **2003** 34 (3) 257 – 290.

61 Hristov, V.; Vasileva, S. Dynamic Mechanical and Thermal Properties of Modified Poly (propylene) Wood Fiber Composites. In *Macromolecular Materials Engineering.* **2003** 288 (10) 798 – 806.

62 Lopez-Manchado, M. A.; Arroyo, M. Thermal and Dynamic Mechanical Properties of Polypropylene and Short Organic Fiber Composites. In *Polymer* **2000** 41 (21) 7761 – 7767.

63 Lopez-Manchado, M. A.; Biagiotti, J.; Kenny, M. J. Comparative Study of the Effects of Different Fibers on the Processing and Properties of Polypropylene Matrix Composites In *Journal of Thermoplastic Composite Materials* **2002** 15 (5) 337 – 353.

64 Ferry, J. D. Viscoelastic Properties of Polymers 3rd Edition. John Wiley and Sons, New York, 1980. p. 266.

APPENDIX

Actual Weights of Materials Used for Wetlaying

Designation	Composition	Fiber weight ratio, %	Fiber weight ratio (g)	Measured reinforcing fiber weight (g)/ 400 liters of white water	Measured matrix (PP) fiber weight, (g) / 400 liters of white water
LP 25	LYOCELL / PP	25 / 75	125 / 375	125	375
LP 35	"	35 / 65	175 / 325	175	325
LP 50	"	50 / 50	250 / 250	250	250
LP 65	"	65 / 35	325 / 175	325	175
COSLP	(CO SEW / PP) / LYOCELL	90 / 10	450 / 50	1177	225
SLP 30/20	SEW / LYO / PP	30 / 20 / 50	150 / 100 / 250	806	250
SLP 35/15	"	35 / 15 / 50	175 / 75 / 250	941	250
SLP 40/10	"	40 / 10 / 50	200 / 50 / 250	1075	250
SLP 45/5	"	45 / 5 / 50	225 / 25 / 250	1210	250

VITA

Richard Kwesi Johnson was born in Ghana on May 16 1971 to Cdr. Abraham Johnson (rtd) and Mrs Margaret Johnson. In February of 1998, he earned his Bachelors Degree in "Natural Resource Management" at the College of Natural Resources, Kwame Nkrumah University of Science and Technology, Kumasi, Ghana. He then worked as an intern with the Forest Products Inspection Bureau for one year after which he joined the Ghana Environmental Protection Agency.

In Fall of 2002, he was admitted to the Virginia Tech Department of Wood Science and Forest Products to pursue a Masters degree where he worked on Cellulose fiber-reinforced Thermoplastic Composites under the supervision of Drs. Wolfgang Glasser and Audery Zink-Sharp. Mr Johnson plans to continue with his research on wood-plastic composites through the PhD at Virginia Tech Department of Wood Science and Forest Products.